W72-02105

17010 DBL 12/70

PB 205 001

COLLOID FLOTATION AND ADSORBING COLLOID FLOTATION

by

Barry L. Karger
Department of Chemistry
Northeastern University
Boston, Massachusetts 02115

for the

FEDERAL WATER POLLUTION CONTROL ADMINISTRATION
DEPARTMENT OF THE INTERIOR

Grant # 17010 DBL

December, 1970

Reproduced by
NATIONAL TECHNICAL
INFORMATION SERVICE
Springfield, Va. 22151

A

83

SELECTED WATER RESOURCES ABSTRACTS
INPUT TRANSACTION FORM

1. Report No.
2.
3. Accession No. W72-02105

4. Title
COLLOID FLOTATION AND ADSORBING COLLOID FLOTATION

5. Report Date
6.
8. Performing Organization Report No.
10. Project No. EPA WQO 17010DRL

7. Author(s)
Karger, Barry L.

9. Organization
Northeastern Univ., Boston, Mass., Department of Chemistry

11. Contract/Grant No.
13. Type of Report and Period Covered

12. Sponsoring Organization

15. Supplementary Notes Final Technical Report, December 1970, 79 p, 30 fig, 69 ref

16. Abstract

Different separation processes are discussed that have potential application in the wastewater treatment field--(a) colloid flotation (b) coagulation of finely divided ion exchange resin for rapid ion removal, and (c) adsorbing colloid flotation. For each method, the implications to waste water treatment are detailed, and potential applications are explored. Colloid flotation can be successfully employed in the removal of clays (kaolin and montmorillonite) from waste water streams. There is a close interrelationship between gas bubble diameter and the size of the particle being removed. Gas bubbles of 1-2 mm require fully dispersed colloidal materials, whereas fine bubbles of 0.2 mm required coagulated sols for best removal. An understanding of the mechanism of flotation removal can be obtained through measurement of the zeta potentials of the colloidal particles. Rapid and total ion removal is potentially possible with the use of coagulated mixed ion exchange resins. One way in which this might be accomplished is in a fluidized bed. A total of 10 ppm Cr^{+3} can be rapidly removed from aqueous media by adsorption on hydrous manganese dioxide and the subsequent flotation of the colloid. The manganese dioxide can be generated in situ by the standard oxygenation reaction.

17a. Descriptors

*Waste water treatment, *Flotation, *Ion Exchange, *Separation techniques, *Water purification, Surfactants, Montmorillonite, Phosphates, Colloids, Cation adsorption, Kaolinite, Manganese, Surface tension

17b. Identifiers

Maganese dioxide

17c. COWRR Field & Group 05D

18. Availability PB-205 001 X PC $3.00 MF .95
19. Security Class. (Report)
20. Security Class. (Page)
21. No. of Pages
22. Price

Send To:
WATER RESOURCES SCIENTIFIC INFORMATION CENTER
U.S. DEPARTMENT OF THE INTERIOR
WASHINGTON, D. C. 20240

Abstractor
Institution

WRSIC 102 (REV. JUNE 1971)
GPO 913.261

ABSTRACT

This report details developments from three different separation processes that have potential application in the waste water treatment field---(a) colloid flotation (b) coagulation of finely divided ion exchange resin for rapid ion removal, and (c) adsorbing colloid flotation. For each method, the implications to waste water treatment are detailed, and potential applications are explored.

(a) An experimental investigation is reported of the effects of several solution parameters on the flotation of colloidal kaolin and montmorillonite using ethylhexadecyldimethylammonium bromide. The parameters examined were the zeta potential of the surfactant-particulate species, the concentration of selected cations, pH, and the ratio of initial surfactant concentration to initial particulate concentration. Two apparatuses were used to assess the effect of aggregation on flotation; one employed bubbles of 1-2 mm average diameter to effect the flotation, while the other used bubbles of about 0.2 mm. In the large bubble system, aggregation adversely affected the flotation of the particulates. For the small bubble (0.2 mm) system, the effect of aggregation on the flotation of particulates was contrary to that in the large bubble (1-2 mm) system. These observations are explained in terms of bubble sizes and their attachment to the particulate species during the flotation process. Studies also showed that several cations and pH variations cause little interference. A general discussion is given relative to the application of the process to large-scale clarification of turbid waters.

(b) Finely-ground ion exchange resin particles remove ions from solution much more rapidly than the conventional-size beads. Such finely-divided solids form suspensions when added to aqueous solutions. A method was required for rapidly removing such suspensions once ion adsorption had occurred, and to this end it is shown that the particles (-400 mesh) can be completely coagulated within a few minutes by the addition of suspensions of oppositely-charged solids. Thus anion exchange resins are coagulated by cation exchange resins (200 to 400), montmorillonite (200), kaolin (30), charcoal (10), silica (10), and glass (5), the figures representing arbitrarily defined relative coagulating abilities. Coagulating power is shown to increase markedly with decreasing particle size. Most suitable for ion removal is a mixed finely-divided resin formed by coagulation of anionic and cationic resins from pure water. The mixed resin, when added to 1 liter of 3×10^{-4} M sodium phosphate solution removes all the phosphorus within 2 min, and when added to 1 liter of 2.5×10^{-4}M calcium chloride, removes over 90% of the calcium within 3 min.

(c) An experimental investigation is reported of the adsorbing colloid flotation of chromium ions using hydrous, colloidal manganese dioxide as the adsorbent. Both the Guyard and the oxygenation reactions for the generation of MnO_2 were investigated and assessed for application to water and waste treatment. While both methods of preparing MnO_2 in situ are useful for water treatment, the oxygenation reaction is the more desirable method owing to the undetectable residual manganese level and the 100% removal of Cr^{+3} over the concentration ranges studied. The adsorption of Cr^{+3} by MnO_2 has been studied as a function of pH, electrophoretic mobility, and concentrations of both Cr^{+3} and Ca^{+2}. Using the results of the adsorption of Cr^{+3} as a function of pH, the optimum removal of the chromium ions was achieved when the flotation removal of MnO_2 was effected. EHDA-Br was used to float the hydrous oxide with the aid of a small amount of ethanol, which acted as a frothing agent. A 100% removal of Cr^{+3} is possible for concentrations of Cr^{+3} up to 10 ppm and a 96% removal for 20 ppm Cr^{+3} when 100 mg/l MnO_2 is used followed by flotation. The flotation does not interfere with adsorption of the chromic ion. A 100% removal of the MnO_2 is effected in less than 1½ minutes of sparging when a small bubble apparatus and a frother are used. A general discussion is given relative to the application of adsorbing colloid flotation to large-scale treatment of industrial aqueous wastes.

This report was submitted in fulfillment of Grant No. 17010 DBL between the Federal Water Pollution Control Administration and Northeastern University.

Key Words: Colloid flotation, adsorbing colloid flotation, small particle ion-exchange resin, coagulation, kaolin, montmorillonite, waste water treatment, ion removal, manganese dioxide.

Contents

Section		Page
I	Conclusions	1
II	Recommendations	2
III	Introduction	3
IV	Studies in the Flotation of Colloidal Particulates: Effects of Aggregation in the Flotation Process	4
V	The Coagulation of Finely-divided Ion Exchange Resins and the Use of the Coagulated Material for Rapid Ion Removal	17
VI	Adsorbing Colloid Flotation of Chromium Ions using Hydrous, Colloidal Manganese Dioxide	26
VII	Acknowledgements	40
VIII	References	41
IX	Tables	45
X	Figures	47

SECTION I

CONCLUSIONS

1. Colloid flotation can be successfully employed in the removal of clays (kaolin and montmorillonite) from waste water streams.

2. There is a close interrelationship between gas bubble diameter and the size of the particle being removed. Gas bubbles of 1-2 mm require fully dispersed colloidal materials, whereas fine bubbles of 0.2 mm required coagulated sols for best removal.

3. An understanding of the mechanism of flotation removal can be obtained through measurement of the zeta potentials of the colloidal particles.

4. Rapid and total ion removal is potentially possible with the use of coagulated mixed ion exchange resins. One way in which this might be accomplished is in a fluidized bed.

5. 10 ppm Cr^{+3} can be rapidly removed from aqueous media by adsorption on hydrous manganese dioxide and the subsequent flotation of the colloid. The manganese dioxide can be generated in situ by the standard oxygenation reaction.

SECTION II

RECOMMENDATIONS

1. A detailed feasibility study of the flotation of colloid clay materials should be undertaken. The use of gas dissolution to form a fine dispersion of bubble to effect flotation should be examined. The results of this work should then be compared with the costs of conventional methods of water clarification, such as coagulation/settling.

2. A continuous coagulated mixed resin fluidized bed column should be built in order to investigate ion removal by this method. Emphasis should be placed on total ion removal rather than a particular species.

3. A large scale study, including economic analysis, should be undertaken to investigate adsorbing colloid flotation via the use of hydrous manganese dioxide. This study should include other cations, besides Cr^{+3}, which are found in waste streams.

SECTION III

INTRODUCTION

The clean-up of waste waters in municipal water supplies is ultimately a separation problem involving the removal of pollutants. Thus there is continual interest in finding new separation methods for potential use in this application. A separation process must be (1) inexpensive, (2) rapid, (3) amenable to large scale operation, and (4) must not contaminate the water with new impurities.

In this project we have explored the applicability of three separation processes to water pollution control (a) colloid flotation for removal of clay materials, (b) coagulated ion exchange resin for removal of electrolyte and (c) adsorbing colloid flotation for removal of electrolyte again. The report will detail each of these studies separately. Some of the important factors controlling separation for each method will be described and potential applications to waste water treatment field will be in part presented and in part suggested.

SECTION IV

STUDIES IN THE FLOTATION OF COLLOIDAL PARTICULATES: EFFECTS OF AGGREGATION IN THE FLOTATION PROCESS

Barry L. Karger and Douglas G. DeVivo

A. INTRODUCTION

Separation processes utilizing selective adsorption at gas-liquid interfaces from bubbles generated in aqueous media have found a number of applications over the past few years. These processes, which have the generic name of adsorptive bubble separation processes, have recently been reviewed and their applications discussed in two articles (1,2). A nomenclature scheme for these methods was published in 1967 (3). Foam separation is a category of the nomenclature scheme pertaining to separations utilizing a foam. Foam separation methods can be subdivided into foam fractionation and flotation, the former dealing with the removal of soluble species and the latter dealing with the removal of particulate species. Foam fractionation has been used to separate radioactive metal ions (4), nonbiodegradable detergents (5), and many other soluble ionic species. Ore flotation, a subdivision of flotation, has been used for many years in the dressing of metallic ores. In this application we are concerned with heterogeneous systems containing macrosized solids of a crystalline nature (6,7).

Although a great deal has been published on ore flotation, very few studies have been concerned with the flotation of colloidal-size particulates (colloid flotation). Clanton et al. (8,9) reported qualitative studies on several sols, while Jaycock and Ottewill (10,11) were among the first workers to present an extensive investigation of the flotation of a colloidal system. These latter authors studied the effect of adsorption of cationic surfactants and electrokinetic properties on the extent of flotation of silver iodide. Workers in the Soviet Union have applied flotation to the removal of colloidal metal oxides from aqueous sols. Colloids have been separated both in the pure form (12, 13) and with adsorbed and occluded isotopes and impurity elements (14-17). A 99.4% removal of ^{134}Cs, present in microquantities, was accomplished by sorption on $K_2Cu_3[Fe(CN)_6]_2$ followed by flotation of the ferrocyanide using gelatin as a foaming agent (14). Skrylev and Nokrushin (18) fitted a first-order rate equation to the removal of colloidal ferric hydroxide, manganese dioxide, and mixed ferrocyanide particulates using gelatin as the surface-active agent.

Grieves and co-workers have successfully applied flotation to several colloidal systems and suspended solids including ferric and stannic oxides (19,20), kaolin clay (21), and active carbon (22). In each of the above

studies an oppositely charged surfactant was used to effect flotation of the colloid or suspended solids. The species to be separated was thus concentrated via a mobile foam generated in the bulk by sparging with air. The studies dealt with the effects of feed colloid concentration, gas rate, and pH. Grieves and co-workers have also reported a study of the rate of removal of positively and negatively charged colloidal ferric oxide from aqueous suspensions (23). The rate of removal of the colloid was correlated with the quantities of surfactant and particulates in the residual suspension. Negatively charged particulates were removed at a rate directly proportional to the surfactant to particulate concentration ratio in the residual suspension and a power function greater than one of the residual concentration of particulates. In contrast to negatively charged ferric oxide, the rate of removal of positively charged ferric oxide was dependent upon an exponential function of the initial surfactant concentration.

The success of these studies in the application of flotation to the removal of colloidal particulates made it seem worthy to examine the flotation of kaolin and montmorillonite in more detail. The purpose of this paper, thus, is to study the effect of a variety of parameters on the rate of flotation of the clays, with special emphasis on the role of zeta potential on this rate. It can be noted that these two species of clays contribute to the turbidity of water in many areas of the world and thus are a major problem in water treatment. The application of flotation to the clarification of water containing colloidal kaolin or montmorillonite appears feasible and advantageous in specialized application such as military field use or in specialized industrial separation problems. Specialized instances are emphasized because of the economic restrictions on the flotation process owing to the surfactant requirement.

B. EXPERIMENTAL

1. Apparatus. A schematic diagram of the first flotation apparatus is given in Fig. 1. Nitrogen gas was passed through, in series, two gas saturator bottles filled with deionized water; a glass-wool water droplet trap; a constant differential flow controller; and a calibrated rotameter. The gas was sparged through a 50-60-μ pore-size glass frit located at the base of the column and the foam produced travelled up the column. A side exit arm on the column was located 19 cm above the initial sol level and led into a heat exchanger where the foam was collapsed and drained into a large beaker.

The second flotation cell used was a modification of one first described by Sebba (24) and is shown in Fig. 2. The cell was constructed

of Pyrex and had the following characteristics: 9 cm diameter, 2 liter capacity, 7 cm diameter sintered glass frit of 5-10 μ porosity. Samples were withdrawn by inserting a pipet into the cell through the top opening.

2. Procedure. A stock sol was prepared by dispersing 0.40 g of either kaolin or montmorillonite in 500 ml of deionized water with a Waring blender for 2 min. The sol was then allowed to stand for about 1 hr to settle out large particles, and the decanted portion was diluted to the desired concentration with deionized water. In all but a few experiments, the concentration of solids in the total initial bulk sol was 100 mg/l. At the start of each experiment, the gas flow rate through the column of the apparatus in Fig. 1 was adjusted to approximately 2000 ml/min and 3600 ml of the required sol was added to the column through an opening in the top. The gas flow was then readjusted to 2000±50 ml/min and the surfactant was added to the column by gas injection of 400 ml of the required surfactant solution. This method proved superior to the previously tried method of premixing the surfactant and the sol before pouring into the column. Mixing of the surfactant and sol was extremely rapid because of turbulence caused by rising gas bubbles. Longer premixing times had no effect on the results obtained and nonequilibrium effects between particulates and surfactant did not appear important in our system. The time $\theta = 0$ was taken when the surfactant was injected into the column. Samples of the bulk sol were then drawn at 2 min intervals and analyzed first for suspended solids and then for zeta potential and surfactant concentration.

The procedure followed in the experiments with the flotation cell (Fig. 2) was the same as with the column apparatus above except that 1400 ml of the required sol was used and the surfactant solution (200 ml) was mixed directly with the sol to give a final volume of 1600 ml. The flow rate was maintained at 170 ml/min and samples were withdrawn with a pipet and analyzed in a similar manner to samples from the column apparatus.

3. Analyses. The initial and residual concentrations of suspended solids were determined with a Hach model 2100 laboratory turbidimeter using appropriate calibration plots. The response of the turbidimeter was linear with respect to concentration of suspended solids and corresponded to 125 Jackson turbidity units (JTU) for 100 mg/l kaolin and 36 JTU for 100 mg/l montmorillonite. The presence of surfactant did not affect the turbidity readings. Precision of these measurements was ± 2%. Total surfactant concentration (free plus adsorbed) was determined by filtering a 10 ml aliquot of the residual bulk through a 0.45μ Millipore filter; washing the retained solids with 25 ml of deionized water; and then determining the quantity of surfactant in the filtrate by a two-phase titration with tetraphenylboron (25). This procedure was accurate to ± 0.6 mg/l. Tests with known amounts of

surfactants showed that essentially all of the adsorbed surfactant was removed by the washing step. Zeta potential measurements were made on a Zeta-Meter (Zeta-Meter, Inc., New York, N.Y.). Measurements had a precision of ± 3mV.

4. Chemicals. The montmorillonite clay used was clay mineral standard no. 23 of the American Petroleum Institute. The sample was purchased from Ward's Natural Science Establishment, Inc., Rochester, New York. The sample was ground on an electric mortar and pestle for several hours to a mesh size greater than 200. It should be noted that the sieving step is only to remove coarse particles. Those particles passing through the screen were further disintegrated by a Waring blender. The kaolin used was a natural, air-separated, untreated clay of relatively uniform stability characteristics and size. The clay was used as received from Fisher Scientific Company. Ethylhexadecyldimethylammonium bromide (EHDA-Br) was technical grade (Eastman Chemical) and was used without further purification. Tetraphenyl-boron sodium (Aldrich Chemical Co., puriss. grade) and bromophenol blue (Fisher Scientific Co., certified reagent) were used as received from the suppliers.

C. THEORY

The removal of colloidal particulates from aqueous sols by foaming is possible because of the electrical charges on the surface of the particulates and the large surface-to-volume ratio. These two properties promote the adsorption of an oppositely charged surfactant, rendering the colloidal species surface-active. Passing gas through a porous frit into the bulk medium generates a large interfacial area on which the surface-active particulates can adsorb and subsequently be removed from the bulk.

The mechanism of interaction on ionic surfactants with colloidal particulates in the flotation process has been studied by Taggart et al. (26) and Jaycock and Ottewill (10). The former authors pointed out that froth flotation of minerals with ionic surfactants involves the attachment of the polar group of the surfactant molecule to the mineral surface; thus, flotation behavior depends on the orientation of the surfactant molecule with respect to the mineral surface after attachment. Jaycock and Ottewill examined the interaction of ionic surfactants with colloidal silver iodide. The authors observed that although silver iodide particulates initially had a negative electrophoretic mobility, the mobility decreased to zero and then increased to a high positive value as the concentration of cationic surfactant was increased. The same effect has been observed in this study for kaolin in the presence of EHDA-Br. Figure 3 shows a plot of zeta potential vs. EHDA-Br concentration. Initially, the particulates have a zeta potential of -25mV.

As the concentration of EHDA-Br is increased, the zeta potential decreases to 0 and then increases to approximately +37 mV.

Jaycock and Ottewill have presented a model to explain the charge reversal phenomenon. When the hydrophobic colloid was contacted with an oppositely charged surfactant, the polar groups were attracted to the charged surfaces of the particulates owing to electrostatic forces. A monolayer was built up as the surfactant concentration was increased. This electrostatically attracted monolayer neutralized the original surface charge and caused the zeta potential to drop to zero. Following the completion of the monolayer, a second layer of surfactant molecules was formed by van der Waals' forces of attraction between the hydrocarbon chains of the surfactant molecules (10). During the formation of this second layer, the charge increased from zero to a positive value. At the completion of the second layer, the charge was opposite to the original charge and likewise, the zeta potential sign was the reverse of the original.

The magnitude of the resultant opposite charge on the colloidal particulates is dependent not only upon the type of concentration of the surfactant present, but also upon the type and concentration of electrolytes and the amount of particulates present in a given mass of sol (27). These same factors which affect the magnitude of the charge of the surfactant-particulate species are also of prime importance in the flotation process (21,23,28). The intimate relationship between the magnitude of the charge of particulates in a sol and the degree of aggregation is well known (29). Aggregation of colloidal particulates increases as the charge and therefore the electrostatic repulsion between particulates is decreased. Since aggregation increases the particle size in the sol, it is not surprising that the flotation process is affected by this factor and is thus dependent upon those parameters which affect the degree of aggregation in a sol. Consequently, the magnitude of the charge of the particulate-surfactant species should be relatable to flotation behavior. The zeta potential or electrophoretic mobility is intimately related to the surface charge and can be used as a convenient quantification of the surface charge (27). Consequently, zeta potential is a measure of the stability of the sol toward formation of aggregates (coagulation) and may thus be used to evaluate the effect of aggregation on the flotation process.

In this work, clay particulates adsorb cationic surfactant and have their charge reversed from negative to positive. The magnitude of this positive charge affects the degree of aggregation and flotation. The zeta potential of the charge-reversed sol can be lowered by decreasing the amount of surfactant present or by adding electrolytes, such as sodium sulfate. The lowering of the zeta potential of this sol increases the degree of aggregation present in the sol. This behavior has been observed in our laboratory for kaolin and montmorillonite sols containing

EHDA-Br. In addition to electrical effects, the rate of aggregation and therefore the size of the aggregates present in a sol at a specific time after sparging at a constant rate is dependent upon the quantity of particulates present according to the Smoluchowski coagulation law (30).

In assessing the effect of aggregation upon the flotation of colloidal particulates using oppositely charged surfactants, it is of value to discuss the empirical results in terms of a mathematical model or rate equation. This allows a quantitative evaluation in addition to a qualitative discussion of the results. A quantitative empirical evaluation of the relation of aggregation, through zeta potential measurements, and particulate quantity to the flotation process can be made by fitting kinetic data for the flotation of a hydrophobic colloid, such as a clay, with an oppositely charged surfactant to a mathematical model or rate equation. This approach allows the assessment of the relative significance of the parameters chosen for investigation and their relationship to the flotation process.

It was decided to examine the correlation of the zeta potential of the surfactant-particulate species and the quantity of particulates present with the flotation rate of kaolin and montmorillonite particulates using EHDA-Br. While any industrial scale flotation unit would be operated in a continuous mode, a batch process can be used in the laboratory to evaluate various parameters affecting the flotation rates. The results obtained can then be used to design or to optimize a continuous system. The batch operations used in this work were described in the experimental section.

The rate of removal of particulates from the bulk sol can be expressed as:

$$\frac{d(Z_F V_F)}{d\theta} = \frac{-d(Z_R V_R)}{d\theta}$$

where $Z_F V_F$ = quantity of particulates in the foam (mg), $Z_R V_R$ = quantity of particulates in the residual sol (mg), θ = time of sparging (min). Thus, $d(Z_F V_F)/d\theta = -d(Z_R V_R)/d\theta$ = instantaneous rate at time θ (mg/min) for a variable volume, batch process (23).

The fit of experimental rates, obtained from smoothed curves through the original data, to a rate equation of the form:

$$\frac{-d(Z_R V_R)}{d\theta} = k \left(\frac{Z_R V_R}{Z_i V_i}\right)^{\alpha} \left(\frac{ZP_\theta}{ZP_i}\right)^{\beta} \qquad (1)$$

[where k = rate constant (mg/min), Z_iV_i = initial amount of particulates present, ZP_0 = zeta potential of surfactant-particulate species at time 0 (mV), ZP_i = initial zeta potential of surfactant-particulate species (mV), and α and β = constants] can be accomplished by a least squares analysis using a digital computer. It may be noted that the use of ratios on the RHS of the rate expression eliminates a major problem in the determination of zeta potential, arising from the indirect calculation of zeta potential from the electrophoretic mobility using the Helmholtz-Smoluchowski equation (27). The equation is only approximate and was derived from a rather simple physical model, which is seldom realized in experimental systems. By using a relative parameter such as ZP_0/ZP_i, the above errors are minimized. It should be noted that it is only necessary to divide the zeta potential by a factor of 13 to convert to electrophoretic mobility, and thus zeta potential and electrophoretic mobility are interchangeable in Eq. (1) .

Grieves and Bhattacharyya have used an approach similar to that reported in this paper to study the flotation of positively and negatively charged surfactants (23). The rate equations developed by these authors were functions of the initial and residual quantities of surfactant and particulates.

D. RESULTS AND DISCUSSION

Data obtained for the batch flotation of kaolin and montmorillonite clays with EHDA-Br were used to evaluate several solution parameters affecting the colloid flotation process. The results for typical batch flotations of kaolin and montmorillonite in the apparatus shown in Fig. 1, utilizing bubbles of approximately 1 - 2 mm diameter, are shown in Fig. 4. The results are expressed in terms of total residual amount of particulates as a function of sparge time. Rates of removal for kaolin and montmorillonite approach zero after 10 - 14 min of sparging at 2000 ml/min for kaolin and 14 - 16 min of sparging at 1000 ml/min for montmorillonite. During these time periods, approximately 95% of the kaolin particulates and 94% of the montmorillonite particulates were removed when EHDA-Br was used as the surfactant.

Several experiments were performed to evaluate the relation between flotation rate and two parameters; the zeta potential of the surfactant-particulate species and the quantity of particulates remaining in the residual sol at any time, θ, for both kaolin and montmorillonite. The experiments involved varying the initial zeta potential of the surfactant-particulate species in the bulk sol from +37 to 0 mV in the kaolin study and from +17 to 0 mV in the montmorillonite. The zeta potentials of the surfactant-particulate species for 100 mg/l particulates and 37.8 mg/l EHDA-Br were +37 and +17 mV for kaolin and montmorillonite, respectively. The variation of the initial zeta potentials through the above ranges was

achieved by adding different amounts of sodium sulfate to the bulk sol except for the zero value of zeta potential (fully coagulated). Coagulation was achieved by addition of a small amount of the surfactant which corresponded to the quantity required to produce the zero electric point and then allowing coagulation to take place before adding the balance of the surfactant to give a total of 37.8 mg/l. It should be noted that the total amount of surfactant used in all the experiments (37.8 mg/l) was chosen on the basis of the quantity needed to produce a suitable foam in terms of stability and reproducibility of measurements. A typical plot of zeta potential vs concentration of sodium sulfate for kaolin-EHDA-Br is shown in Fig. 5. During the flotation experiments, the amount of particulates and surfactant present and the zeta potential were determined simultaneously at periodic time intervals.

The initial zeta potential, and therefore the extent of aggregation in the sol, affected the flotation rate and maximum removal of both kaolin and montmorillonite. Figures 6 and 7 show the effect of initial zeta potential, ZP_i, on the percent removal of kaolin and montmorillonite as a function of sparge time, θ. For a given set of conditions, the percent removal of both kaolin and montmorillonite for each value of θ decreased as ZP_i was decreased. The poorest flotation in our system was observed when the initial sol was coagulated ($ZP_i = 0$).

The trends shown in Figs. 6 and 7 indicate that the flotation of clay particulates using the system of Fig. 1 is adversely affected by aggregation of the particulates. As discussed in the theory section, the degree of aggregation existing in a sol, for example a kaolin or montmorillonite sol, is dependent on the magnitude of the surface charge on the particulates. Thus, the flotation trends observed reveal an inverse relationship between the flotation and the size of the particulate species. This argument is strengthened by the fact that montmorillonite particulates are floated much faster than are the kaolin particulates, montmorillonite particulates being much smaller than kaolin particulates according to turbidimetric measurements.

A discrepancy exists between the results in Fig. 6 and 7 and those of other investigators who have studied the affects of aggregation on the flotation of certain colloidal bacterial organisms. Rubin and Lackey (31) found that aggregation of Bacillus cereus with alum considerably improved tne flotation of the organisms. In their experiments, Rubin and Lackey used a flotation cell which utilized much smaller and much slower sparge rates to affect the flotation of the organisms. We decided to examine the effect of aggregation on the flotation of kaolin and montmorillonite using a cell similar to that employed by Rubin and Lackey, as seen in Fig. 2. The results for the colloid flotation of the two clay species using the above cell are shown in Fig. 8. An examination of the flotation data in Fig. 8 shows that the coagulated form of both clays floats considerably better than does the dispersed form. This

behavior is contrary to the trend observed for the same species when the larger column apparatus was used with its concomitant larger bubbles, much higher flow rates, and larger convection currents.

The explanation of the disparity between the flotation behavior observed in the two different systems appears to involve bubble size and the transport of the particle attached to the bubble across the interface between the bulk liquid and the foam. The large column unit employs a 50-60 μ porosity frit to generate bubbles while the small cell utilizes a fine porosity, 5-10 μ frit. On the basis of Spargo's work on bubble diameters (32), it is reasonable to assume that a difference of an order of magnitude exists between the average bubble diameters in the two apparatuses. This is indeed supported by observations of a qualitative nature. Bubble size should affect the buoyancy imparted to the surfactant-particulate species by attachment to the bubble at the gas-liquid interface. In the 50-60 μ frit system, the bubbles are approximately the same size or larger than the aggregates in the sol (i.e., 1-2 mm). The large size of the bubbles makes the attachment of more than one bubble to a single aggregate unlikely, while the attachment of several aggregates to a single bubble is probable. Buoyancy of the aggregates is therefore poor and the flotation of large aggregates proceeds at a slower rate than dispersed particulates. In the case of the fine-fritted cell with bubbles of average diameter of approximately 0.2 mm or less (32), the possibility of multiple bubble attachment to single aggregates is reasonable. The larger the aggregates, the larger the number of bubbles which can become attached to the aggregates, with improved buoyancy. Flotation is therefore enhanced by aggregation in the small bubble system contrary to the behavior in the large bubble system.

The above behavior implies many advantages of a small bubble system employing low flow rates over a large bubble, high flow rate system for the removal of colloidal particulates. Not only does the small bubble system require less sparge gas, but the amount of surfactant actually needed to effect a good removal should be considerably less. The surfactant concentration need only be that which causes coagulation of the particulates. In the large bubble system, enough surfactant must be used to effect charge reversal and thus keep the particulates in a fairly dispersed state.

In addition, the stability of the foam is somewhat dependent on the bubble size (33). The dependency is indirect and therefore foams formed from fairly large bubbles are unstable unless enough surfactant is present to stabilize the foam. The results of a study in the large bubble cell using the 50-60 μ frit of residual particulate concentration vs the initial ratio of surfactant to particulate ratio (X_i/Z_i) are shown in Fig. 9. Examination of the data

reveals that optimum removal of particulates occurred at X_i/Z_i equal to 0.76. It is to be noted that this value is higher than the minimum quantity of surfactant needed (Fig. 3) to obtain the maximum charge reversal. Based on studies by Rubin and Lackey (31), the surfactant requirements for a small bubble system are much less than the amount needed in the large bubble system described in this paper. In addition, frothers can be used to lower the amount of surfactant needed in the small bubble system (31). The amount of surfactant needed to effect good flotation is extremely important since it is the limiting factor in the economic evaluation of flotation for commercial application. While the capital expenditure for flotation equipment is low, the cost of surfactant is high compared to the cost of reagents used in conventional processes.

A least squares analysis of the batch flotation data obtained with the large bubble system shown in Fig. 1 for the flotation experiments involving the effect of zeta potential was performed on a CDC-3300 computer using a Fortran program written for this application. A copy of the program is available from the authors upon request. For kaolin floated with EHDA-Br, a total of 22 data points was used to obtain the following equation for the best fit of the data:

$$\frac{-d(Z_R V_R)}{d\theta} = 78 \left(\frac{Z_R V_R}{Z_i V_i}\right)^{0.15} \left(\frac{ZP_\theta}{ZP_i}\right)^{1.4} \qquad (2)$$

The values of θ included in this equation were 10 min and less; at longer times, $-d(Z_R V_R)d\theta$ was very close to zero. The average of the percentage deviations calculated with Eq. (2) from the experimental values for 20 out of 22 data points (two points were disregarded owing to disproportionately high error) was approximately 10%. An identical treatment was applied to data for the batch flotation of montmorillonite. The best fit for 24 data points is shown in Eq. (3):

$$\frac{-d(Z_R V_R)}{d\theta} = 42 \left(\frac{Z_R V_R}{Z_i V_i}\right)^{0.34} \left(\frac{ZP_\theta}{ZP_i}\right)^{0.97} \qquad (3)$$

The values of θ used to get Eq. (3) were 14 min and less. Equation (3) showed an average percentage deviation of approximately 11 %. The fits between experimental data and Eqs. (2) and (3) are shown in Figs. 10 and 11, respectively. Comparison of experimental and calculated rates was chosen as an evaluation of Eqs. (2) and (3) in preference to using the integrated form of the equations. This method of comparison obviated long graphical integrations and proved satisfactory for our purpose.

Equations (2) and (3) show the dependency of the flotation rate of kaolin and montmorillonite on the amount of particulates present and on the zeta potential ratio of the surfactant-particulate species. Mathematical relationships such as the above equations are useful in analyzing a specific flotation process. The results can be used to help in the optimization process or in the design of a continuous process from batch process data. There are several weaknesses, as well as the above advantages. For instance, an examination of Eqs. (2) and (3) shows that the degrees of significance of the two terms on the RHS of the two equations differ considerably. In Eq. (2) the significance ratio (β/α) is almost ten, while in Eq. (3) the ratio is less than three. While the differences in the chemical properties of kaolin and montmorillonite, such as exchange capacity and wettability, could account for the disparity, it is also likely that other variables or factors in the flotation system, in addition to particulate concentration and charge effects, must be considered. With the exception of the initial values of variables chosen, none of the solution variables available for consideration in the flotation process are independent of one another. Once the flotation process has begun, variables such as electrokinetic potentials, surfactant concentration, and particulate concentration all become interrelated in a very complicated manner. This is especially true for the electrokinetic properties. In our work, we found that ZP_0/ZP_i at a particular θ value depended not only on ZP_i as expected, but was obviously affected in an irregular way by some other parameters in the flotation process. The reproducibility of the ZP_0/ZP_i measurements was good (~10%), though, for all but the lowest ZP_0 values where the precision decreased considerably owing to experimental difficulties in measuring very low mobilities. Another problem is the variation, though small, of the average bubble diameter during the foaming process. This variation results from changes in the surfactant concentration during the foaming period. The fact that the zeta potential term on the RHS of Eqs. (2) and (3) is more significant than the particulate amount term is in agreement with the hypothesis that aggregation plays a very important role in the flotation of colloidal particulates. As mentioned earlier, aggregation effects should be reflected in the zeta potential term.

The quantitative approach using kinetic models could not be made when the fine frit apparatus was used because the kinetics of the removal process were too fast. In addition, any equations obtained would have been useless owing to their inapplicability at the optimum removal conditions when the zeta potential was equal to zero (fully aggregated).

Flotation Interference by Inorganic Cations. Experiments reported in this section were conducted to establish the influence of several inorganic cations, commonly found in natural waters, on the flotation of colloidal kaolin in the large bubble apparatus shown in Fig. 1. The

cations chosen were Na^+, Ca^{2+}, and Fe^{3+} added as NaCl, $CaCl_2$, and $FeCl_3$, respectively. Turbidimetric measurements were unsatisfactory for analyses of suspended solids in sols containing Fe^{3+}. Samples containing ferric ion were thus assayed gravimetrically. Figure 12 shows the data for experiments in which the concentrations of the above ions were varied prior to addition of the surfactant. The results are expressed in terms of percent removal after 6 min of sparging as a function of initial cation concentration. The presence of mono- and divalent cations in the bulk sol created no difficulties at concentrations below approximately 10^{-2} and 10^{-3} M, respectively. A pronounced interference was provided by trivalent iron at initial concentrations greater than 10^{-5} M. An examination of Fig.12 shows that the interference of these ions is not wholly an aggregation effect. If interference was due only to aggregation effects, the percent removal after 6 min of sparging should not have differed greatly from 50%, which was the value obtained for the removal of fully aggregated kaolin particulates in the large bubble apparatus after 6 min of sparging. The decrease in removal up to the 50% value (shown as a dotted line on Fig. 12) appeared to be due to increasing aggregation while the decrease beyond 50% suggests a different mode of interference. A plausible explanation of this behavior is based on the interference of the ions with the adsorption of the cationic surfactant by the negatively charged particulates. Reduction of the negative charge on the particulates by electrostatic interactions not only promotes aggregation, but above certain concentrations of ions the surfactant adsorption step becomes more difficult and, therefore, the flotation process is less efficient. The concentrations at which this secondary interference occurs depends on the charge on the cation and are indicated by arrows in Fig. 12.

Effect of pH on Flotation of Kaolin. The effect of pH on the flotation of kaolin was studied in the large bubble apparatus and the results are shown in Table 1 for the residual concentration of particulates, Z_R, as a function of initial pH. Results are shown for Z_R after 6 and 8 min of sparging had elapsed. The pH values are for the initial bulk sol. A statistical examination of the data showed that for 95% confidence limits, pH variation from 2.6 to 11.2 produced no interference in the flotation of kaolin. Any pH value outside this range would be of no interest and the extremes of the pH range were thus eliminated from consideration. The initial concentrations of particulates and EHDA-Br were 100 and 37.8 mg/l, respectively. The results obtained are in agreement with those found by Grieves for the flotation of a sol containing illite clay, Fuller's earth, and natural dirt and sand (34). Since pH has little or no effect on the flotation of clay particulates, an extra degree of freedom is allowed in the flotation process. This is especially desirable in water treatment where one wishes to avoid the addition of any unnecessary reagents.

E. CONCLUSION

An experimental investigation has been carried out on the flotation of colloidal kaolin and montmorillonite with ethylhexadecyldimethylammonium bromide. Zeta potential measurements of the surfactant-particulate species have proved useful in assessing the effect of aggregation on the flotation of clays.

The optimum flotation in a system employing bubbles of 1-2 mm average diameter is obtained for the dispersed particulates as opposed to the aggregated ones. A comparison study has been made between the system employing 1-2 mm bubbles and a system using bubbles of average diameter of approximately 0.2 mm to effect the flotation of the two clay species. This study indicated that bubble size plays an important role in the flotation process. In the two systems compared, the affect of coagulation on flotation was directly opposite..

The superior flotation of coagulated clay sols in the fine bubbles (0.2 mm) system has important economic implications. A much smaller quantity of surfactant is required in this system owing to the increased stability of a fine structured foam and lack of the need for charge reversal, which is required in the large bubble (1-2 mm) system. Only a surfactant concentration at or below that needed to achieve the zero electric point must be considered. Inexpensive reagents, such as alum, may be used to promote coagulation, thus aiding flotation in the fine bubble system (31). The proper combination of coagulant and surfactant would minimize the surfactant needed and, therefore, keep the operating cost of a commercial flotation process competitive with other methods of water clarification. While a detailed economic study has not been made of such a flotation process, the cost might be minimized to allow flotation to compete successfully with conventional clarification methods.

In addition, it should be pointed out that while flotation systems utilizing large bubbles of the order of 1-2 mm do not appear to operate as efficiently as a fine bubble system, such systems may find use in specific situations in which the colloids present cannot be coagulated by alum or polyelectrolytes. An example of such a situation is the clarification of waters in asphalted catchment basins used in the arid southwestern United States. These waters contain colloids which are so highly peptized that they cannot be coagulated. While large-scale electrophoresis has been proposed for clarification of these waters (35), flotation should be tried. Such an application could be optimized using a quantitative approach such as discussed in this paper. Optimization of a large bubble system can be achieved by maintaining the colloid in the dispersed form. This can be done by adding sufficient surfactant to effect charge reversal or, perhaps by use of dispersants such as polyphosphates.

SECTION V

THE COAGULATION OF FINELY-DIVIDED ION EXCHANGE RESINS AND THE USE OF THE COAGULATED MATERIAL FOR RAPID ION REMOVAL

B.L. Karger and T.A. Pinfold

A. INTRODUCTION

Ions may be removed from large volumes of dilute aqueous solutions by adsorption on ion exchange resins. The solutions are passed through columns packed with resin beads of about 0.5 mm diameter, and exchange of the counter-ions of the resin occurs with ions of the same sign from the solution. The rate of this exchange is inversely proportional to the square of the radius of the resin particles (36), and hence the finer the state of subdivision of the beads, the more rapid the ion removal. There is a practical limit, however, to continued subdivision in that as the particle sizes approach the colloidal range, suspensions are formed. Such particles can no longer be used in columns because the fines are washed out while the larger particles, which are still relatively small, settle and then necessitate the use of high pressures to force the liquid past them. Such suspensions, however, are admirably suited for the rapid removal of ions from large volumes because besides being able to adsorb ions rapidly, they can be dispersed throughout the bulk in short time with efficient stirring. The advantage in time, however, is dissipated unless a comparably rapid method can be found for subsequently removing the suspension. As filtration of large volumes is too slow, another means was sought for removing the dispersed resins.

Hydrophobic colloids are stabilized by the charges that exist on the surfaces of their particles. It is well known that one hydrophobic colloid can be coagulated by the addition of another of opposite charge since the repulsions between particles of one species are reduced by intervention of oppositely-charged particles of the other. As the resin particles used were not greatly in excess of colloidal dimensions, it was decided to attempt the coagulation of an anion exchange resin (positively-charged) with solids that were negatively-charged. It was found that glass, silica, carbon, and kaolin were suitable. Of markedly greater efficiency were montmorillonite or a cation exchange resin, and the addition of an optimum amount of these led to rapid and complete removal of the suspended particles. The purpose of the present investigation, then, is to examine the above phenomena more closely, both from the standpoint of mutual coagulation of suspensions as well as the rapid removal of ions from aqueous systems.

B. EXPERIMENTAL

1 Materials. The anion exchange resins used were Amberlite IRA 400, IRA 401 (both Mallinckrodt Chemical Company) and IRA 904 (Rohm and Haas), all of the $RN(CH_3)_3^+Cl^-$ form. They differ in nominal divinylbenzene (DVB) content being 8, 4, and 16%, respectively. Amberlite IRA 400 and IRA 401 are gelular-type resins whereas Amberlite IRA 904 is a macroreticular resin. The gelular-type loses its pore structure on dehydration while the latter does not. It is relevant to the present discussion that macroreticular resins reduce to samples of uniform particle distribution on grinding because their beads are made up of a number of much smaller beads of uniform size and the grinding process merely breaks down the larger particles into their smaller constituents (37).

The cation exchange resins used were Amberlite IR 120 (Mallinckrodt Chemical Company), Dowex-50W-X8 (Dow Chemical Company) and AG50W-X16 (BioRad Laboratories) all of the $RSO_3^-H^+$ type and nominally of 8,8, and 16% DVB content, respectively. An aqueous suspension of Amberlite XE 254 ultrafine resin (Rohm and Haas) of the $RSO_3^-Na^+$ form was also used; the amount of solid material in the suspension was 23% w/w and the average particle size, as declared by the manufacturers, was 1 μ.

The solid resins, as well as soda glass, silica, charcoal, montmorillonite, and kaolin, were ground and separated into fractions using U.S. Standard sieves of 60, 200, and 400 mesh. Examination of the -400 mesh fraction under a microscope showed the resin samples to be made up of an appreciable range of particle sizes (except IRA 904, which has been discussed), while the other solids were relatively uniform. The montmorillonite, kaolin, and silica were finely divided in relation to the resins, while the charcoal and glass particles were, relatively, of medium and large sizes, respectively. The montmorillonite (coaguloid) was supplied by the Baroid Division, National Lead Company, Texas; the soda glass was obtained by crushing clean watch glasses; and the silica, charcoal, and kaolin were from reliable laboratory stocks.

2. Procedure. The experimental procedure for the study of the coagulation of suspensions involved the dispersion of a weighed amount of resin in a 1-liter measuring cylinder containing 1 liter of water, using a magnetic stirrer. A known mass of coagulant was wetted with a small amount of water, introduced into the cylinder, and stirred for 5 min; thereafter 5 ml samples were withdrawn at known time intervals from approximately 5 cm below the surface of the solution. The extent of coagulation was estimated in terms of the turbidity of these samples. As a measure of turbidity, the optical densities of the samples were determined in 1 cm cells in a Beckman DU 2 spectrophotometer at an arbitrary wavelength of 500 nm.

3. Analysis. The phosphorus contents of the solutions were determined colorimetrically using ammonium molybdate (38). To 5.00 ml of sample were added 2 ml of 2.5 M sulfuric acid, 2 ml of 2.5% ammonium molybdate, and 1 ml of reducing solution (made by dissolving 0.5 g of 1-amino-2-naphthol-4-sulfonic acid in 185 ml of 15% sodium bisulfite and 5% sodium sulfite). The solution was then made up to 25.00 ml with water, allowed to stand for 10 min, and examined spectrophotometrically in 1 cm cells at a wavelength of 660 nm.

The calcium contents of the solutions were determined (39) colorimetrically using ammonium purpurate (murexide). A solution of this dye was made by dissolving 40 mg. of ammonium purpurate in 75 ml of water and making up to 250 ml. A volume of 10.00 ml of unknown solution was diluted to 80 ml, the pH adjusted to 11.3 with 0.4% sodium hydroxide solution, 10.00 ml of murexide solution added, and the whole made up to 100 ml in a standard flask. The optical density was then determined without delay in 1 cm cells at 506 nm against a blank sample formed from the same reagents.

The zeta-potentials of the particles in a sample were determined by measuring their electrophoretic mobility using a zeta-meter (Zeta-Meter Inc.).

B. RESULTS AND DISCUSSION

Coagulation. The manner in which suspended particles of one charge could be coagulated by others of opposite charge was examined first. Figure 13, in which the optical density of the solution is plotted against time, illustrates the mutual coagulation of IRA 401 resin and glass (both -400 mesh). Curve A shows the decrease in turbidity as the resin particles settled out in the absence of glass, a slow process which even after 24 hr could not reduce the optical densities to values below 0.38. The addition of finely-divided glass, as shown by Curves B and C, caused a lowering of the repulsions of the positively-charged resin particles by intervention of the glass particles between them. In this way coagulation was enhanced and the optical densities decreased.

It became clear early in the investigation that the state of subdivision of the coagulant was of importance. In Fig. 14, Curve D shows the rate of settling of 0.50 g of IRA 401 resin (-400 mesh) alone with time, while Curves A, B, and C reflect the coagulating ability of samples of glass of the same mass but of different particle size. The best coagulation was achieved among the measurements made when the particles of glass were smallest, but it is not known how effective glass of a finer state of subdivision would have been because a sieve of smaller mesh was not available.

As explained in the Introduction, it was found that the most efficient coagulations occurred when one suspension of a resin was added to another. The spectacular way in which this happened is shown in Fig. 15. The curve between Points A and B reflects the gradual settling of 0.50 g of IR 120 (-400 mesh). At B, 0.50 g of IRA 401 (-400 mesh) was added and the mixture stirred vigorously for 30 sec. Within a minute, both solids had settled out almost completely.

It was found that when one suspension of resin was added to another of opposite charge there was an optimum ratio of masses of the two resins for best coagulation. If too little of the added resin was present, the solution was turbid due to incomplete coagulation. If more of the second resin was added than was required for complete coagulation, the turbidity increased. A minimum in the relationship between turbidity and mass of added resin, as found in Fig. 16, was therefore to be expected. From Curve 1 of this figure, for example, it is clear that the addition of about 0.4 g of IR 120 (-400 mesh) is the most satisfactory for removal of 0.50 g of IRA 401. With less than this amount, coagulation was incomplete, as shown by the positive zeta-potentials of the suspended particles, whereas an excess resulted in turbid suspensions of IR 120, the particles having negative zeta-potentials. In this experiment the oppositely-charged suspensions were mixed by stirring together for 5 min and were allowed to settle for 2 min before the turbidities were recorded. (The coagulated material settled within the 2 min period and a sharp decrease in turbidity was found; it was this value that was recorded, as it reflected the extent of coagulation. Thereafter the usual slow decrease in turbidity occurred, comparable to that shown in Fig. 13, Curve A; no cognizance was taken of this decrease as it was merely a measure of the settling out with time of the uncoagulated resin.)

The importance of particle size of the coagulant is emphasized by Fig. 16, Curve 2, for which the IR 120 resin was in the -200/400 mesh range. Four times as much of this coarser fraction was required for the same extent of coagulation within the 2-min period as for the -400 mesh particles. A more finely-divided sample of IR 120 was not available but a comparison can be made with XE 254 ultrafine resin when used as coagulant. The latter is similar to IR 120 in that both are of the RSO_3^- type although they differ in being of the Na^+ and H^+ forms, respectively. The optimum amount of XE 254 required to coagulate 0.50 g of IRA 401 was 0.20 g as opposed to 0.40 g for IR 120, and the resulting solutions were completely clear. The finer state of subdivision is probably responsible for these results.

The information embodied in Fig. 16 for a resin coagulant can be used to anticipate the probable effect on turbidity of adding greater quantities of glass as coagulant than were used in Figs. 13 and 14. Had the variation of turbidity with time been plotted in Fig. 13 for larger

masses of glass, for example, the curves would most likely have been above that for the 6.0 g because, with all the resin coagulated, the increased turbidity would have arisen from excess glass. Turning to Fig. 14, it is shown that, for a fixed mass of coagulant, a decrease in particle size led to lower turbidities, but a study of Fig. 16 indicates that this will only necessarily be true if the fixed mass of coagulant is less than the optimum amount for maximum coagulation for any of the particle size fractions used. For example, in Fig. 16 the turbidity at A for the coarse fraction is greater than that at B for the fine fraction because the mass of resin used was below the optimum amounts of both fractions needed for maximum coagulation. If, however, the fixed amount of resin used had been between the two optimum values, it is possible that a more turbid solution would have resulted with the fine resin (Point C) than with the coarse one (Point D). As the quantity of glass used for Fig. 14 was 3.0 g, which is below the optimum coagulating mass for each of the three fractions considered, the turbidities necessarily decreased with increasing state of subdivision. Figure 16, however, may be used to anticipate that this need not always be the case when masses of glass other than 3.0 g are added to 0.50 g of Amberlite IRA 401.

The importance of particle size on coagulation was again evident when using IRA 400 resin. Two (-400 mesh) samples which had been differently ground showed markedly different particle sizes and size distributions when examined under a microscope. In consequence the masses of IRA 120 resin (-400 mesh) required to coagulate 0.50 g of each sample were about 0.2 and 0.4 g, respectively. Further, 0.50 g of IRA 904 resin required 1.0 g of IR 120 (both -400 mesh) for complete removal. This appreciably greater quantity of IR 120 was due to the finely-divided nature of the macroreticular resin. It is in keeping with the conclusion, which appears to be true as a first approximation, that in the complete coagulation of two oppositely-charged resins, less is required of the one that is more finely divided.

"Finally, it is worth noting two results that are to be expected from the experiments described above. Addition of one resin to a suspension of another of the same charge led to increased turbidity in the solution and no coagulation. Second, the ratio of the masses of oppositely-charged resins required for coagulation remained the same irrespective of which was suspended and which was used as coagulant. Reversal of the roles, therefore, led to no unexpected behavior.

The relative abilities of negatively-charged solids for coagulating 0.50 g of IRA 401 (-400 mesh) are shown in Table 2. The values, based on an arbitrary scale of 400 for the best coagulant, were determined by comparing the mass of each solid required for complete coagulation after stirring together for 5 min and allowing 2 min for settling. Some variation in the relative coagulating power is to be expected, depending on

how finely the solids have been ground. Thus, although all were -400 mesh, continued grinding would lead to smaller average particle sizes and enhanced coagulating power, as was shown for IRA 400 resin. How much influence efficiency of grinding will have on coagulating power will depend on the hardness of the solid, but it is not anticipated that the relative coagulating power would change by more than a factor of 2. The exchange capacities, densities, and zeta-potentials of the solids have been included for comparison. The same sample of IRA 401 was used for all the coagulants.

It is clear from Table 2 that the wide variation in the efficiencies of the coagulants is not matched by similar changes in zeta-potential, exchange capacity, or density. Coagulant particles must have charged surfaces and appreciable zeta-potentials; however, in Table 2 the best coagulants do not necessarily have the highest potentials. It is clear that, in general, there must be a relationship between zeta-potential and the extent of coagulation, but in the system under investigation other factors must also play important roles. As also seen in Table 2, exchange capacity is not related to coagulation. Exchange capacity, of course, is dependent not only on surface charges, but also on charges existing within a particle. Since it is surface charges which keep particles from coagulating, it is not surprising that exchange capacity bears no relationship to coagulation. Note that of the solids listed in Table 2, exchange occurs entirely on the surface for glass, silica, and kaolin; for charcoal and montmorillonite exchange occurs both on and in the solid; whereas for the resins it occurs overwhelmingly in the pores.

It might have been expected that the densities in Table 2 would be significant in that substances with values close to that of the resin would tend to settle at the same slow rate and thus remain in intimate contact with resin particles more readily. The chances of coagulation would then be greater. The particles, however, are small and the electrical effects of their surface charges are of much greater consequence than those caused by gravity.

A clearly dominant factor in coagulating ability is that of particle size, the one bearing an inverse relationship to the other. This result is not surprising as the greater the number of particles for a given mass of coagulating material, the more efficiently they can be packed around a suspended particle, thus reducing its zeta-potential and rendering it more susceptible to coagulation. This cannot, however, be the only effect, as a great difference exists in the coagulating power of montmorillonite and kaolin, although their particle sizes were approximately the same. Further, the silica sample used was more finely divided than those of the resins, although it coagulating power was insignificant in comparison. Had some solids been less easily wetted than others, agglomeration to larger particles may have occurred

before coagulation was possible; the increase in particle size of the coagulant would then ostensibly have led to lower efficiencies. The poor coagulants in Table 2, however, are all easily wetted provided their surfaces have not been contaminated. To examine the possibility of such contamination for the case of glass, the powdered sample which had been used was washed repeatedly with ethanol and then tested once again. No change in its coagulating ability was found.

It is tentatively suggested that coagulating power is related to the ability of the solid particles to swell and hence to have sufficient deformability for efficient packing. Total rigid particles of glass, silica, charcoal, and kaolin may pack around a particle of opposite charge but will do so in a way not conducive to the addition of further layers of alternately charged particles. Strains will develop in these agglomerates which will prevent their growth, thereby reducing the efficiency of the process. This explanation would account for the marked difference in efficiency between montmorillonite which swells and kaolin which does not. It would also account for the marked efficacy of resins. It is clear that more work will be necessary before a complete understanding of the factors involved in the mutual coagulation of two solids can be attained.

Ion Removal. Because of the rapidity with which finely-divided resins adsorb ions and are coagulated, the overall process of ion removal and subsequent resin coagulation was investigated. First it was shown that 2.5 g of underground -20/50 mesh IRA 401 resin required 50 min to adsorb 96% of the phosphorus from 1 liter of a 3×10^{-4} M solution of sodium phosphate. (This was done by stirring the resin for the requisite time, allowing it to settle for 2 min, and then withdrawing a 5-ml sample of liquid in the usual way. It was unnecessary to add oppositely-charged resin in this case since the particles settle rapidly on their own and no coagulation is needed.) It was then required to compare this rate of removal to that achieved by a finely-ground resin. In this context, it was necessary to recognize that the resin dried during grinding because the water adsorbed in the pores was released. An adjustment therefore had to be made for this loss of water so that the total exchange capacities of the two samples would be the same. As the unground resin contained 60% of water, 1.0 g of -400 mesh IRA 401 should have the same exchange capacity as 2.5 g of unground resin. A mass of 1.0 g of -400 mesh resin was stirred with 1 liter of a 3×10^{-4} M solution of sodium phosphate and then coagulated by adding an optimum amount of XE 254 ultrafine resin and stirring for 5 min. By performing this experiment a number of times, and on each occasion decreasing the period for which the resin was stirred with the solution prior to coagulation, it was shown that the finely-ground resin required only 0.5 min for 96% removal of phosphate, a rate which was 100 times faster than when using unground resin. If allowance is made for the 5 min required for coagulation of the fine resin, the overall process is about 10 times faster than when using unground resin.

An even more rapid removal can be achieved by the use of a coagulated cationic-anionic mixed resin. This mixture was prepared by coagulating 1.0 g of IRA 401 (-400 mesh) with 0.40 g XE 254 ultrafine resin in pure water. The resulting resins, although coagulated, retain a fine state of subdivision and the concomitant ability to adsorb ions rapidly. The mixed resin was added to 1 liter of the phosphate solution, stirred for 1.5 min, and a sample taken 0.5 min later. As shown in Fig. 17, Curve A, removal of 96% of the phosphate was achieved; recoveries were not as good if the period of stirring was less than 1.5 min. (The sample taken above was withdrawn before the resin had settled completely, which usually took 2 min. This was done because after 0.5 min a sufficient volume at the top of the solution was completely clear of resin.) The optical densities of such samples and of the final solutions were all zero. Curve C in Fig. 17 is for 2.5 g of unground IRA 401 resin as described previously, while Curve B is for 2.0 g of (-40/60 mesh) IRA 401 resin. This latter fraction is the finest to which the resin can be ground and yet retain the ability to settle out rapidly and completely when stirring is discontinued. The mass of 2.0 g used was once again an attempt to maintain comparable exchange capacities, heed being taken of the moisture content of the samples.

Care should be exercised in the choice of the coagulating resin in that if it is in the hydrogen form, exchange with the Na^+ ions in solution leads to a decrease in pH with subsequent hydrolysis of the PO_4^{-3} ion to uncharged H_3PO_4 molecules which are not adsorbed. When, for example, IR 120 resin in the acid form was used as coagulant, recovery of phosphorous was only 50% and the pH of the final solution was 3.4 . Using XE 254 resin, however, which is in the sodium form, resulted in 96% removal and a final pH value of 7.3 .

If the same quantity of the finely-divided mixed resin described above was stirred with 1 liter of a 2.5×10^{-4} M calcium chloride solution, over 90% of the calcium present was adsorbed within 3 min.

Fluidized Bed Operation. In order for this method of ion removal to be applicable to large scale processes it is necessary that the coagulated, mixed resin be used in a continuous process. We decided to do a preliminary investigation of the use of this material in a fluidized bed for the removal of phosphate.

The apparatus was a simple 3 liter cell, 1 meter high by 2 cm wide. A coarse porous glass frit was attached at the bottom of the cell to be certain that the resin was not lost from the cell. In addition, it was found that a medium porous glass frit was necessary at the top of the cell. The coagulated resin consisted of IRA 401 (400 mesh) and Rohm and Haas' XE-254. It was suspended in distilled water in the cell and the flow of the synthetic water was begun from the bottom of the cell. For the high flow rates in this study it was

necessary to pump the water into the cell. Samples of 1 liter volume were collected out of the top of the cell and analyzed. As previously, we used phosphate as the test electrolyte ($1.5 \times 10^{-3}\mu$).

Figure 18 shows a plot of phosphate concentration in the effluent vs. volume of effluent collected as a function of the amount of anion exchange resin used. As expected, the larger amount of resin results in better removal of phosphate. For 1 gm, the phosphate in the effluent reaches the initial concentration after 5 liters, whereas with the 5 gm sample, it takes over 10 liters to reach the initial concentration. Figure 19 shows the influence of feed flow rate on removal of phosphate. We find that the phosphate is more effectively removed at the high feed rate. This may be due to the resin being better suspended in the cell at the higher flow rate. For both flow rates the turbidity of the water collected was measured and found to be negligible.

These preliminary, and admittedly crude measurements do illustrate that coagulated ion exchange resins could be used to remove ions from aqueous media in a continuous fashion. Note that both cations and anions could be removed at the same time. From these initial results, the process deserves future study.

SECTION VI

ADSORBING COLLOID FLOTATION OF CHROMIUM IONS USING HYDROUS, COLLOIDAL MANGANESE DIOXIDE

Barry L. Karger and Douglas G. DeVivo

A. INTRODUCTION

At present, most methods for disposal of liquid waste containing dissolved species, such as heavy metal cations, fit into two general categories. The waste is either concentrated and contained, or it is diluted and dispersed (40). The first method has been applied to those wastes containing either radioactive species which have levels of activity too great to be released to the environment or, to those containing valuable materials in sufficient quantity to justify reclamation. The current concern over water pollution will most likely lead to the lowering of the minimum allowable concentrations of soluble species which can be discharged to the environment. This will necessitate the development of new separation methods for the removal of a wide variety of materials from aqueous media which are currently being discharged to the environment without regard for the long term ecological effects which are threatening our existence on earth.

One group of species which is of importance relative to water pollution is that consisting of metals such as chromium, copper, zinc, etc. These metals are either extremely toxic in the free ionic state or enter into reactions to form toxic entities. An example of the latter is the oxidation of trivalent chromium to chromate ion, which is toxic to all life forms. The standard methods of removal of these metals is by precipitation of the metal hydroxide or by passage through an ion exchange column. Both these methods have limitations. The hydroxide precipitation is difficult because these metal hydroxides are gelatinous in nature and thus settle poorly. The waste is usually passed through a sand or other filter to remove the unsettled hydroxide precipitate, which often leads to clogging of the filter bed. Ion exchange methods are expensive to use and the throughput rate is often quite low.

New complications in industrial waste treatment have been introduced by the growing number of sources of low-level radioactive waste. Examples of such sources are power reactor installations, reactor fuel preparation facilities, and medical and educational installations. Recognizing the problem of low-level radioactive wastes, many users of radioactivity on a large scale have installed treatment plants which lower the amount of radioactive species released to the environment. Many of these treatment plants employ chemical precipitation methods similar to water treatment procedures and are generally based

upon empirical techniques. Owing to the cumulative damaging effects of such highly active radioisotopes as Cs^{137} and Sr^{90}, it is desirable to remove all of the isotope from the liquid waste before discharging the waste to the environment. Manganese dioxide has been used for radiochemical separations both in the laboratory and in chemical processing plants. The colloidal oxide with its adsorbed radioisotope is usually coagulated and allowed to settle out in large settling tanks over a period of several hours (41).

It appears that adsorbing colloid flotation might offer an alternative method to settling for the removal of small quantities of valuable or toxic cations.

B. HISTORICAL SURVEY

1. Methods for Producing Hydrous Manganese Dioxide. In this section we will be concerned with the various methods of producing hydrous manganese dioxide. This is important to the application of the oxide to water treatment since the generation method, if the colloid is produced in situ, must satisfy several factors including low residual manganese ion concentration, ease of generation, and economic considerations. It will be shown later on that generation in situ is an easy and efficient way of producing a dispersed hydrous manganese dioxide sol.

Hydrous manganese dioxide can be formed by a variety of reactions, of which the earliest was proposed by Guyard and is known as the Guyard reaction (42). This reaction involves both the oxidation and the reduction of manganese in aqueous solution:

$$3\,Mn^{+2} + 2MnO_4^- + 2H_2O \rightarrow 5MnO_2 + 4H^+$$

Laitinen has pointed out that the rate of reaction increases with increasing pH. In neutral solution the reaction takes place almost simultaneously (43). Humphrey and Eikleberry found that the stoichiometry must be determined empirically because the theoretical amount of $KMnO_4$ is never required (44).

A second method for forming manganese dioxide is used in water treatment for the removal of manganous ions and involves the oxidation of manganous ion by oxygen in alkaline solution. A pH of 9.5 to 10.0 is required to effect rapid oxidation to the tetravalent state (44). This method of forming manganese dioxide in water treatment has been described in detail by Humphrey and Eikleberry (44) and Nordell (45), who pointed out that theoretically one part per million of dissolved oxygen would oxidize seven parts per million of divalent manganese. Nordell proposed the following two-step reaction: (45)

$$Mn^{+2} + 2\,OH^- \rightarrow Mn(OH)_2$$

$$2Mn(OH)_2 + O_2 \rightarrow 2MnO_2 + 2H_2O$$

Morgan and Stumm found that this oxidation reaction was non-stoichiometric (46). It should be noted that the kinetics of the above reaction are determined by the rate at which oxygen can diffuse into the reaction solution. For convenience, the above reaction will be referred to as the "oxygenation reaction."

A third method for forming manganese dioxide involves the reduction of potassium permanganate by hydrogen peroxide. This reaction has been described by Mellor (47):

$$2KMnO_4 + H_2O_2 \rightarrow 2MnO_2 + 2KOH + 2O_2$$

The reaction proceeds as written only in alkaline solution; in acid solution the MnO_4^- is reduced to the divalent manganous ion. Hence, hydrogen peroxide is often used to dissolve manganese dioxide in acid media. The above reaction is difficult to control, and the use of hydrogen peroxide in industrial or municipal water treatment would be too costly. Thus, this method of preparing manganese dioxide is not of great value relative to the work in this report.

2. Adsorption of Inorganic Ions from Solution by Manganese Dioxide. The early work on the adsorption of inorganic ions from solution by manganese dioxide was done by Indian investigators (48-53). Chatterji published the major initial work, which has retained its validity over the years (49). He noted that the adsorption of inorganic ions by MnO_2 was very rapid and that cations were more strongly adsorbed than anions. This latter point was explained by Ganguly and Dhar who found that the colloidal MnO_2 was negatively charged (51). Dhar and coworkers were able to show that hydrous MnO_2 adsorbed hydroxyl ions very strongly in preference to other anions (50), while Ghosh showed that the negative charge on the MnO_2 could be increased by increasing the concentration of the hydroxyl ion (53).

A long series of papers on MnO_2 adsorption studies was published by Geloso and Levy (54-60). Geloso also noticed that the formation reactions for MnO_2 were non-stoichiometric (54). He found that Ni^{+2} and Cu^{+2} ions could be adsorbed, as well as Fe^{+2} (55), and proposed an adsorption equation similar to Freundlich's formula (55-57). A summary of the work on adsorption of inorganic ions by MnO_2 performed by Geloso and Levy was published in 1931 (60).

Morgan and Stumm published a detailed study of the adsorption of

Mn^{+2} by colloidal MnO_2, which was formed by the oxygenation reaction (46). They found that Mn^{+2} was adsorbed with a concomitant release of H^+ ions. The uptake of Mn^{+2} and release of H^+ occurred rather rapidly, with 5 minutes or less required for 50% exchange. At pH 7.5, the exchange capacity of the oxide for Mn^{+2} was 0.5 moles of Mn^{+2} per mole of MnO_2, while at pH 9 the capacity was ca. 2 moles of Mn^{+2} per mole of MnO_2.

It should be noted that the large cation sorption capacities observed for hydrous MnO_2 are in accord with the high specific surface areas exhibited by the oxide when prepared in situ. Buser and Graf found surface areas of ca. 300 meters^2 per gram for δ-MnO_2 (61), which, as mentioned earlier, is one of the forms of MnO_2 produced by the Guyard reaction.

Morgan and Stumm have also made an interesting observation relative to the adsorption by hydrous MnO_2 of metal ions which tend to form hydroxo complexes (46). They found that the MnO_2 dispersions showed a higher adsorption for Mn^{+2} and Zn^{+2} than for Mg^{+2} and Ca^{+2}. This results from the fact that the coordination requirements of the metal ions which form hydroxo complexes are satisfied by incorporation into the hydrous oxide-hydroxide solid structure. This behavior is important relative to the adsorption of Cr^{+3} reported in this report and will be discussed again later. The role of hydroxyl ions in the MnO_2 particle will be discussed in detail in the Theory section.

3. Adsorbing Colloid Flotation. At present, few reports of the investigation of adsorbing colloid flotation have appeared in the literature. Skrylev and Pushkarev reported the use of adsorbing colloid flotation, although they did not use this terminology, to separate microquantities of Cs^{134} from aqueous media (62,63). Their experiments showed that cesium could be essentially removed completely from a solution in which the Cs^{134} was present as a microcomponent by using mixed ferrocyanides of copper, zinc, manganese, nickel, and cobalt as sorbents and gelatin as the foaming agent (62). The above authors used approximately 100 mg/l of colloidal phase of the composition $K_2Fe(Fe(CN)_6)$ and $KFe(Fe(CN)_6)$. The cesium removal was observed to fall off when considerable quantities (in excess of 10 g/l) of several sodium salts were introduced into the system, owing to the competition between the Na^+ and Cs^+ ions for the adsorptive sites on the ferrocyanide particle surfaces. The removal of Cs^{134} dropped to 18.3% when 1 g/l of ferric sulfate was present, owing to the preferential adsorption of Fe^{+3} because of its higher positive charge. The process used by Skrylev and Pushkarev required 20 to 30 minutes of foaming to remove 97.0 to 99.0% (63).

Grieves and Crandall used adsorbing colloid flotation fortuitously when they added bentonite to alleviate the interference of

trivalent iron in the flotation of a mixture of dirt and sand, Fuller's earth, and illite clay (64). The interfering ions were adsorbed by the bentonite and removed during the flotation of the bentonite. However, no investigation of the adsorbing colloid flotation process was performed.

C. THEORY

1. Potential Determining Ions. The origin of the surface charge on the MnO_2 particle is different from that of a clay particle, which was discussed in Section IV. The surface charge on the MnO_2 particle is a result of the adsorption of so-called "potential-determining" ions at the surface of the particle (65,66). These ions are adsorbed onto the surface of the colloidal MnO_2 particle because of active centers on the imperfect crystals (66). In the case of colloidal MnO_2, the potential determining ions are almost entirely OH^- ions (46), and, therefore, for most conditions the MnO_2 particles appear negatively charged. Except for the origin of the surface charge, the remainder of the theory concerned with the electrical double layer, etc., for colloidal MnO_2 particles is identical with that discussed in Section IV, which should be consulted for further information.

2. Adsorption of Ions by Hydrous Manganese Dioxide. The adsorption of inorganic ions on MnO_2 may be interpreted as surface complex formation or as an ion exchange process. The first mode of adsorption occurs with metal ions that have a tendency to form hydroxo complexes, because incorporation into a hydrous oxide-hydroxide solid structure satisfies the coordination requirements of the metal ions (46). Those metal ions which are strongly hydrolyzable are adsorbed to a greater extent. For example, Morgan and Stumm found that MnO_2 dispersions showed a higher adsorption capacity for Mn^{+2} and Zn^{+2} than for Mg^{+2} and Ca^{+2}. Results for the adsorption of Cr^{+3} by MnO_2, which are reported in this work, are in qualitative agreement with the findings of Morgan and Stumm and will be discussed in detail in the Results and Discussion section.

For non-hydrolyzable ions, an ion exchange process occurs during adsorption. The ion exchanged for a typically adsorbed cation is the H^+ ion, with one H^+ exchanged for each charge on the cation. This ion exchange process also occurs for hydrolyzable cations. For instance, the removal of Mn (II) from solutions in contact with colloidal MnO_2 dispersions at pH values up to about 8 has been interpreted as resulting primarily from ion exchange between Mn (II) and H^+ (46).

The H^+ ion is displaced from the Stern layer and from the adjacent portion of the diffuse outer layer. Since the adsorption process is

dependent principally upon the electrical double layer of the colloidal MnO_2 particle, it would appear that there should be an interrelationship between the adsorption and the electrokinetic properties of the particle. This important aspect will be discussed in more detail, relative to some correlations between electrophoretic mobility and adsorption found in this report, in the Results and Discussion section.

D. EXPERIMENTAL

1. Apparatus. The apparatus used in the flotation experiments on the colloidal MnO_2 was the small bubble system described in Section IV.

Electrophoretic mobility measurements were made with the Zeta-Meter. A Perkin-Elmer, model 303, atomic absorption spectrometer fitted with the appropriate spectral lamps was used in the analyses for Cr and MnO_2 (as Mn). Two burettes (Kimax; no. 8593) were used to dispense the reagents for the Guyard and oxygenation reactions. Mixing and flocculation of the MnO_2 was accomplished with the use of a laboratory multiple mixer having 6 stainless steel stirring paddles (Phipps-Bird, Inc., Richmond, Va.). The Millipore filter apparatus described in Section IV was used in the analyses. A Beckman DU-2 was used in the spectrophotometric analysis of MnO_4^- at a wavelength of 525 nm.

2. Chemicals. The manganese sulfate was reagent grade (Fisher Scientific) and was used in solution, concentration: 5 mg $MnSO_4$ per ml, prepared gravimetrically. The potassium permanganate was reagent grade (Fisher Scientific) and was used to prepare a solution having a concentration of 10.52 mg/ml (0.3330 N), standardized with sodium oxalate (certified reagent; Fisher Scientific). The sodium hydroxide used was reagent grade (Fisher Scientific) in solution having a concentration of 0.0984 N, standardized with potassium acid phthalate (certified reagent; Fisher Scientific). Ethylhexadecyldimethylammonium bromide was technical grade (Eastman Chemical) and was used without further purification. Deionized water was used to prepare all the aqueous solutions and MnO_2 sols.

3. Optimum Conditions for Forming Colloidal MnO_2 in Aqueous Media. For the sake of convenience, a concentration of 100 mg/l MnO_2 was chosen as the basis for the experimental calculations.

Guyard Reaction: For this reaction, experiments were performed to determine the amount of $KMnO_4$ needed to react with the theoretical amount of Mn^{+2} required to give 100 mg/l MnO_2. Theoretically, 73.2 mg/l $KMnO_4$ are required to completely react with 104.2 mg/l $MnSO_4$ to give 100 mg/l MnO_2. Five samples, each containing 104.2 mg $MnSO_4$

were placed in 1 liter beakers. Different amounts corresponding to 50%, 70%, 80%, 90%, and 100% of the theoretical amount (73.2 mg) of $KMnO_4$ were added to each beaker while mixing vigorously with a magnetic stirrer. Burettes were used to dispense the required volumes of standard $MnSO_4$ and $KMnO_4$ solutions. After mixing for about 2 minutes, 10 ml of 1 mg/ml alum ($Al_2(SO_4)_3.18H_2O$) solution were added and the samples were transferred to the Phipps-Bird mixer and mixed at 40 r.p.m. for about 30 minutes. The alum caused the MnO_2 to coagulate. The samples were then filtered through 0.45μ Millipore filters. A 100 ml aliquot of the filtrate was then taken and analyzed spectrophotometrically for MnO_4^- and total Mn content according to the persulfate method given in Standard Methods.

The effect of alum on the analysis for MnO_4^- was studied by measuring the optical density before and after the addition of 10 mg/l alum to each of eight 100 ml samples containing different concentrations of MnO_4^-. However, it was later found that alum was not needed since the MnO_2 sols were unstable enough to flocculate by mixing only.

Oxygenation Reaction: Experiments were performed to determine the amount of NaOH needed for the complete oxidation of 173.7 mg/l $MnSO_4$, which was the theoretical amount of $MnSO_4$ needed to give 100 mg/l MnO_2. To a series of samples containing 173.7 mg/l $MnSO_4$, NaOH solution was added in varying amounts in each sample while the mixture was mixed with a magnetic stirrer. After mixing for about 3 minutes, a small amount of alum was added and the sols were mixed at 40 r.p.m. on the Phipps-Bird mixer until fully flocculated (about 30 minutes). Aliquots were then filtered through a Millipore filter and the filtrate was analyzed spectrophotometrically for total Mn content.

4. Electrophoretic Mobility Measurements. The procedure followed in measuring the electrophoretic mobility of the colloidal MnO_2 was identical with the procedure followed in Section IV with the exception that particle migration times were converted to electrophoretic mobility (μ/sec./volt/cm) instead of zeta potential. Calibration plots based on voltage used, average tracking time, and cell dimensions were furnished with the Zeta-Meter for determination of the electrophoretic mobility.

The manganese dioxide to be measured was formed by either the Guyard reaction or the oxygenation reaction. For each reaction, the optimum formation conditions, as determined empirically, were used. These conditions corresponded to 70% theoretical amount of $KMnO_4$ in the Guyard reaction and 100% theoretical amount of NaOH in the oxygenation reaction. The preparation procedure for the Guyard reaction involved reacting 10.24 mg of $KMnO_4$ with 20.84 mg $MnSO_4$ in

200 ml of solution to give approximately 88 mg/l MnO_2. For the oxygenation reaction, 18.4 mg NaOH was reacted with 34.74 mg $MnSO_4$ in 200 ml of solution to give 100 mg/l MnO_2.

The pH was adjusted immediately after the MnO_2 was formed in the rapid mixing step by inserting the pH electrodes into the sol with the magnetic stirrer still in place and then adding appropriate amounts of H_2SO_4 or NaOH from plastic squeeze bottles. After adjustment of the pH, a portion of the sol ($\simeq$ 28 ml) was placed in the plastic electrophoresis cell and an average of 20 particles was tracked in each experiment according to the procedure given in Section IV of this report.

5. Cr^{+3} Adsorption Measurements. The adsorption of Cr^{+3} by the hydrous, colloidal manganese dioxide was studied for MnO_2 formed by the oxygenation reaction. In these experiments, the MnO_2 was generated in the presence of varying amounts of Cr^{+3} (added as $CrCl_3$). A volume of 200 ml was used in each of the experiments which corresponded to 18.4 mg NaOH reacting with 34.74 mg $MnSO_4$ for the oxygenation reaction. The respective amounts of reagents were added as standard solutions. The pH was adjusted as described in the previous section under Electrophoretic Mobility Measurements. The residual concentration of Cr was determined by flocculating the MnO_2 on the Phipps-Bird mixer for 30 minutes, filtering a 100 ml aliquot through a 0.45μ Millipore filter, and then analyzing on the Perkin-Elmer atomic absorption spectrometer. The concentration of the sample was then found by comparing the absorption peak on the recorder with the peaks of chromium standards.

It was observed that no coagulant was needed since MnO_2 produced by either reaction flocculated within a reasonable time on the Phipps-Bird mixer owing to the instability of the MnO_2 sol.

6. Flotation Experiments. Two series of flotation experiments were performed. The first was to determine the flotation of colloidal MnO_2 as a function of sparge time using EHDA-Br as the surfactant. In the second series, the MnO_2 was formed in the presence of Cr^{+3} and then the EHDA-Br was added followed by flotation of the MnO_2. In both series, 1 liter of the MnO_2 sol was used.

In the first series of experiments to determine the flotation of MnO_2 with sparge time, the sol containing the EHDA-Br was poured into the flotation apparatus and the sparge rate was adjusted to 170 ml/min. In some of the experiments, 2 ml of ethanol were added as a frother. Frothers will be mentioned in the Results and Discussion section. Samples were then withdrawn by inserting a pipette through the open top of the flotation cell. A 50 ml aliquot of the residual sol was taken and analyzed for MnO_2 by the following procedure. The sample was acidified by adding a little H_2SO_4 and then

dissolved by adding 5 ml of 30% H_2O_2. The volume was made up to 100 ml in a volumetric flask and the contents analyzed for Mn by atomic absorption. The Mn concentration was converted to MnO_2 concentration by multiplying by a constant.

In the adsorbing colloid flotation experiments, the residual sol was analyzed for Cr with an atomic absorption spectrometer. All these experiments involved MnO_2 produced by the oxygenation reaction and a pH of 11.6.

7. Interference of Ca^{+2}. The procedure followed in this series of experiments was identical to that described under Cr^{+3} Adsorption Measurements except that varying amounts of Ca^{+2} (as $CaCl_2$) were added to the solution prior to the formation of the MnO_2 in the presence of Cr^{+3}. As in the above experiments, MnO_2 produced by the oxygenation reaction was used and the pH was adjusted to 11.6 .

E. RESULTS AND DISCUSSION

1. Stoichiometry of Reactions for Forming Manganese Dioxide. As mentioned earlier, the stoichiometry of both the Guyard and the oxygenation reactions must be determined empirically. Studies were made of the residual concentration of manganese left in solution as a function of the percent theoretical amounts of $KMnO_4$ added in the Guyard reaction and of NaOH added in the oxygenation reaction. The minimum allowable concentration set by the U.S. Public Health Service is 0.05 mg/l.

Guyard Reaction: The residual concentration of manganese left in solution was studied as a function of the percent theoretical amount (73.2 mg/l) of $KMnO_4$ added to 104.2 mg/l $MnSO_4$. These are the theoretical amounts to produce 100 mg/l MnO_2 according to the reaction:

$$2KMnO_4 + 3MnSO_4 + 2H_2O \rightarrow 5MnO_2 + K_2SO_4 + 2H_2SO_4$$

The results, shown in Figure 20, reveal that the residual quantity of Mn^{+2} is approximately zero at 75 to 100% stoichiometry. However, 70% stoichiometry proved to be the overall optimum value since at higher percentages of $KMnO_4$, visually objectionable quantities of MnO_4^- were present. At the 70% level, however, the residual Mn^{+2} concentration is about 0.2 mg/l, which exceeds the minimum allowable concentration of 0.05 mg/l.

Oxygenation Reaction: The results of the stoichiometric study of the oxygenation reaction are shown in Figure 21. The results are expressed in terms of residual manganese concentration as a function

of the theoretical amount (92.0 mg/1) of NaOH needed to react with 173.7 mg/1 $MnSO_4$. These are the theoretical amounts required to produce 100 mg/1 MnO_2 according to the reaction:

$$MnSO_4 + 2NaOH \rightarrow Mn(OH)_2 + Na_2SO_4$$

$$2Mn(OH)_2 + O_2 \rightarrow 2MnO_2 + 2H_2O$$

It can be seen that the residual manganese concentration was zero when 100% of the theoretical amount (92.0 mg/1) of NaOH was reacted with the 173.7 mg/1 $MnSO_4$. About three minutes were required to complete the formation of the MnO_2 when the solution was rapidly mixed with a magnetic stirrer. As mentioned earlier, the oxygenation reaction rate is limited by the rate of diffusion of air (O_2) into the aqueous solution.

2.Electrophoretic Mobility of Manganese Dioxide. As discussed in the Theory section, the properties of the electrical double layer surrounding a manganese dioxide particle are very sensitive to changes in pH since hydroxyl ions form the potential determining layer. Figure 22-24 show the results of a study of electrophoretic mobility (μ/sec./v/cm) vs. pH for the Guyard reaction and for two permutations of adding the reagents in the oxygenation reaction. For both reactions, the electrophoretic mobility becomes more negative as the hydroxyl concentration is increased over the major part of the pH range. For the manganese dioxide produced by the Guyard reaction, saturation of the potential determining layer by OH^- occurs at about pH 7. After this pH value, the mobility approaches zero owing to charge neutralization by the increasing cation concentration. At about pH 8.3, the mobility begins to increase negatively again owing to the oxidation of the residual Mn^{+2} ions by O_2. This reaction is the oxygenation reaction, which occurs in alkaline solution and forms more MnO_2, which subsequently adsorbs OH^-. Hence, the mobility increases negatively until saturation of the potential determining layer occurs once again.

For the oxygenation reaction, the electrophoretic mobility also increases negatively as the pH is raised, thus indicating an increase of the negative charge on the MnO_2 particles as the hydroxyl ion concentration is raised. The mobility increases until the potential determining layer becomes saturated and then decreases owing to the neutralization of the particle charges by the sodium cations in solution. When the NaOH was added to the $MnSO_4$ solution, higher mobilities were observed for the manganese dioxide particles overall than when the $MnSO_4$ was added to the NaOH. The former order of addition was used in the remainder of the studies for producing oxygenation reaction MnO_2.

The above results indicate that hydroxyl ions are preferentially adsorbed and form the potential determining layer of the colloidal manganese dioxide particulates formed in both the Guyard and the oxygenation reactions. Although previous papers in the literature have dealt with the preferential adsorption of hydroxyl ions by MnO_2 (46), none of these earlier works employed electrokinetic measurements to study the adsorption of hydroxyl ions in the potential determining layer of the MnO_2 particles.

3. Adsorption of Cr^{+3} by Manganese Dioxide as a Function of pH. In an earlier section, it was shown that when the Guyard reaction was used to generate MnO_2, the residual Mn^{+2} concentration exceeded the limit of 0.05 mg/l set by the U.S. Public Health Service. However, the oxygenation reaction results in no residual Mn^{+2} concentration. Thus, it was decided to use the oxygenation reaction to generate in situ the MnO_2 for the remainder of the studies.

In this section, the adsorption of Cr^{+3} ions by oxygenation reaction MnO_2 is described as a function of pH and electrophoretic mobility. The results of this study, expressed in terms of percent removal of chromium from solution versus pH and versus electrophoretic mobility (μ/sec./v/cm), are shown in Figures 25-26. When $CrCl_3$ was added to give an initial concentration of 5 ppm Cr^{+3}, and 100 mg/l of MnO_2 were used as generated in situ by the oxygenation reaction, complete removal of the chromium ions was achieved for pH 2.5 to 6.7 and for pH greater than 10.7. In the lower pH range, the high removal of Cr^{+3} is not expected if the adsorption occurs by ion exchange, which predicts cation adsorption to be directly related to the negative charge and, thus, to the electrophoretic mobility of the MnO_2 particles. In the pH region of 2.5 to 6.7, the range in electrophoretic mobility was -0.75 to -1.5 (μ/sec./v/cm), which indicated a low negative charge. However, as mentioned in the Theory section, strongly hydrolyzable metal ions are probably adsorbed by incorporation into a hydrous oxide-hydroxide solid structure, which satisfies the coordination requirements of the metal ions (46). This appears to be the case for the adsorption of chromium ions, which have a strong tendency to form hydroxo complexes (47, 67). Actually, this adsorption mechanism should predominate throughout the pH range and thus, adsorption due to ion exchange would be minor even at the higher pH values. As the MnO_2 is generated in situ, the Cr^{+3} ions form hydroxo complexes at the surface of the particles as rapidly as the particles are formed. An ion exchange process should predominate for non-hydrolyzable cations such as cesium ions.

The decrease in adsorption between pH 6.7 and pH 10.7, which is shown in Figure 25, is not understood. Based on the data obtained

in these studies, an explanation of this anomalous decrease would not be possible without a high degree of speculation. It should be noted, however, that the decrease shown on Figure 25 is not due to experimental error.

4. Adsorption of Cr^{+3} by Manganese Dioxide as a Function of the Initial Concentration of Cr^{+3}. In this section, the results of a study of the adsorption of Cr^{+3} by oxygenation reaction MnO_2 as a function of initial Cr^{+3} concentration will be discussed. The results for a series of experiments in which 100 mg/l MnO_2 was generated in the presence of varying concentrations of Cr^{+3} are shown in Figure 27. In each experiment, the pH was adjusted to 11.6 immediately after the MnO_2 was fully generated. This pH value was used since it was close to the natural pH of the system ($\simeq$ 10.1) after the oxygenation reaction was complete, and this pH value was well within the range of maximum adsorption (Figure 25). It should be noted that at a pH of 11.6, any Cr^{+3} which was not adsorbed by the MnO_2 during the formation of the MnO_2 would precipitate out as $Cr(OH)_3$.

An examination of Figure 27 shows that the removal of Cr^{+3} from solution decreases gradually when the concentration of Cr^{+3} present initially exceeds 10 ppm. This behavior could be a result of the exceeding of the adsorptive capacity of the MnO_2 and the subsequent formation of $Cr(OH)_3$ in the liquid medium. This $Cr(OH)_3$ would be detected as chromium source in the analysis by atomic absorption.

5. Effect of Calcium Ion Concentration on the Adsorption of Chromium Ions by Manganese Dioxide. The effect of calcium ion concentration on the adsorption of chromium ions by manganese dioxide was studied because of the common occurrence of Ca^{+2} ions in industrial waste waters (40). The results are shown in Figure 28 for experiments using 100 mg/l of oxygenation reaction MnO_2 at a ph of 11.6 . The results are expressed in terms of percent removal of chromium from solution as a function of initial concentration of Ca^{+2} . In each experiment, the initial concentration of Cr^{+3} was 10 ppm. An examination of Figure 28 shows that complete removal of the chromium was achieved when calcium was present in concentrations below 10 ppm. When the calcium concentration present was above 10 ppm, the percent removal of chromium by the MnO_2 decreased as the concentration of calcium was raised. However, 93% of the chromium originally present in the solution was removed when the calcium concentration was as high as 60 ppm. This behavior indicates the preferential adsorption of chromium ions owing to their stronger tendency to form hydroxo complexes than that of calcium ions (47, 67).

6. Adsorbing Colloid Flotation of Chromium Using Manganese Dioxide as the Adsorbent. The results for the flotation of oxygenation reaction MnO_2, using EHDA-Br in the small bubble apparatus described in Section IV, are shown in Figure 29. The results are expressed in terms of percent removal of the MnO_2 as a function of sparge time, θ . Three sets of experimental results are shown; the first set shows the results of the flotation of flocculated MnO_2 when 2 ml of ethanol were added as a frothing agent. Frothing agents decrease the bubble size considerably owing to the frother's ability to make the bubble walls more rigid and to prevent coalescence of the small bubbles (68). The results for this flotation experiment show that complete removal of the MnO_2 (100 mg/1) was achieved after approximately 1½ minutes of sparging at 170 ml/min. gas rate. Very little redispersion of the floated MnO_2 occurred at the bulk foam interface owing to the high stability of the foam. The second set of experimental results shown in Figure 29 is the flotation of flocculated MnO_2 without the aid of the frother. The results show that the flotation rate was slower than that when the frother was present. In addition, more redispersion of the floated MnO_2 occurred, as can be seen by the drop in the percent removal of MnO_2 after 6 minutes of sparging. The third set of experimental results shown in Figure 29 is for the flotation of oxygenation reaction MnO_2 before flocculation took place and without a frother. The flotation under these conditions was inefficient and removals of MnO_2 were poor compared with the previously discussed results.

In all the experiments, the percent removal of chromium, which was present at a concentration of 10 ppm prior to the formation of the MnO_2, corresponded to the percent removal of the MnO_2 during flotation. The 15 mg/1 EHDA-Br added with the ethanol frother did not interfere with the adsorption of the Cr^{+3} by the MnO_2. Under optimum conditions, i.e. MnO_2 flocculated prior to flotation and ethanol added, 100% of the chromium ions were removed by adsorbing colloid flotation after 1½ minutes of sparging at 170 ml/min.

7. Settling Characteristics of Flocculated MnO_2 . For the sake of comparison of settling methods with flotation for the removal of flocculates MnO_2, the settling of MnO_2 flocs as a function of time was studied. The results, expressed as mg/1 MnO_2 in the supernatant as a function of standing time, are shown in Figure 30. The results clearly show that flotation is at least 2 orders of magnitude faster than settling.

F. CONCLUSION

An experimental investigation of the removal of chromium ions from aqueous media using adsorbing colloid flotation has been carried out. Hydrous manganese dioxide was used as the adsorbing colloid and methods for generating this colloid in situ were studied. The Guyard reaction was unsatisfactory as an in generation method owing to the excessive residual concentration of Mn^{+2} ions remaining after the reaction; this high residual Mn^{+2} concentration would constitute a staining problem if used on a commercial scale (69).

The oxygenation reaction appears to be an efficient method for generating manganese dioxide in situ. No detectable residual concentration of Mn^{+2} results and the process would be relatively inexpensive on a commercial scale. The oxygenation reaction produces solutions in which SO_4^{-2} and Na^{+} are relatively high compared with normal concentrations of these ions in water supplies. However, the sulfate concentration which results from the generation of 100 mg/l MnO_2 is below the U.S. Public Health Service's limit of 250 mg/l (69). There is no limit set by the Public Health Service for Na^{+}.

For 100 mg/l MnO_2, complete removal of up to 10 ppm Cr^{+3} was achieved. The presence of up to 60 ppm Ca^{+2} ions produced very little interference in the adsorption process and thus, the separation method is applicable in hard waters. The manganese dioxide produced by the oxygenation reaction can be floated very efficiently in a small bubble apparatus using EHDA-Br, especially when a small amount of ethanol is used as a frother. For instance, 100% removal of MnO_2 was effected in 1½ minutes of sparging at 170 ml/min. The flotation process does not interfere with the removal of Cr^{+3} and, therefore, up to 10 ppm Cr^{+3} can be easily removed by generating approximately 100 mg/l MnO_2 in situ in the presence of Cr^{+3} and then floating out the MnO_2. The most efficient flotation occurred when the MnO_2 was flocculated prior to flotation and a frother was used.

Adsorbing colloid flotation appears to hold promise for industrial waste treatment for the removal of certain metal ions present in small quantities. Although this study was concerned with the removal of Cr^{+3}, the process should be applicable to a large number of metal ions.

SECTION VII

ACKNOWLEDGEMENTS

The author wishes to acknowledge the National Institute for Metallurgy, Johannesburg and the Council for Scientific and Industrial Research, Pretoria, South Africa who made a travel grant available to Dr. Thomas A. Pinfold to study at Northeastern University.

The partial support of this research by Northeastern University is gratefully acknowledged.

Finally, the support of this project by the Federal Water Pollution Control Administration and the assistance of Dr. Sidney Hannah, the Grant Project Officer and Mr. Jesse Cohen are gratefully acknowledged.

SECTION VIII

REFERENCES

1. B.L. Karger and D. G. DeVivo, Separ. Sci., 3, 393 (1968).

2. R. Lemlich, Ind. Eng. Chem., 60, 16 (1968).

3. B.L. Karger, R.B. Grieves, R. Lemlich, A.J. Rubin, and F. Sebba, Separ. Sci., 2, 401 (1967).

4. E. Schonfeld and A.H. Kibbey, Nuclear Appl., 3, 353 (1967).

5. E. Rubin, R. Everett, J.J. Weinstock, and H.M. Schoen, U.S. Public Health Publ. AWTR-5, Cincinnati, 1963.

6. H.M. Schoen (ed.),"New Chemical Engineering Separation Techniques," Wiley, New York, 1962, pp. 319-85.

7. K.L. Sutherland and I.W. Wark, "Principles of Flotation,"Australian Institute of Mining and Metallurgy, Melbourne, Australia, 1955.

8. B.R. Clanton, Text. Res. J., 8, 301 (1938).

9. J.E. Magofinn and B.R. Clanton, Text. Res. J., 8, 357 (1938).

10. M.J. Jaycock and R.H. Ottewill, Inst. Mining Met. (Br.), 72, 497 (1963).

11. M.J. Jaycock and M.C. Rastogi, World Congress of Surface Active Agents, 2, 283 (1960).

12. S.G. Mokrushin, Soobshch. o Nauchn. Issled. Rabot. Chlenov Primorsk. Otd. Vses. Khim. Obshchestva, 2, 26 (1953).

13. V.V. Pushkarev and E.A. Budenkov, Kolloid. Zh., 25, 589 (1963).

14. L.D. Skrylev and V.V. Pushkarev, Kolloid. Zh., 24, 738 (1962).

15. V.V. Pushkarev, Radiokhimiya, 3, 498 (1962).

16. V.V. Pushkarev,"Radiochemical Methods for Determination of Trace Elements" (in Russian), Iyd. "Nauka," Moscow-Leningrad, 1964, p. 124.

17. L.D. Skrylev and L.N. Kalitina, Kolloid. Zh., 29, 396 (1967).

18. L.D. Skrylev and S.G. Mokrushin, Zh. Prikl. Khim., 37, 211 (1964).

19. R.B. Grieves and D. Bhattacharyya, A.I.Che.E. J., 11, 274 (1965).

20. R.B. Grieves and D. Bhattacharyya, Can. J. Chem. Eng. (December 1965).

21. R.B. Grieves, D. Bhattacharyya, and C.J. Crandall, J. Appl. Chem. (London), 17, 163 (1967).

22. R.B. Grieves and E.F. Chouinard, J. Appl. Chem. (London), 19, 60 (1969).

23. R.B. Grieves and D. Bhattacharyya, J. Appl. Chem. (London), 18, 149 (1968).

24. F. Sebba,"Ion Flotation", Elsevier, Amsterdam, 1962.

25. J.T. Cross, Analyst (London), 90, 315 (1965).

26. A.F. Taggart, T.C. Taylor, and C.R. Ince, Trans. Amer. Inst. Min. Engrs., 87, 285 (1930).

27. K.J. Mysels,"Introduction to Colloid Chemistry," Wiley (Interscience), New York, 1959.

28. I. Sheiham and T.A. Pinfold, J. Appl. Chem. (London), 18, 217 (1968).

29. T.M. Riddick,"Control of Colloid Stability Through Zeta Potential," Zeta-Meter, Inc., New York (1968).

30. P.W.J. Debye, Trans. Amer. Electrochem. Soc., 82, 265 (1942).

31. A.J. Rubin and S.C. Lackey, J. Amer. Water Works Ass., 60, 1156 (1968).

32. P.E. Spargo and T.A. Pinfold, Separ. Sci., submitted.

33. J.J. Bikerman, "Foams: Theory and Industrial Applications", Reinhold, New York, 1953.

34. R.B. Grieves, J. Sanit. Eng. Div. Amer. Soc. Civil Eng., SA1, 4650 (1966).

35. S.D. Faust and J.V. Hunter (eds.), "Principles and Applications of Water Chemistry", Wiley, New York, 1967, p. 235.

36. G.E. Boyd, A.W. Adamson, and L.S. Myers, J. Amer. Chem. Soc., 69, 2836 (1947).

37. R. Kunin, E. Meitzner, and N. Bortnick, J. Amer. Chem. Soc., 84, 305 (1962).

38. C.H. Fiske and Y. Subbarow, J. Biol. Chem., 66, 375 (1925).

39. G. Schwarzenbach and H. Gysling, Helv. Chim. Acta, 32, 1314 (1949).

40. N.L. Nemerow, "Theories and Practices of Industrial Waste Treatment," Addison-Wesley, Reading, Mass. (1963).

41. C.B. Amphlett, "Treatment and Disposal of Radioactive Wastes," Pergamon Press, New York (1961).

42. A. Guyard, Bull. Soc. Chim., 1, 89 (1964).

43. H.A. Laitenen, "Chemical Analysis," McGraw-Hill, New York (1960).

44. S.B. Humphrey and M.A. Eikleberry, "Water and Sewage Works", (1962).

45. E. Nordall, "Water Treatment for Industrial and Other Uses," Reinhold, New York (1961).

46. J.J. Morgan and W. Stumm, J. Colloid. Sci., 19, 347 (1964).

47. J.W. Mellor, "Inorganic and Theoretical Chemistry", Vol. 7, Longmans Green, New York (1932).

48. M.N. Chakravardi and N.R. Dhar, J. Phys. Chem., 31, 997 (1927).

49. N.G. Chatterji, Jour. Proc. Asiatic Soc., Bengal Proc. 8th Ind. Sci. Cong., 17 CXXX (1921).

50. N.R. Dhar, K.C. Sen, and S. Ghosh, J. Phys. Chem., 28, 457 (1924).

51. P.B. Ganguly and N.R. Dhar, J. Phys. Chem., 26, 701 (1922).

52. P.B. Ganguly and N.R. Dhar, J. Phys. Chem., 26, 836 (1922).

53. B. Ghosh, J. Chem., Soc., 1926 pt. 2., 2605 (1926).

54. M. Geloso, Compt. Rend., 174, 1629 (1922).

55. M. Geloso, Compt. Rend,, 176, 1884 (1923).

56. M. Geloso, Compt. Rend., 178, 1001 (1924).

57. M. Geloso and L.S. Levy, Compt. Rend., 186, 35 (1928).

58. L.S. Levy, Compt. Rend., 186, 1619 (1928).

59. L.S. Levy, Compt. Rend., 192, 1376 (1931).

60. L.S. Levy, Ann. Chim., 16, 85 (1931).

61. W. Buser and P. Graf. Helv. Chim. Acta., 38, 830 (1955).

62. V.V. Pushkarev. L.D. Skrylev, and V.F. Batresov, Radiokimiya, 1, 709 (1959).

63. L.D. Skrylev and V.V. Pushkarev. Kolloidn. Zhur., 24, 738 (1962).

64. R.B. Grieves and C.J. Crandall, Water & Sewage Works, 113, 432 (1966).

65. E.J.W. Verwey and J.T.G. Overbeek,"Theory of the Stability of Lyophobic Colloids," Elsevier, Amsterdam (1948).

66. H.B. Weiser, "A Textbook of Colloid Chemistry", John Wiley and Sons, New York (1949).

67. H. Remy, "Treatise on Inorganic Chemistry", Vol. 2, Elsevier, Amsterdam (1956).

68. A.J. Rubin and S.C. Lackey, Jour. AWWA, 60, 1156 (1968).

69. "Standard Methods for the Examination of Water, Sewage, and Industrial Wastes," 10th Ed., Am. Pub. Health Assn., Am. Water Works Assn., Fed. Sewage and Ind. Wastes Assn. (1955).

SECTION IX

TABLE 1

Results for Variable pH

θ=6 min		θ=8min	
pH	Z_R(mg/l)	pH	Z_R(mg/l)
2.6	24	2.7	13
4.1	30	4.3	17
6.2	29	6.1	17
6.5	26	6.5	14
8.0	24	8.1	13
9.2	27	9.0	16
10.0	30	10.0	16
11.1	23	11.2	17

$2\sigma = \pm 4.8$ mg/l

TABLE 2

Coagulating Power of Some Negatively-Charged Solids

Coagulant	Relative coagulating power	Exchange capacity (meq./100 g)	Density (g cm^{-3})	Negative zeta-potential (mV)
Amberlite XE 254	400	500	1.4	26.1 ± 3.0
Amberlite IR 120	200	500	1.4	44.2 ± 1.2
Dowex 50W	200	500	1.4	34.1 ± 3.3
AG50W-X16	200	490	1.4	28.8 ± 3.4
Montmorillonite	200	40-45	2.8	30.6 ± 1.5
Kaolin	30	10-12	2.6	28.1 ± 0.5
Charcoal	10	---	1.3	18.8 ± 4.8
Silica	10	---	2.4	21.4 ± 1.6
Glass	5	---	2.5	36.0 ± 2.4

SECTION X

FIGURE CAPTIONS

Figure 1. Plexiglass flotation column apparatus. (1) Needle valve; Swagelok no. IRS4. (2) 500 ml. gas saturator bottles filled with deionized water. (3) Water droplet trap; 1 m x 3 cm o.d., packed with glass wool. (4) Needle valve; Swagelok no. IRS4. (5) Constant differential flow controller; Moore Products Co., Model 63 BU-L. (6) Calibrated rotameter; Kontes Glass Co., no. K-626500. (7) Mercury manometer. (8) Porous glass frit; 8 cm diameter, 50-60μ pore size; Kontes Glass Co. (9) Flotation column; Plexiglas, 90 cm x 10 cm o.d. (10) Exit arm; Plexiglas, $\frac{5}{8}$ cm o.d. (11) Heat exchanger; stainless steel, 60 cm x 6 cm o.d., two tandem coils of no. 22 Chromel wire. (12) Variac controls for heat exchanger coils. (13) Collapsed foam collector; 200 ml beaker. (14) Surfactant injection system; 500 ml vacuum flask with $\frac{1}{4}$ in. o.d. stainless steel tubing. (15) Needle valve; Swagelok no. IRS4.

Figure 2. Pyrex flotation cell with 5-10μ pore size frit.

Figure 3. Zeta potential of kaolin related to molar concentration of EHDA-Br. Kaolin concentration of 100 mg/l .

Figure 4. Residual amounts of kaolin and montmorillonite particulates related to time for initial conditions of 100 mg/l particulates and 37.8 mg/l EHDA-Br. Plexiglas flotation column (50-60μ frit).

Figure 5. Zeta potential related to concentration of Na_2SO_4 for a kaolin sol of initial concentrations of 100 mg/l kaolin and 37.8 mg/l EHDA-Br. Plexiglas flotation column (50-60μ frit).

Figure 6. Percent removal of kaolin particulates related to time for different values of ZP_i and initial concentrations of 100 mg/l kaolin and 37.8 mg/l EHDA-Br. Plexiglas flotation column (50-60μ frit).

Figure 7. Percent removal of montmorillonite particulates related to time for different values of ZP_i and initial concentrations of 100 mg/l montmorillonite and 37.8 mg/l EHDA-Br. Plexiglas flotation column (50-60μ frit).

Figure 8. Percent removal of kaolin and montmorillonite particulates related to time for dispersed and coagulated sols. Pyrex flotation cell (5-10μ frit).

Figure 9. Residual concentration of kaolin after 14 min. of sparging related to the initial ratio of surfactant concentration to particulate concentration. Plexiglas flotation column (50-60μ frit).

Figure 10. Rate data for kaolin particulates for initial concentrations of 100 mg/1 kaolin and 37.8 mg/1 EHDA-Br. Plexiglas flotation column (50-60$_\mu$ frit).

Figure 11. Rate data for montmorillonite particulates for initial concentrations of 100 mg/1 montmorillonite and 37.8 mg/1 EHDA-Br.

Figure 12. Percent removal of kaolin after 6 min of sparging related to ion concentration for Na^{+}, Ca^{2+}, and Fe^{3+}. Plexiglas flotation column (50-60$_\mu$ frit).

Figure 13. Coagulation of 0.50 g liter^{-1} of Amberlite IRA 401 resin using glass (both solids -400 mesh): A, nil; B, 3.0 g; C, 6.0 g glass.

Figure 14. Coagulation of 0.50 g liter^{-1} Amberlite IRA 401 (-400 mesh) with 3.0 g of glass of various mesh sizes: A, -400; B, -200/400; C, -60/200; D, no glass.

Figure 15. The effect of mixing resins with opposite charges. A to B: 0.50 g Amberlite IR 120 (-400 mesh) alone. At B, 0.50 g Amberlite IRA 401 (-400 mesh) added.

Figure 16. Coagulation of 0.50 g Amberlite IRA 401 (-400 mesh) with Amberlite IR 120 of two different mesh ranges: Curve 1, -400 mesh; Curve 2, -200/400 mesh.

Figure 17. Removal of HPO_4^{2-} ions by various resins: A, 1.0 g of a coagulated cationic-anionic mixed resin; B, 2.0 g of IRA 401 (-40/60 mesh size); C, 2.5 g of unground IRA 401 (-20/50 mesh size).

Figure 18. The effect of amount of IRA-401 (400 mesh) on the removal of phosphate by coagulated resin ion removal. Flow of feed = 370 ml/min, initial conc. of phosphate 1.5×10^{-4} M.

Figure 19. The effect of feed flow rate on the removal of phosphate by coagulated resin ion removal. Initial concentration of phosphate 1.5×10^{-4}M, 2.5 g IRA 401 (400 mesh) + XE 254.

Figure 20. Guyard reaction stoichiometry.

Figure 21. Oxygenation reaction stoichiometry.

Figure 22. Electrophoretic mobility related to pH for Guyard reaction manganese dioxide.

Figure 23. Electrophoretic mobility related to pH for oxygenation reaction manganese dioxide. Series I.

Figure 24. Electrophoretic mobility related to pH for oxygenation reaction manganese dioxide. Series II.

Figure 25. Removal of chromium ions from solution by adsorption onto oxygenation reaction manganese dioxide related to pH.

Figure 26. Removal of chromium ions from solution by adsorption onto oxygenation reaction manganese dioxide related to electrophoretic mobility.

Figure 27. Removal of chromium ions from solution related to initial concentration of Cr^{+3}.

Figure 28. Interference of Ca^{+2} with the adsorption of Cr^{+3} by oxygenation reaction MnO_2.

Figure 29. Flotation of oxygenation reaction MnO_2 related to sparge time.

Figure 30. Settling of flocculated MnO_2 related to standing time.

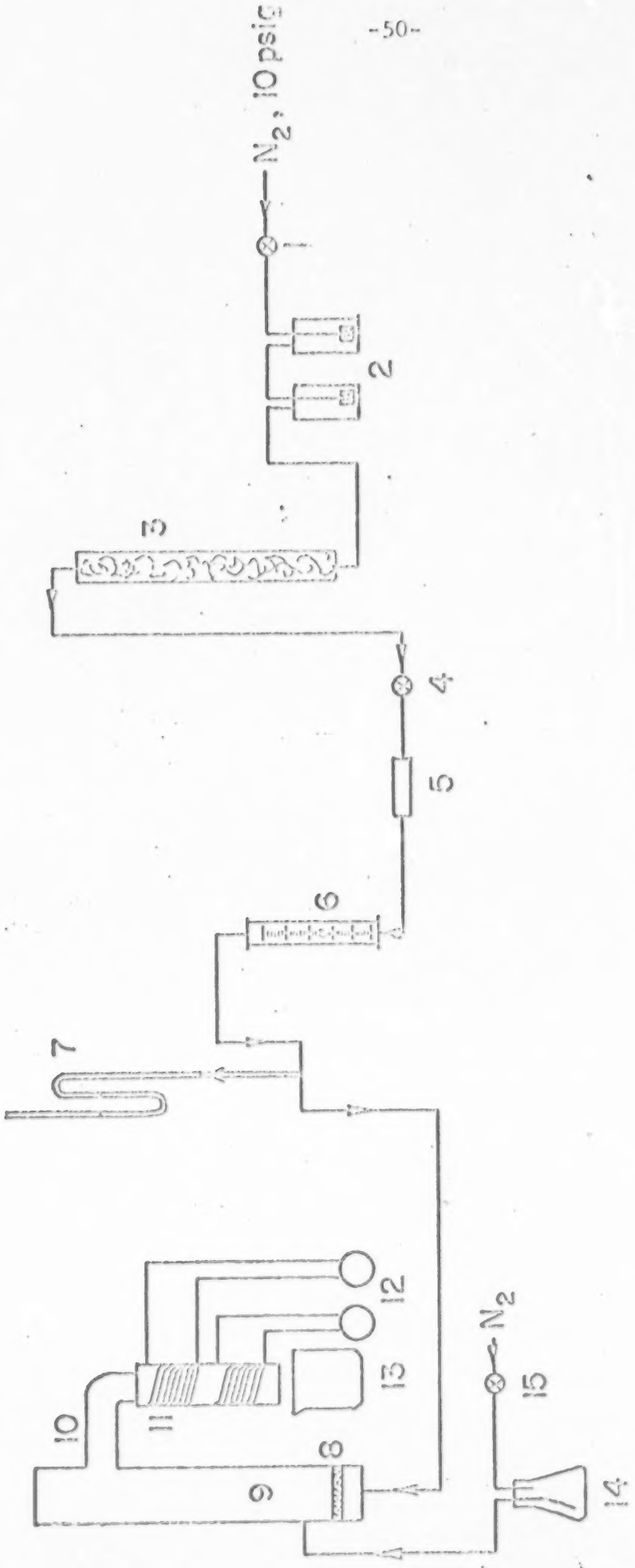

Fig. 1

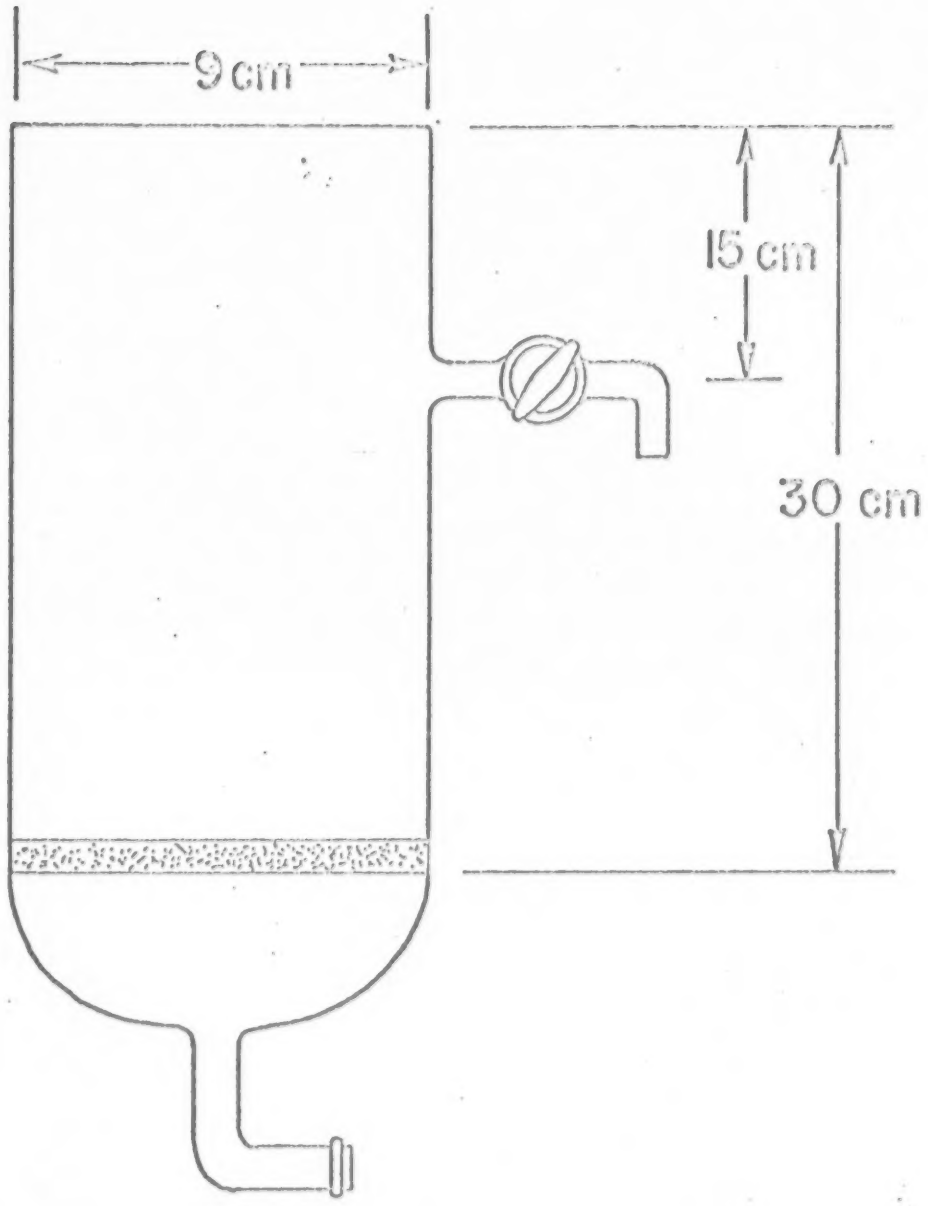

Fig. 2.

52

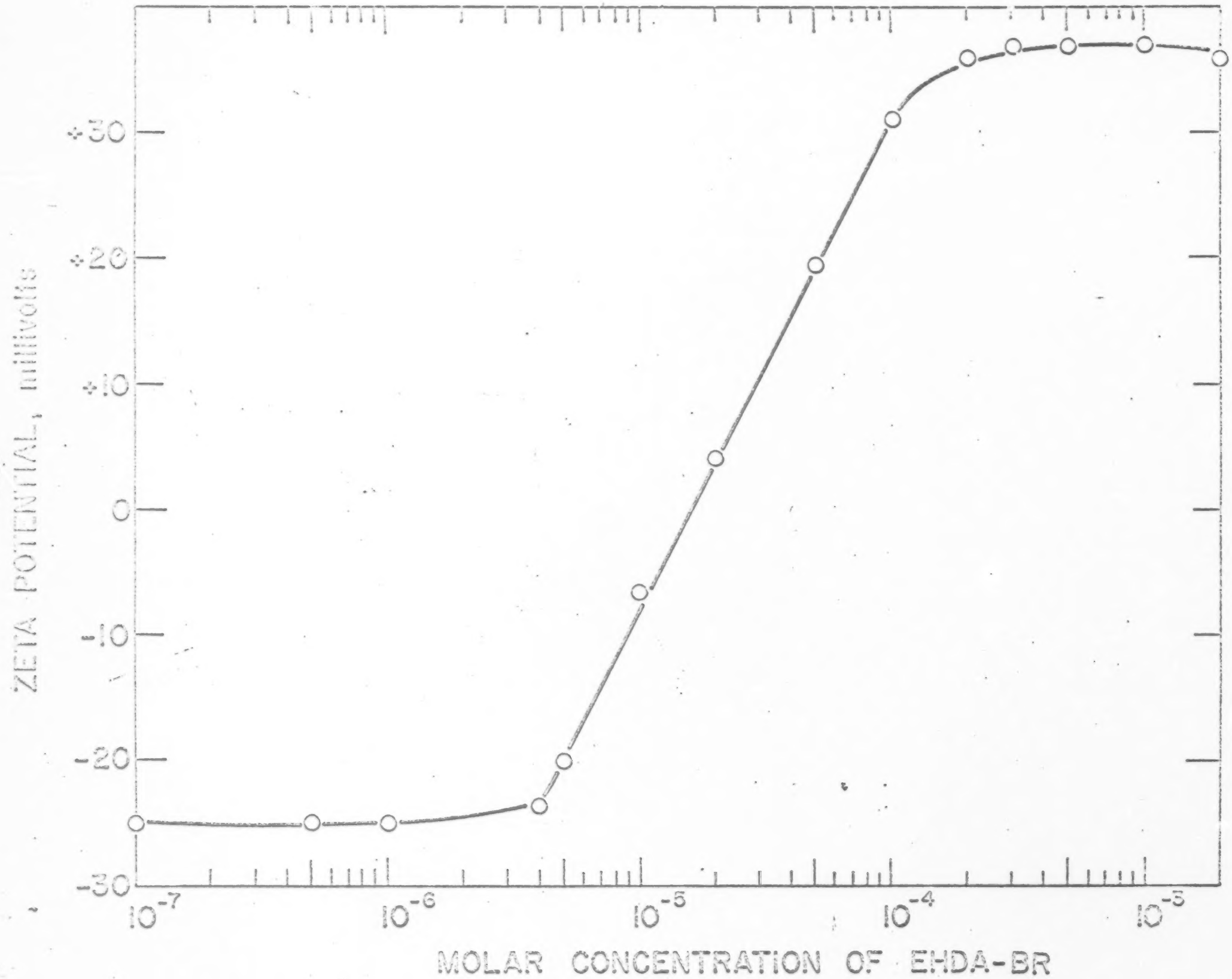
+30
+20
+10
0
-10
-20
-30
ZETA POTENTIAL, millivolts
10^{-7}
10^{-6}
10^{-5}
10^{-4}
10^{-3}
MOLAR CONCENTRATION OF EHDA-BR

Fig. 3

FIG. 4

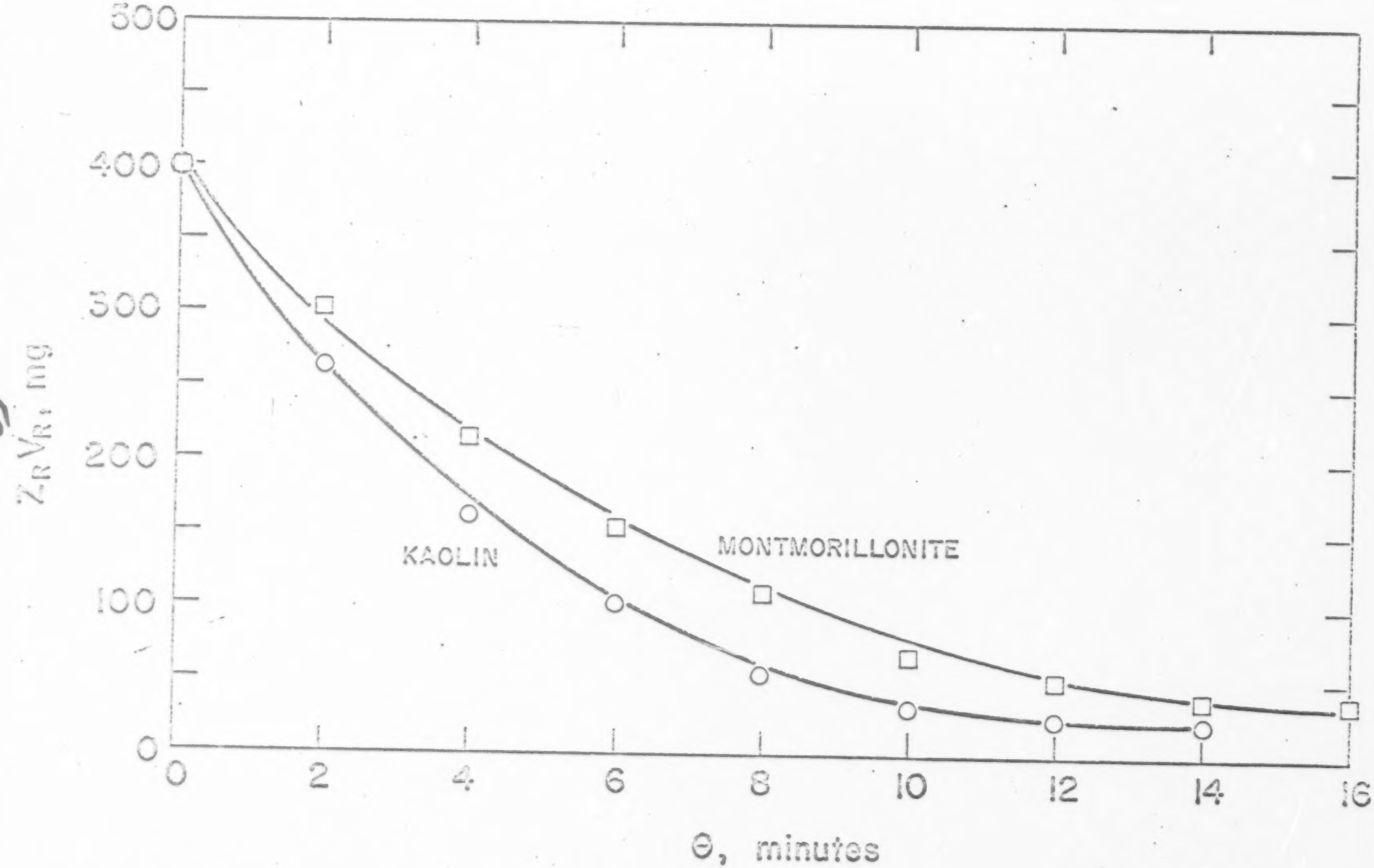
500
400
300
200
100
0
0
2
4
6
8
10
12
14
16
$Z_R V_R$, mg
KAOLIN
MONTMORILLONITE
θ, minutes

Fig. 5

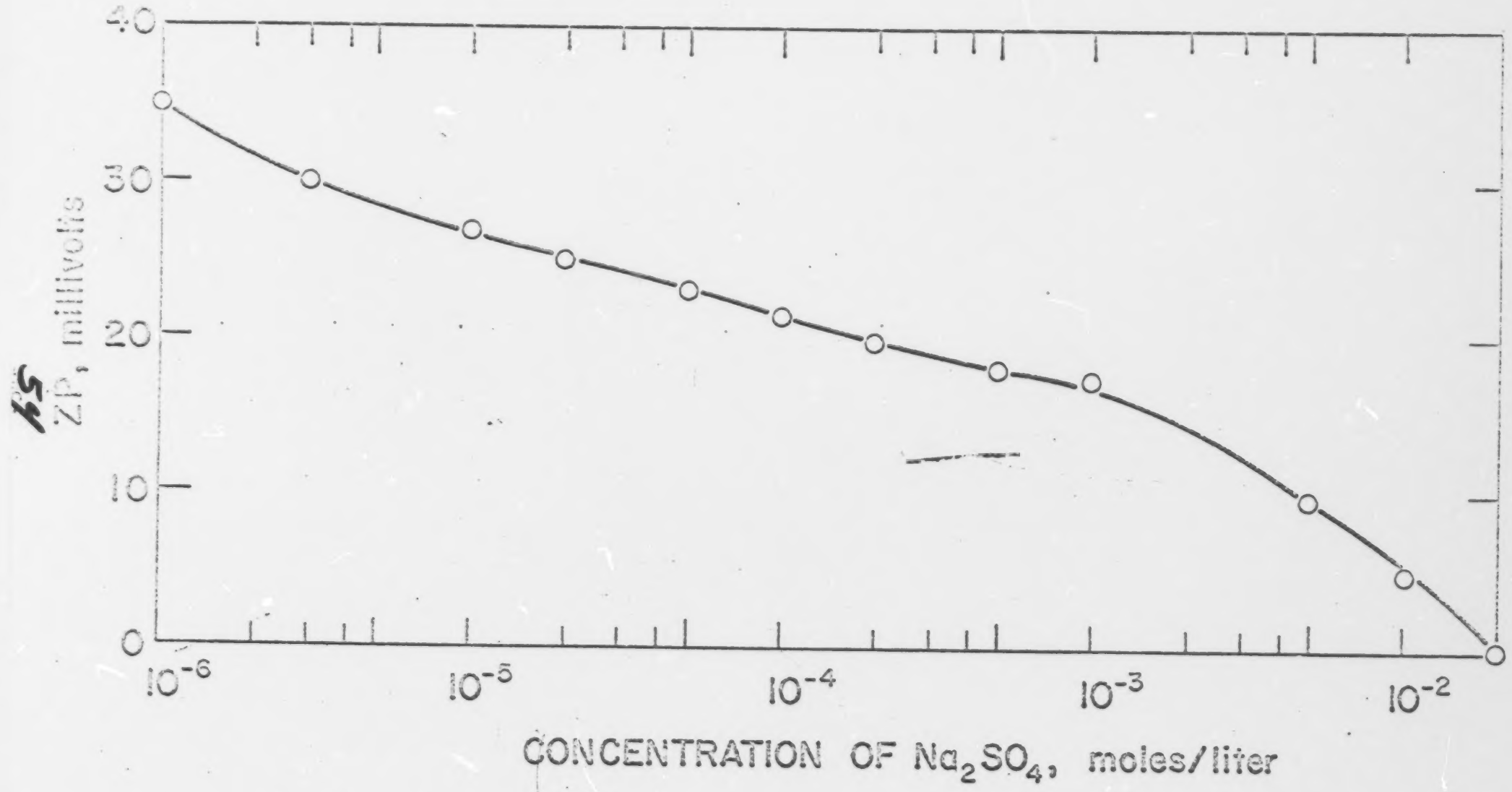
40
30
20
10
0
ZP, millivolts
10^{-6}
10^{-5}
10^{-4}
10^{-3}
10^{-2}
CONCENTRATION OF Na_2SO_4, moles/liter

Fig. 5

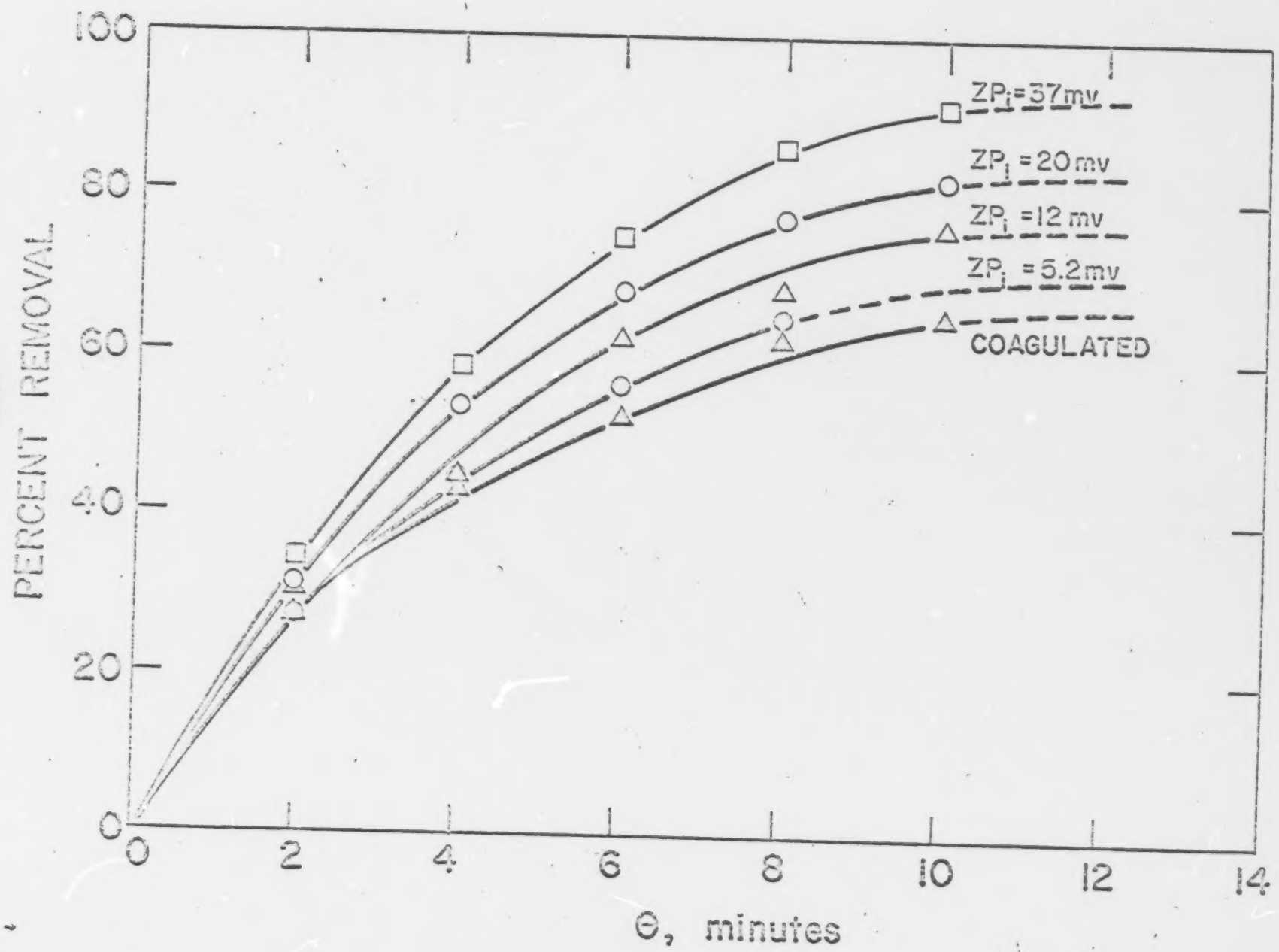
PERCENT' REMOVAL
100
80
60
40
20
0
0
2
4
6
8
10
12
14
θ, minutes
ZP$_i$=37mv
ZP$_i$ =20 mv
ZP$_i$ =12 mv
ZP$_i$ =5.2mv
COAGULATED

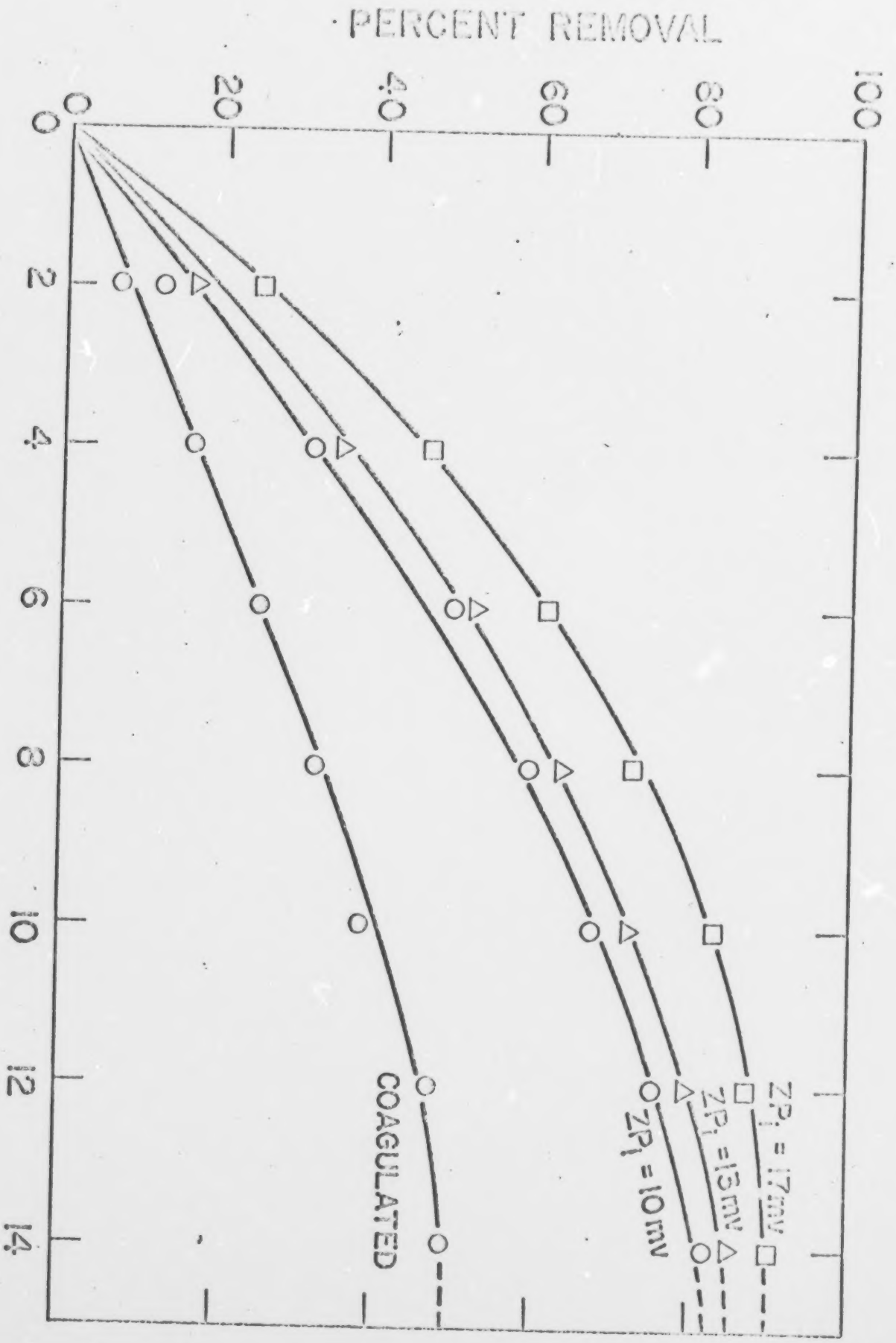
PERCENT REMOVAL
0
20
40
60
80
100
2
4
6
8
10
12
14
Θ, minutes
ZP, = 17mv
ZP, = 15mv
ZP, = 10mv
COAGULATED

Fig. 7

Fig. 5

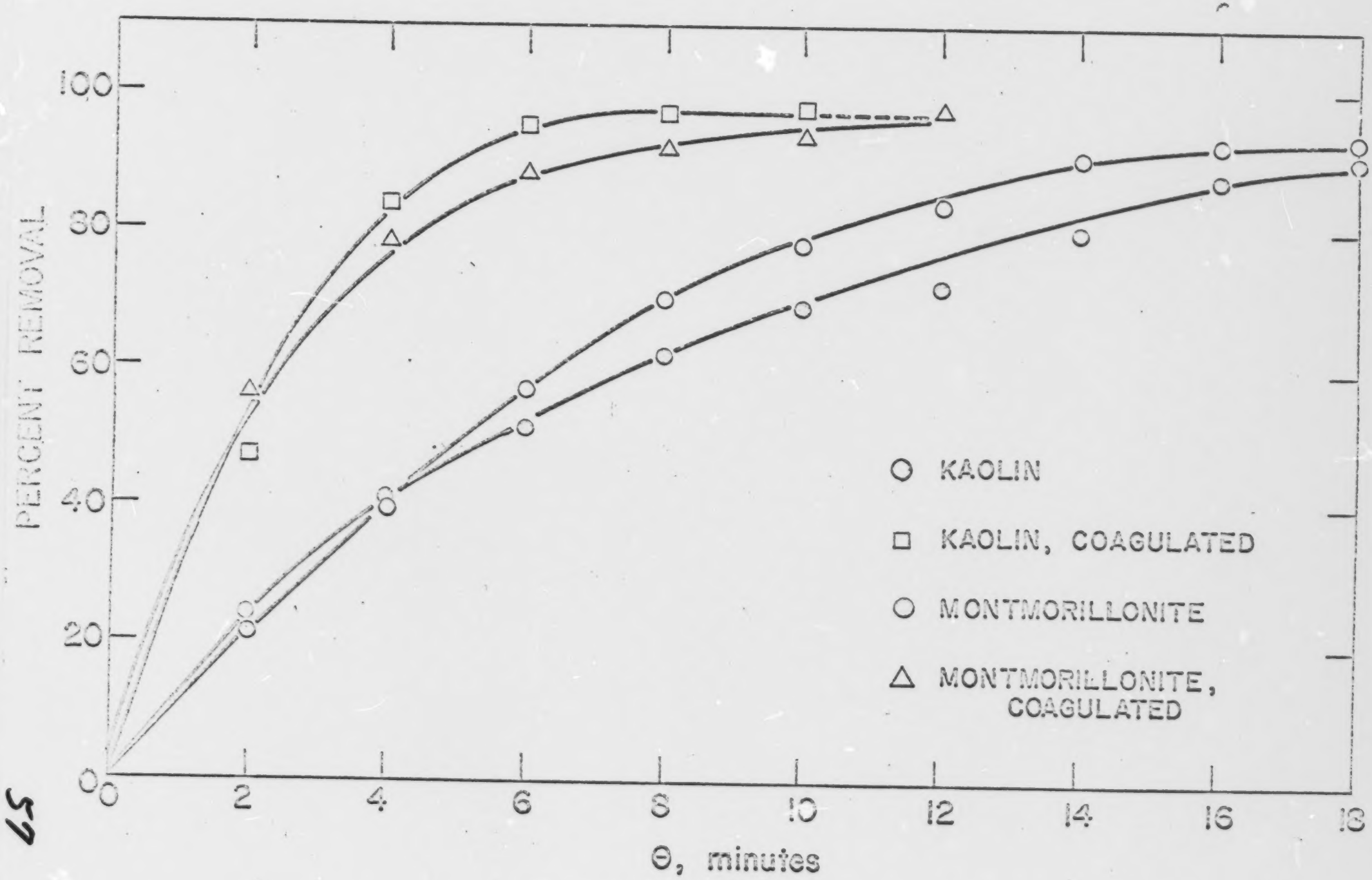
PERCENT REMOVAL
100
80
60
40
20
0
0
2
4
6
8
10
12
14
16
18
θ, minutes
KAOLIN
KAOLIN, COAGULATED
MONTMORILLONITE
MONTMORILLONITE, COAGULATED

45

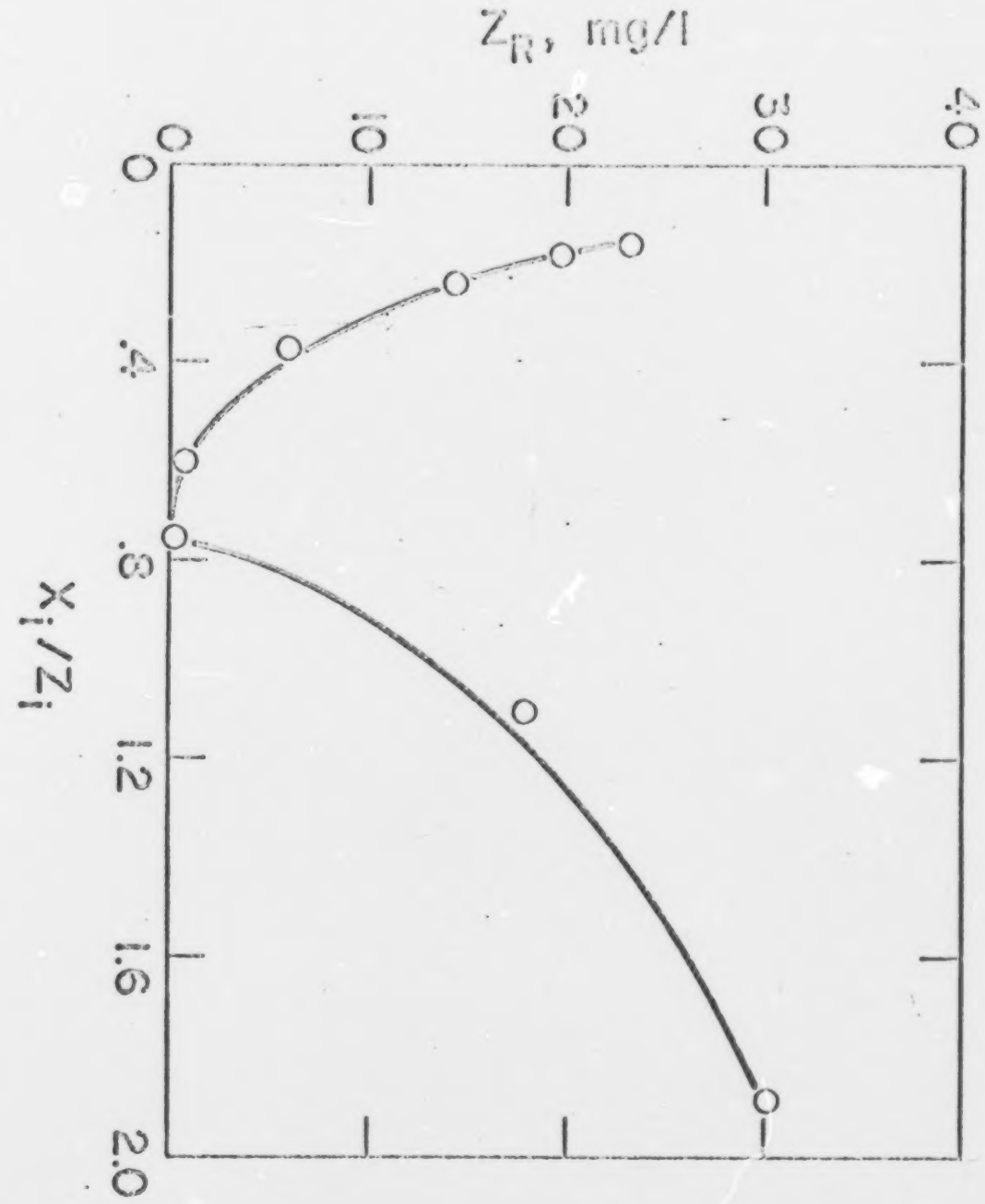

Fig. 9

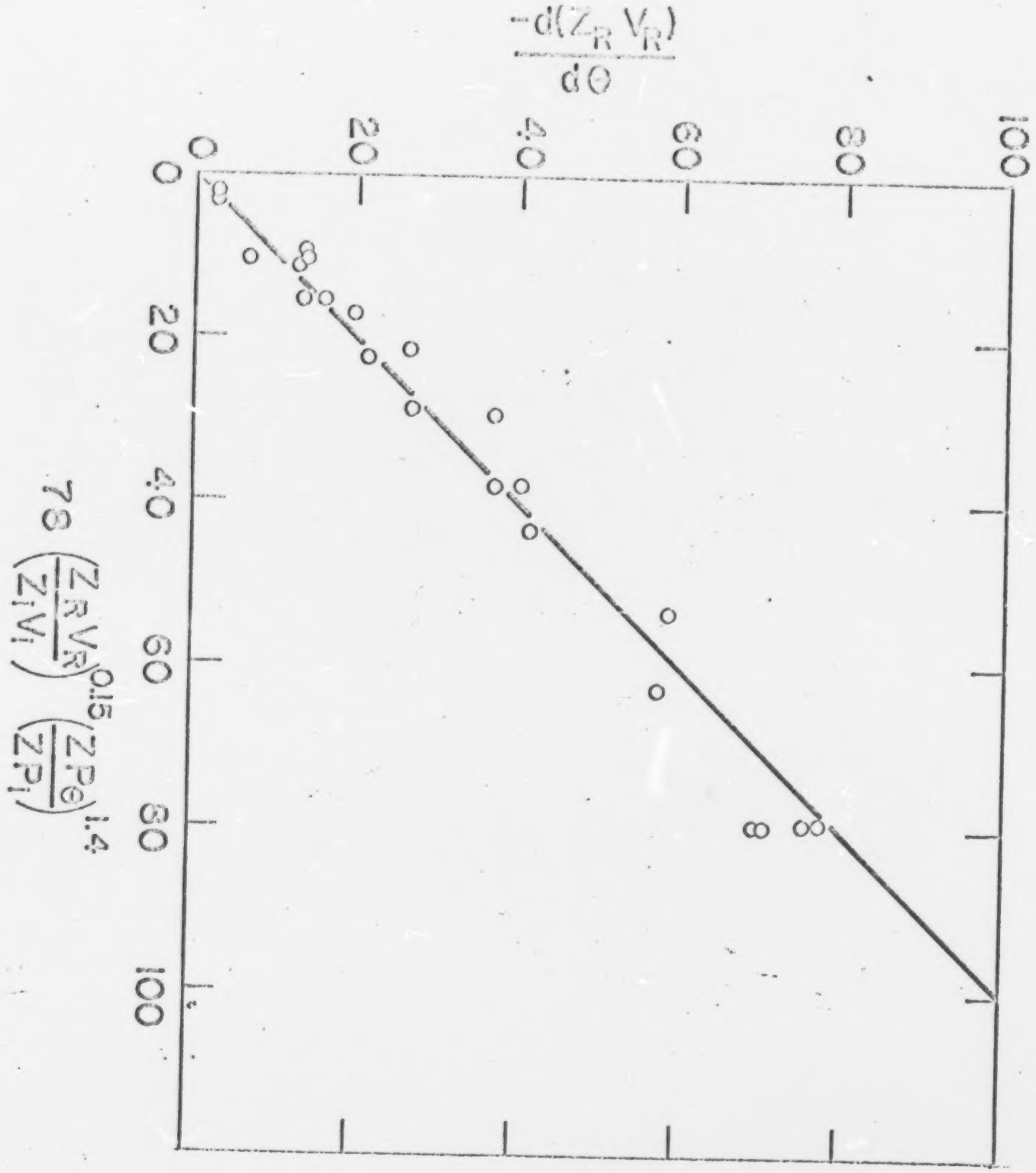
$\frac{-d(Z_R V_R)}{d\theta}$
0
20
40
60
80
100
$\left(\frac{Z_R V_R}{Z_i V_i}\right)^{0.15} \left(\frac{Z_R \theta}{Z_i \rho_i}\right)^{1.4}$
0
20
40
60
80
100

Fig. 10

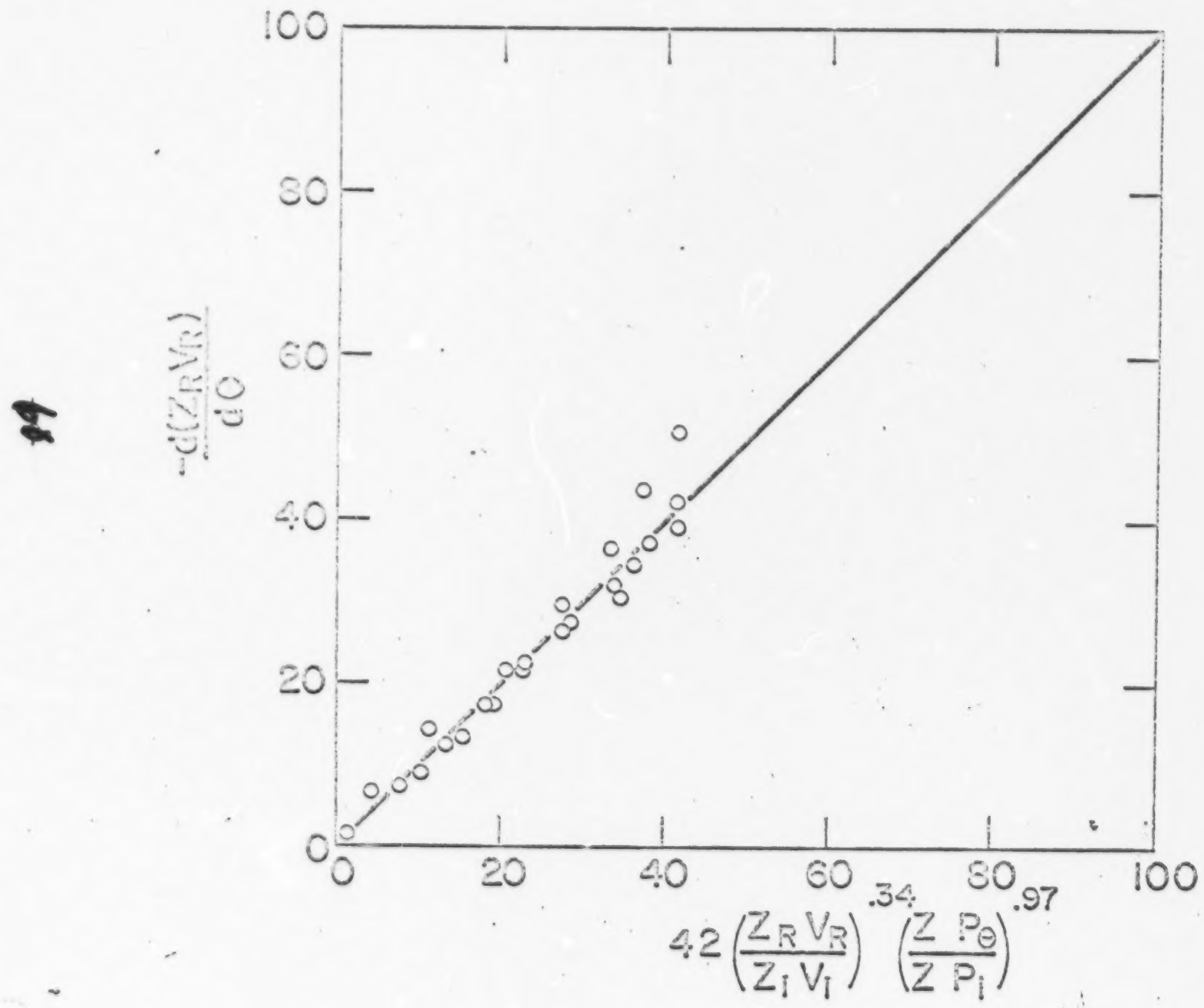
100
80
60
40
20
0
0
20
40
60
80
100
$-\frac{d(Z_R V_R)}{d\theta}$
$42\left(\frac{Z_R V_R}{Z_1 V_1}\right)^{.34}\left(\frac{Z P_\theta}{Z P_1}\right)^{.97}$

Fig. 12.

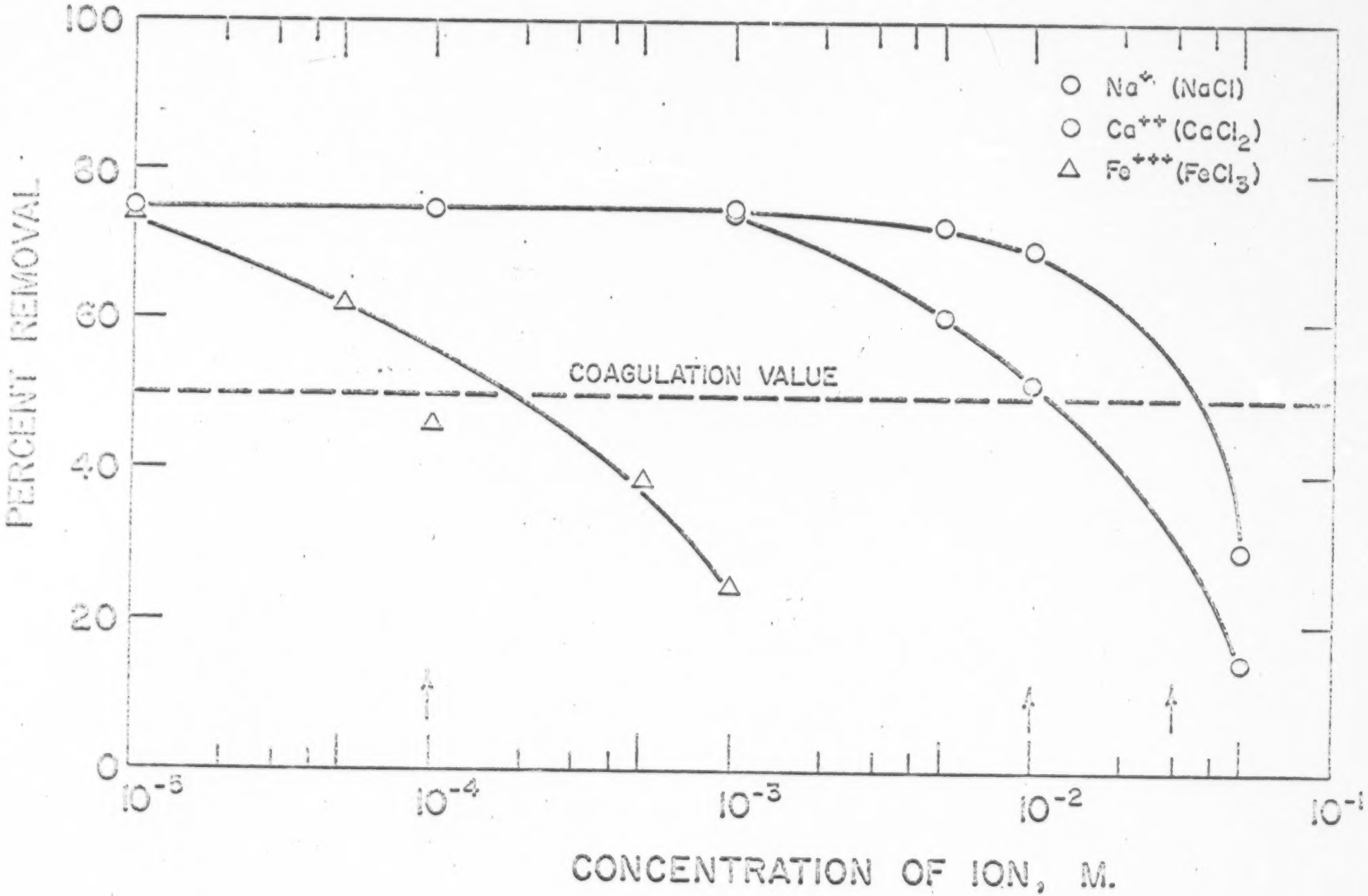
100
80
60
40
20
0
PERCENT REMOVAL
COAGULATION VALUE
Na^{+} (NaCl)
Ca^{++} ($CaCl_2$)
Fe^{+++} ($FeCl_3$)
10^{-5}
10^{-4}
10^{-3}
10^{-2}
10^{-1}
CONCENTRATION OF ION, M.

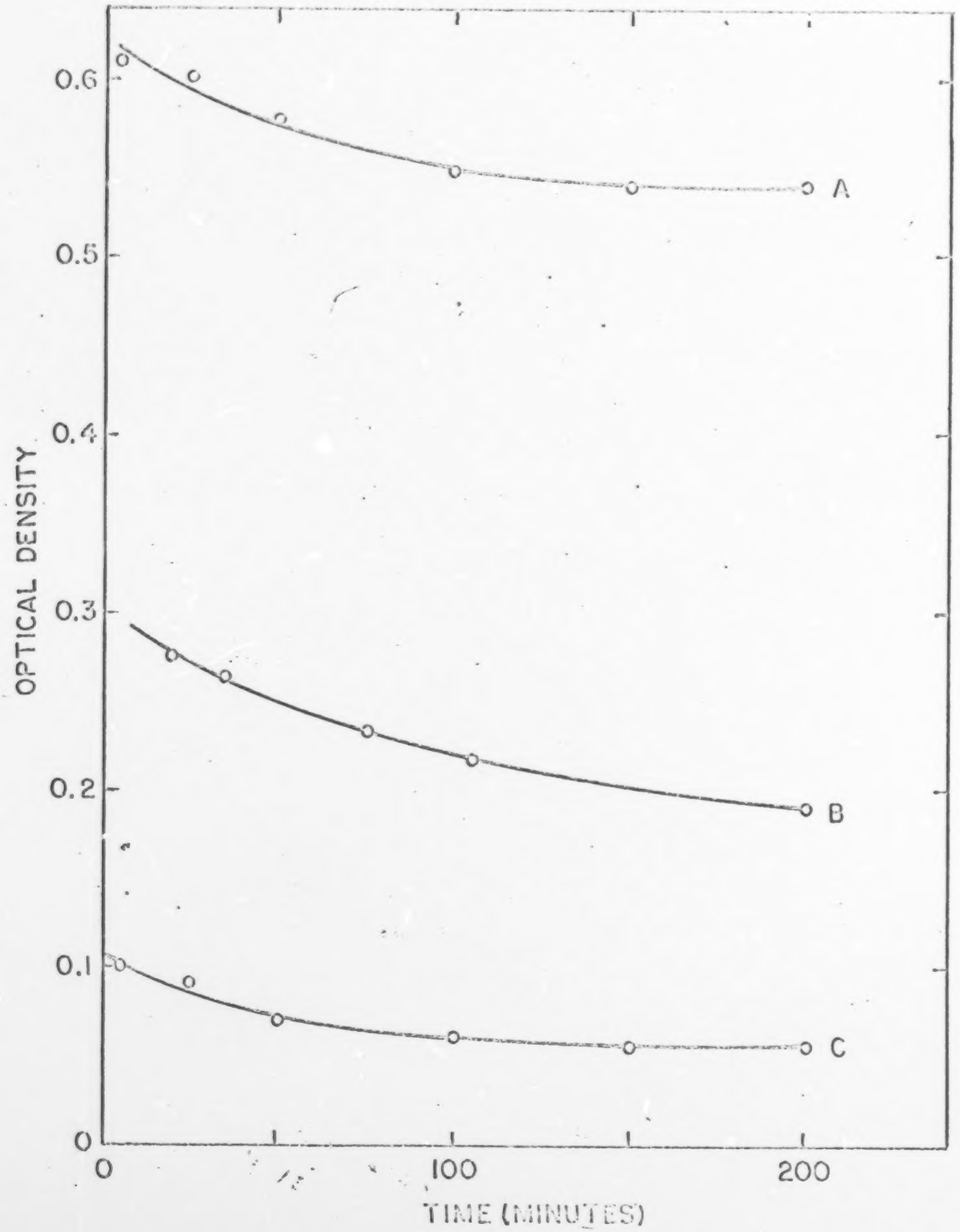

Fig. 13

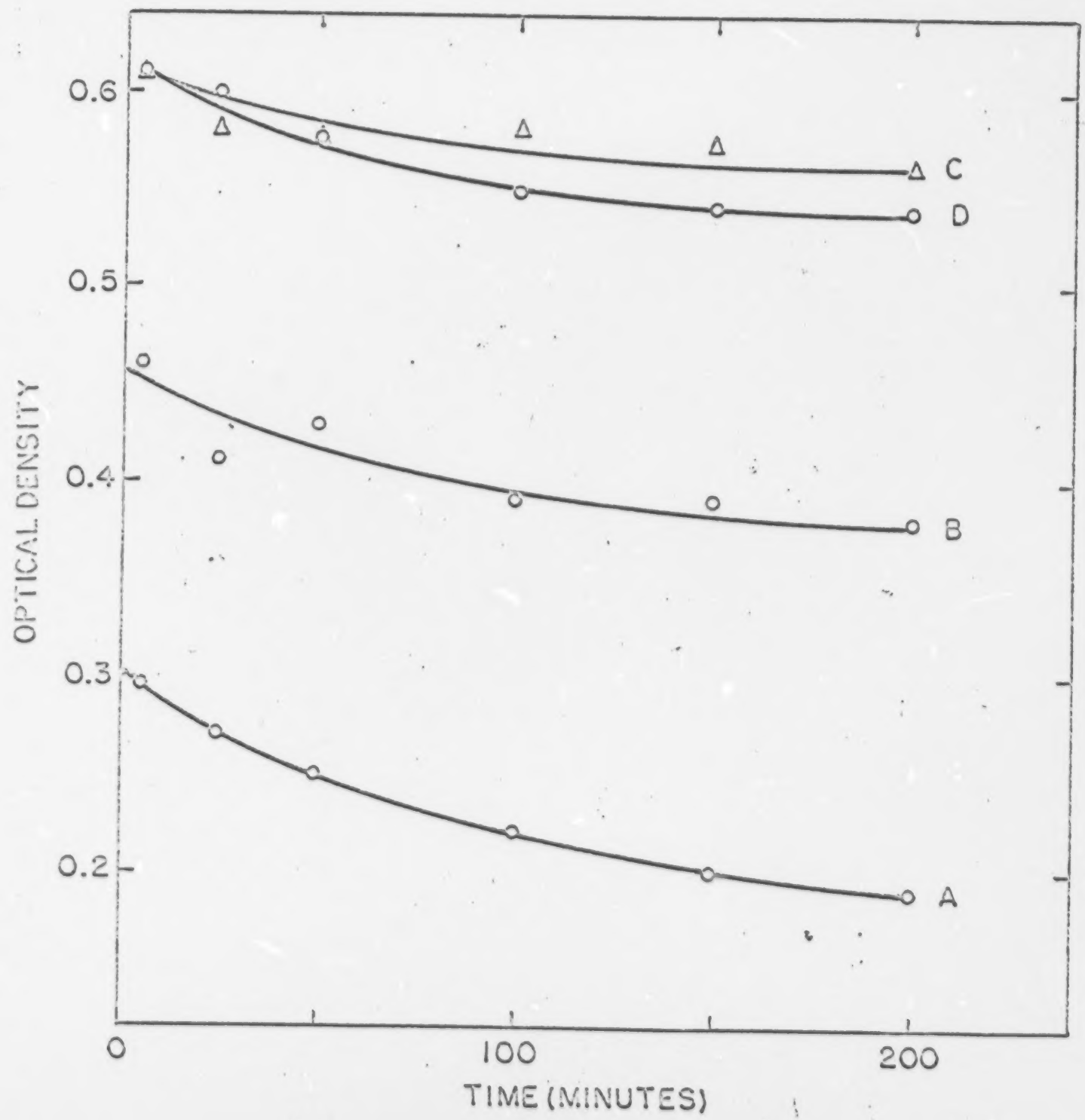

Fig. 14

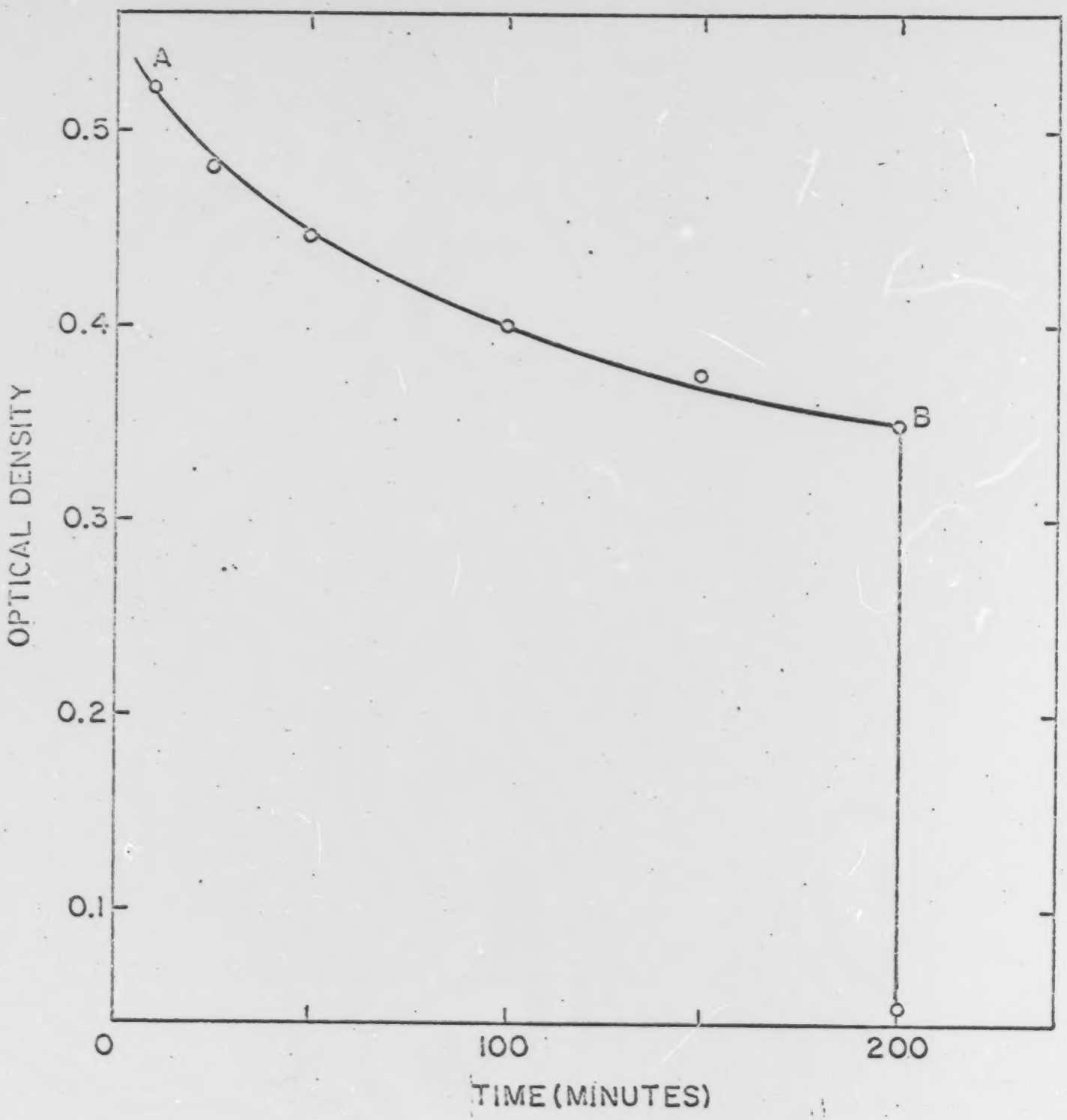

FIG. 15

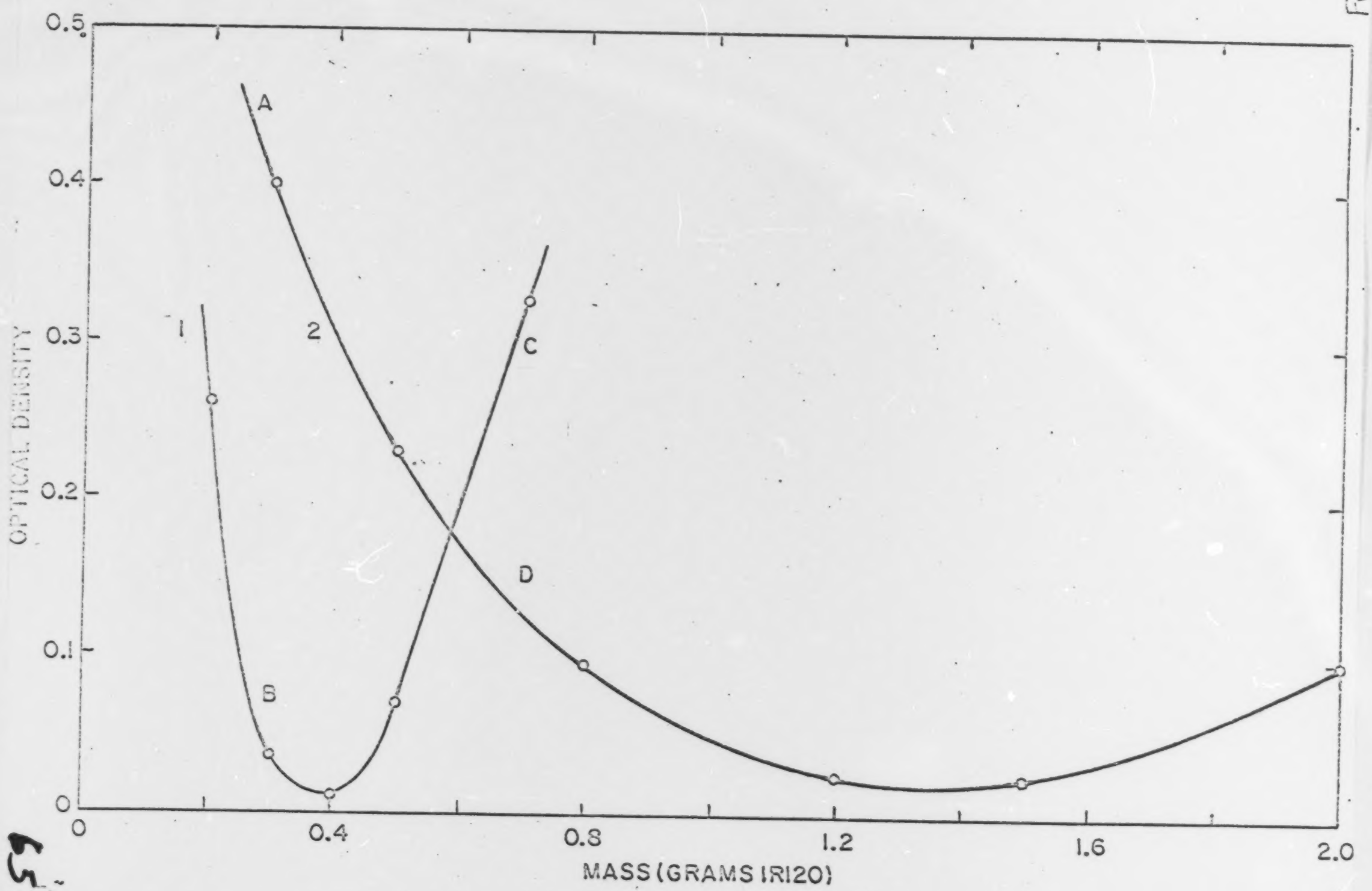
0.5
0.4
0.3
0.2
0.1
0
OPTICAL DENSITY
A
1
2
C
D
B
0
0.4
0.8
1.2
1.6
2.0
MASS (GRAMS IR120)

Fig. 17

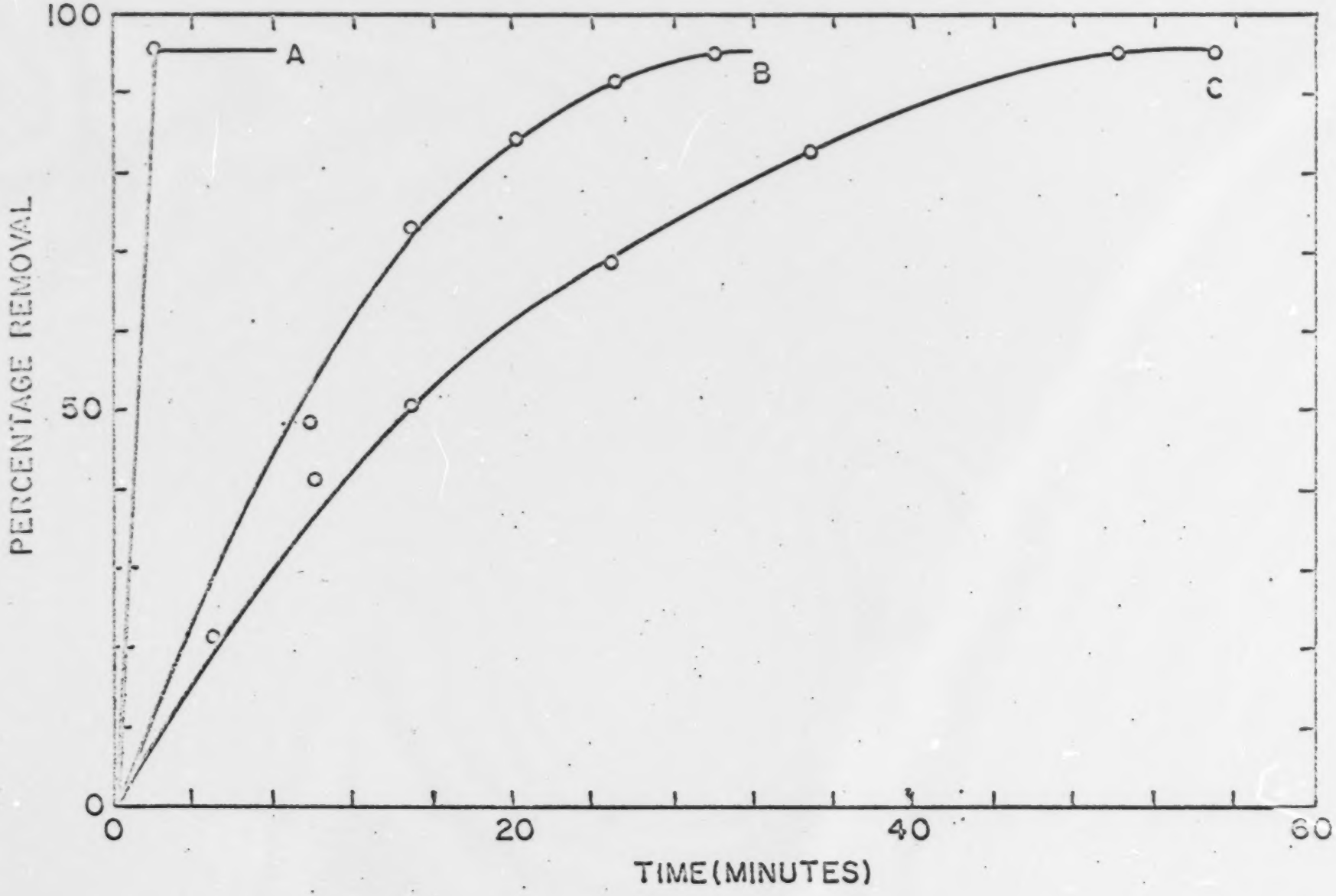

19

Fig 13

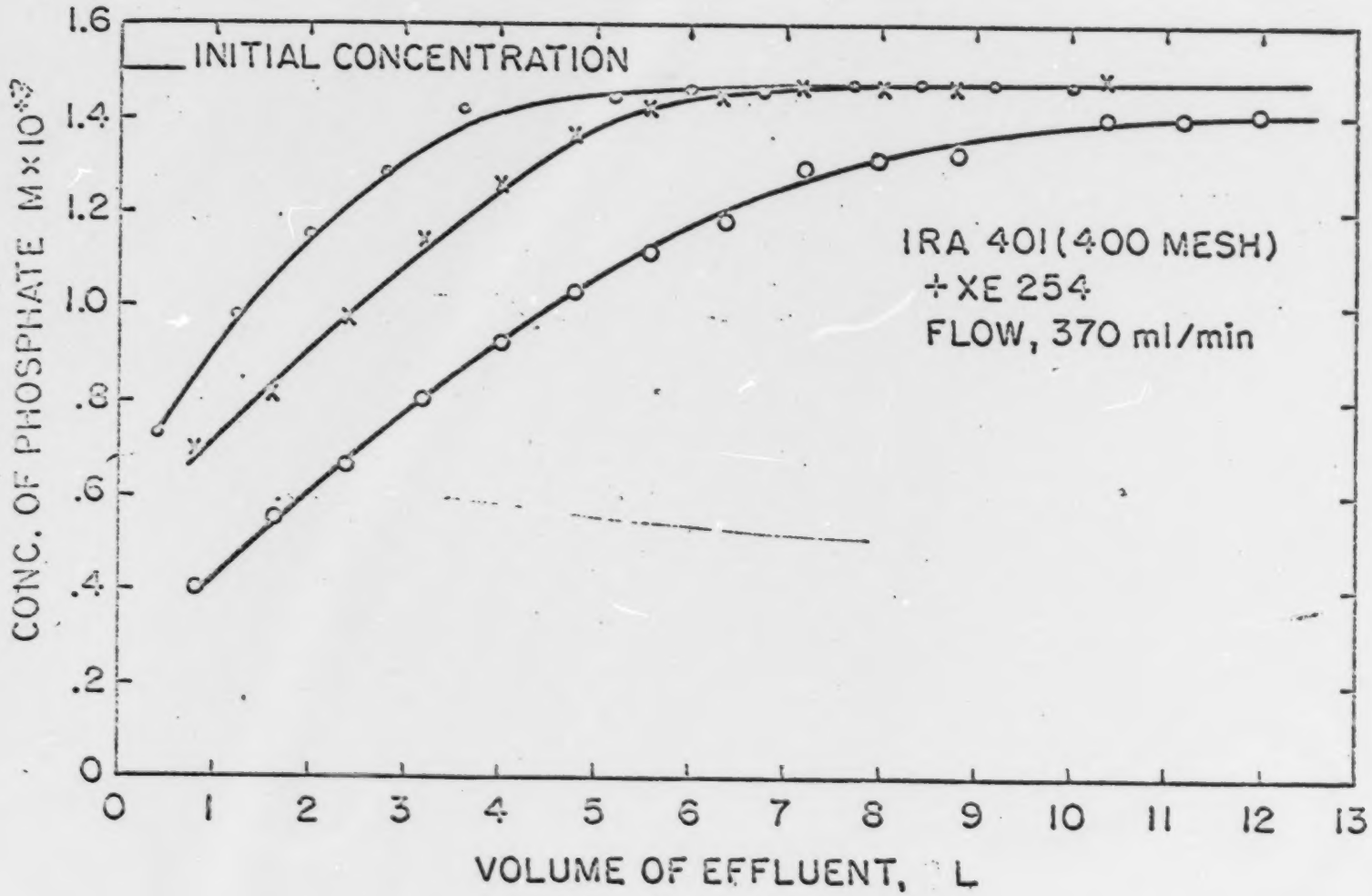
INITIAL CONCENTRATION
IRA 401 (400 MESH)
+XE 254
FLOW, 370 ml/min
CONC. OF PHOSPHATE M×10⁻³
1.6
1.4
1.2
1.0
.8
.6
.4
.2
0
0 1 2 3 4 5 6 7 8 9 10 11 12 13
VOLUME OF EFFLUENT, L

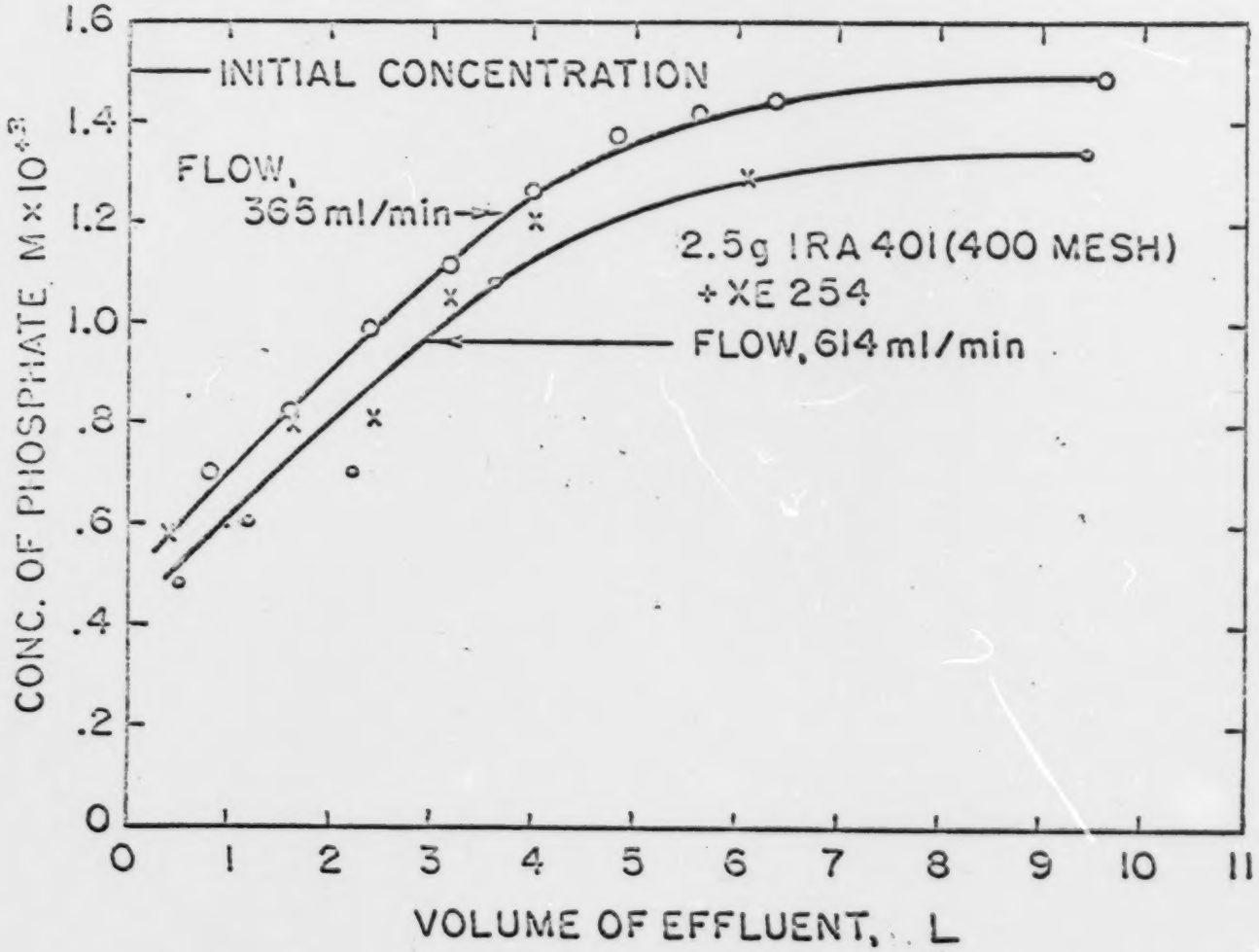
INITIAL CONCENTRATION
FLOW,
365 ml/min
2.5g IRA 401(400 MESH)
+XE 254
FLOW, 614 ml/min
CONC. OF PHOSPHATE M x 10⁻³
1.6
1.4
1.2
1.0
.8
.6
.4
.2
0
0 1 2 3 4 5 6 7 8 9 10 11
VOLUME OF EFFLUENT, L

Fig. 17

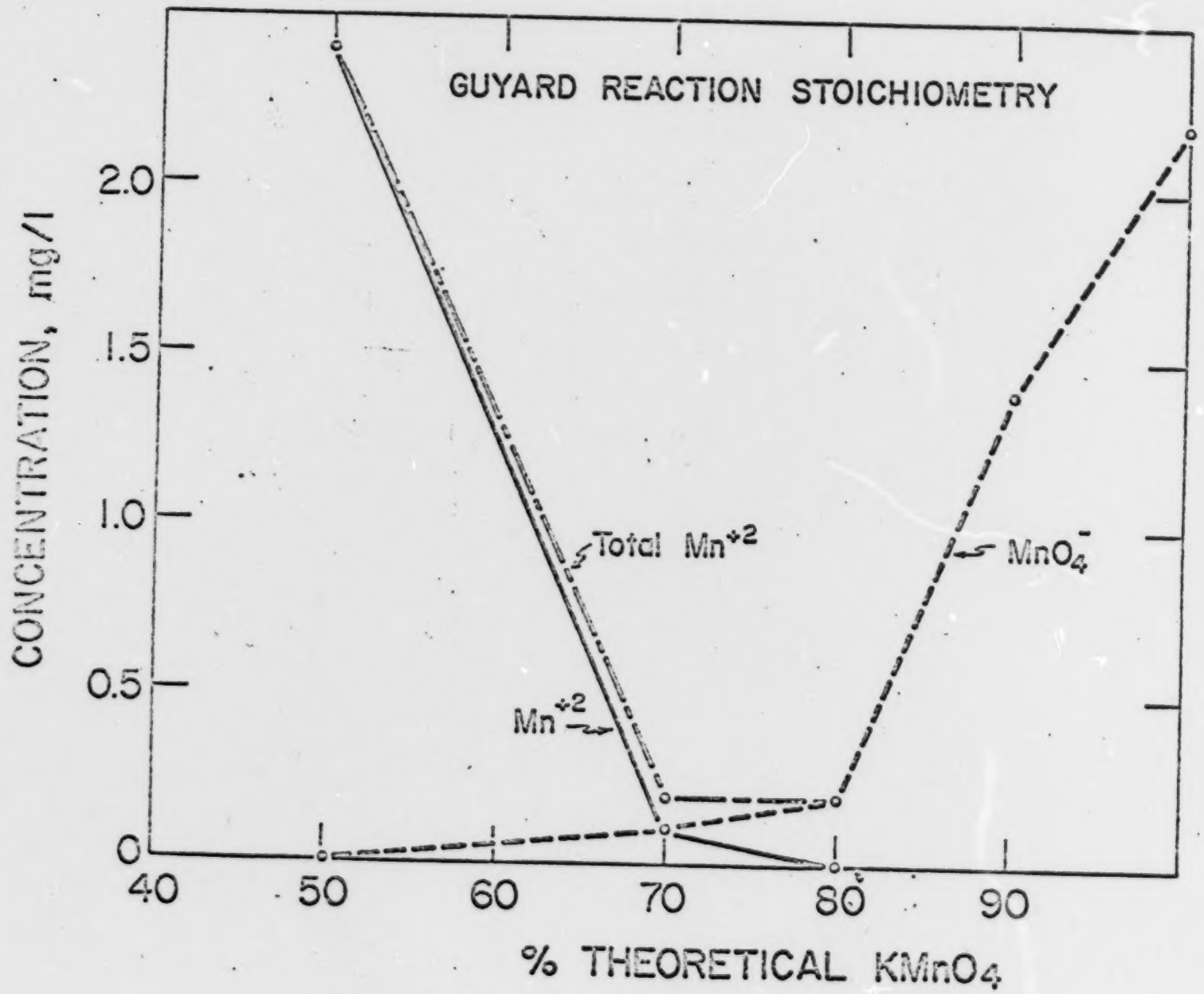
GUYARD REACTION STOICHIOMETRY
CONCENTRATION, mg/l
2.0
1.5
1.0
0.5
0
Total Mn+2
MnO4-
Mn+2
40
50
60
70
80
90
% THEORETICAL KMnO4

Fig. 20

Fig. 21

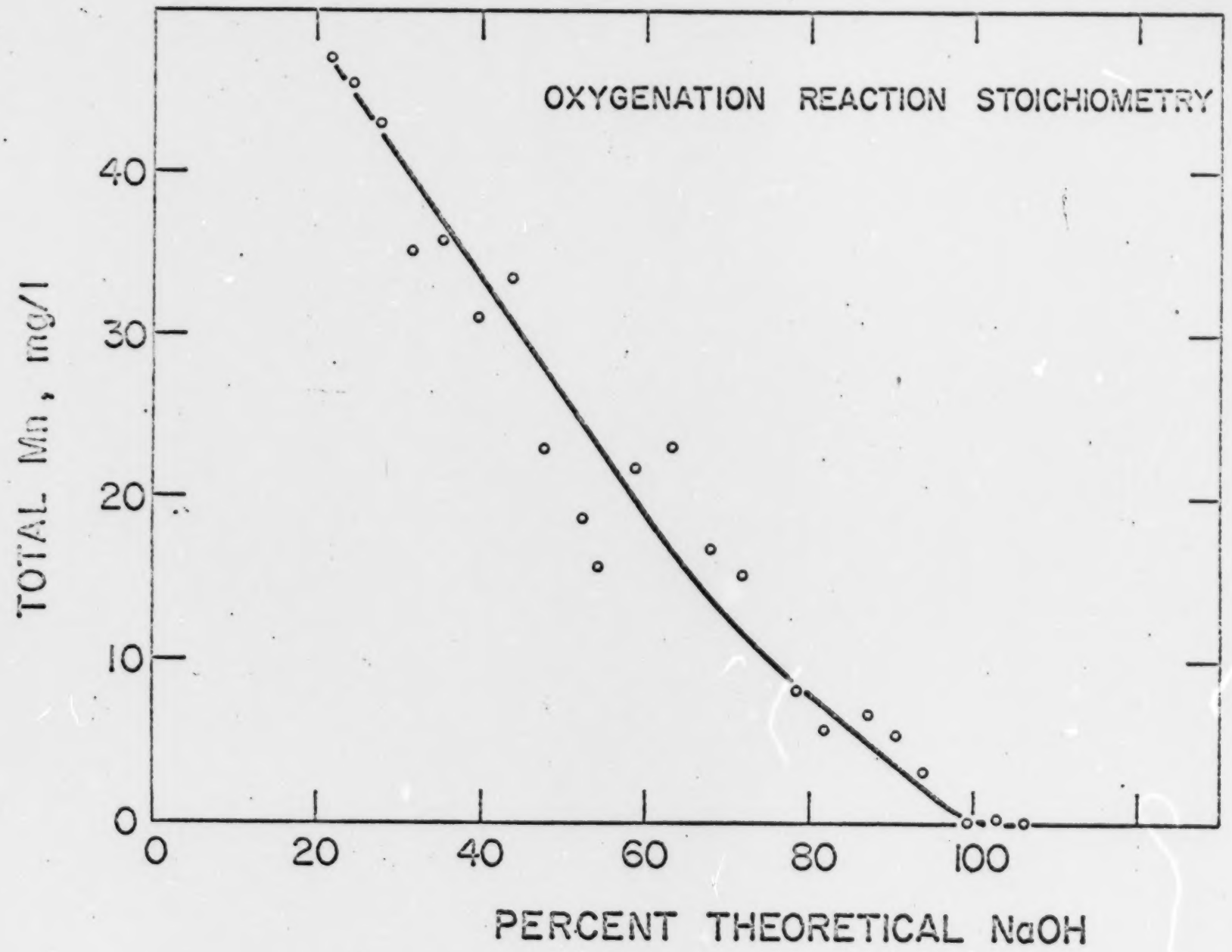
OXYGENATION REACTION STOICHIOMETRY
TOTAL Mn, mg/l
0
10
20
30
40
0
20
40
60
80
100
PERCENT THEORETICAL NaOH

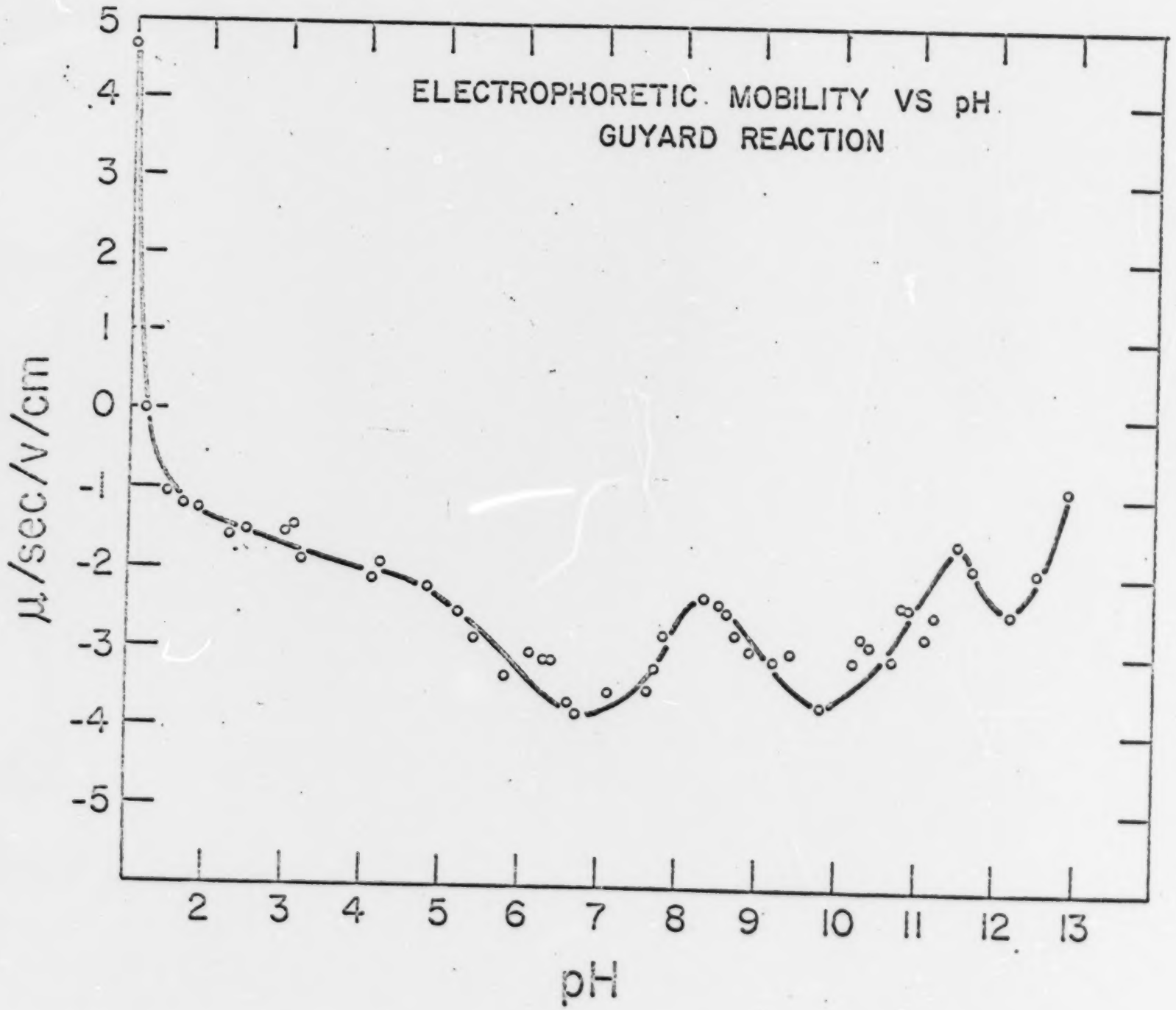
ELECTROPHORETIC MOBILITY VS pH
GUYARD REACTION
μ/sec/V/cm
5
4
3
2
1
0
-1
-2
-3
-4
-5
2
3
4
5
6
7
8
9
10
11
12
13
pH

Fig. 22

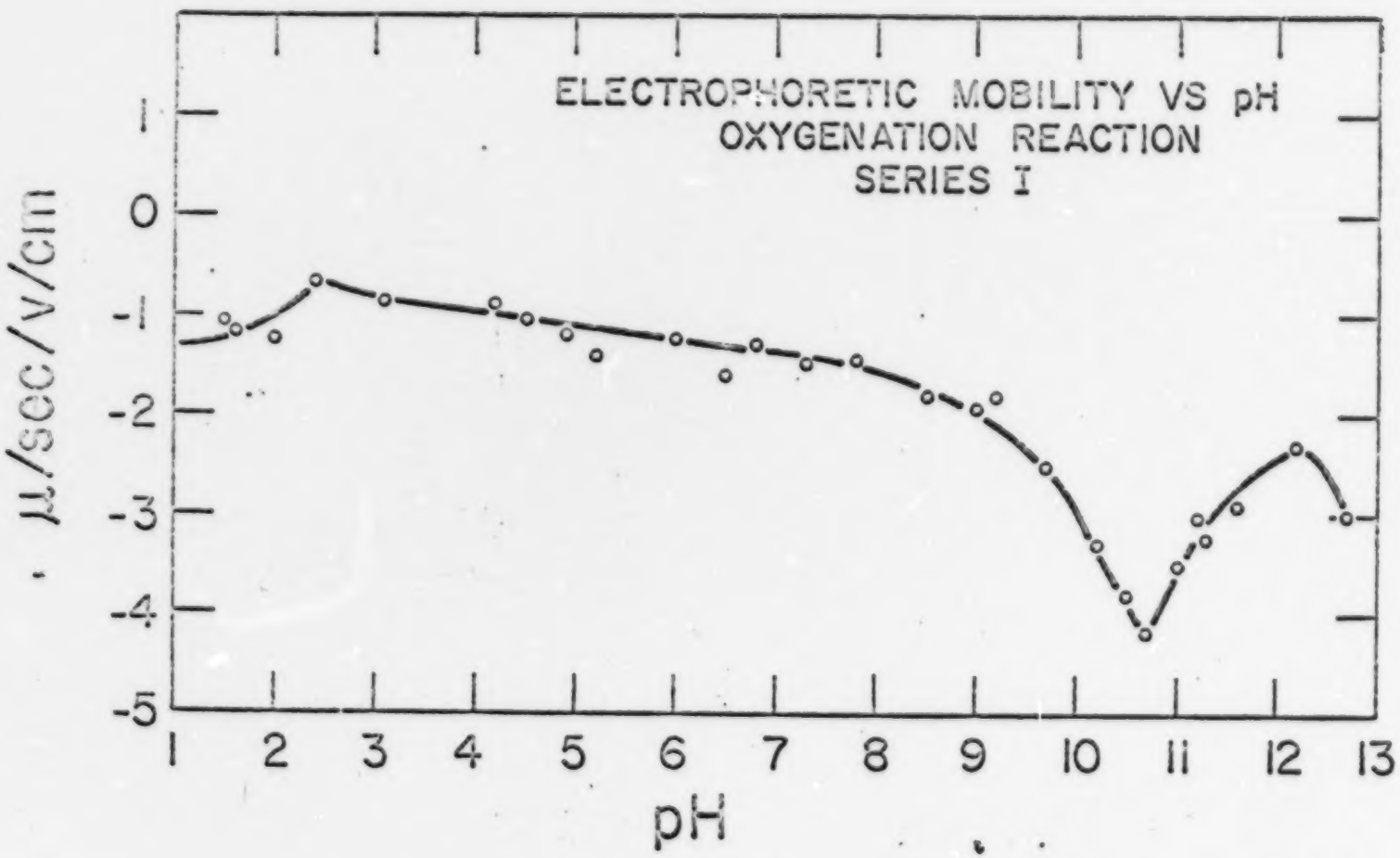
ELECTROPHORETIC MOBILITY VS pH
OXYGENATION REACTION
SERIES I
μ/sec/V/cm
1
0
-1
-2
-3
-4
-5
1
2
3
4
5
6
7
8
9
10
11
12
13
pH

Fig. 23

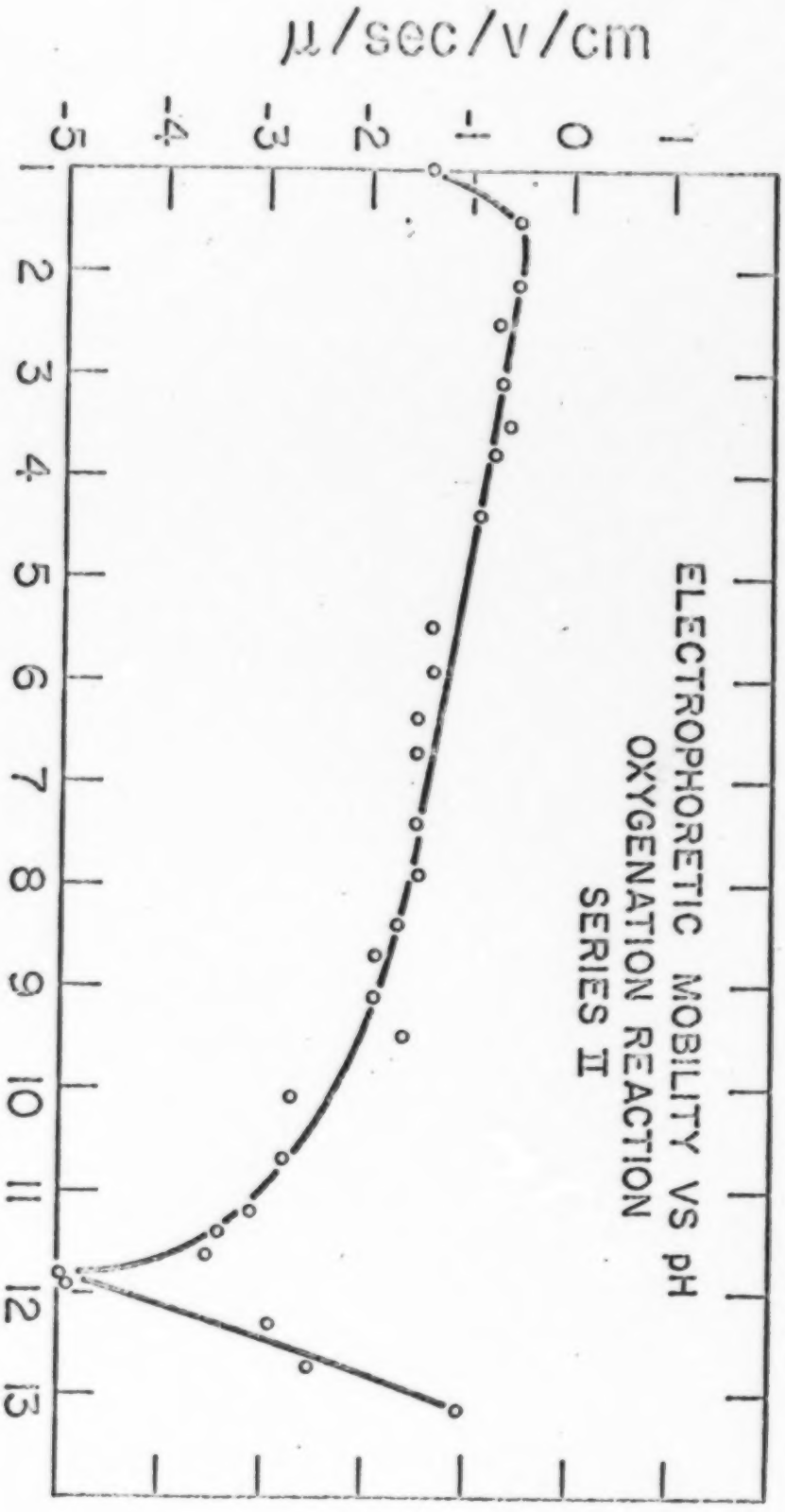
μ/sec/v/cm
-5
-4
-3
-2
-1
0
+
2
3
4
5
6
7
8
9
10
11
12
13
pH
ELECTROPHORETIC MOBILITY VS pH
OXYGENATION REACTION
SERIES II

Fig. 24

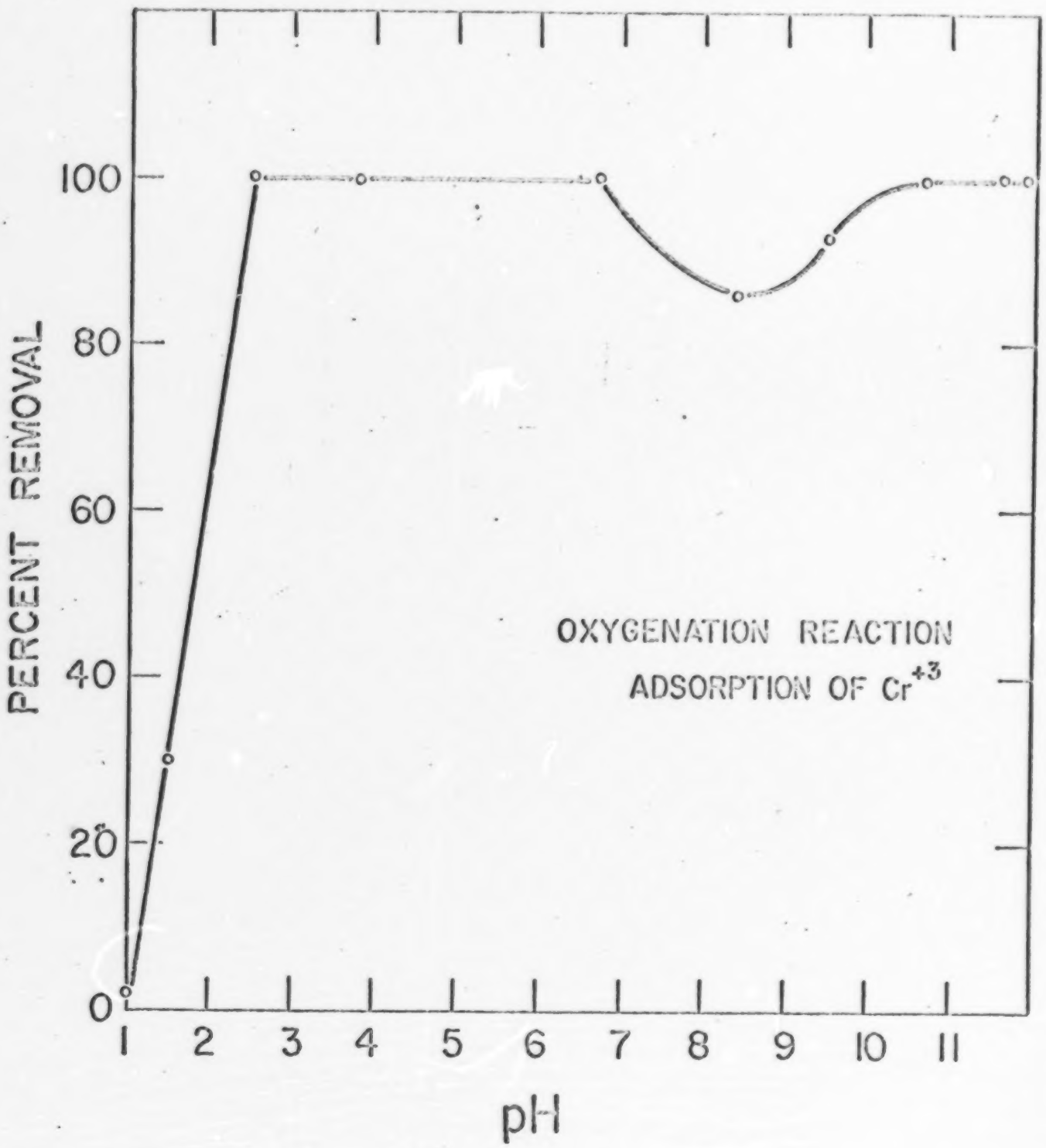
PERCENT REMOVAL
100
80
60
40
20
0
1
2
3
4
5
6
7
8
9
10
11
pH
OXYGENATION REACTION
ADSORPTION OF Cr^{+3}

Fig. 2.5

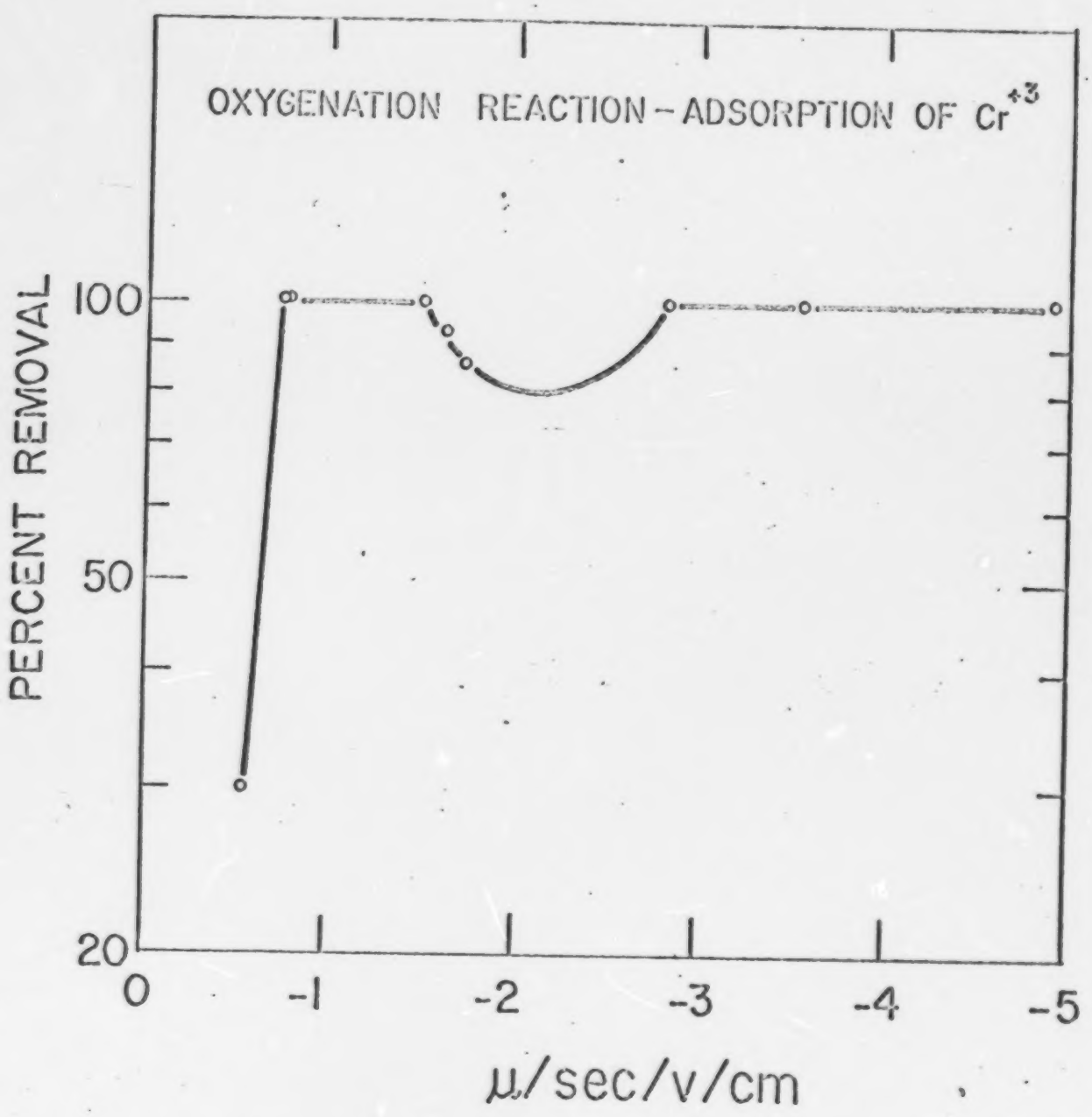
OXYGENATION REACTION – ADSORPTION OF Cr^{+3}
PERCENT REMOVAL
100
50
20
0
-1
-2
-3
-4
-5
μ/sec/v/cm

Fig. 26

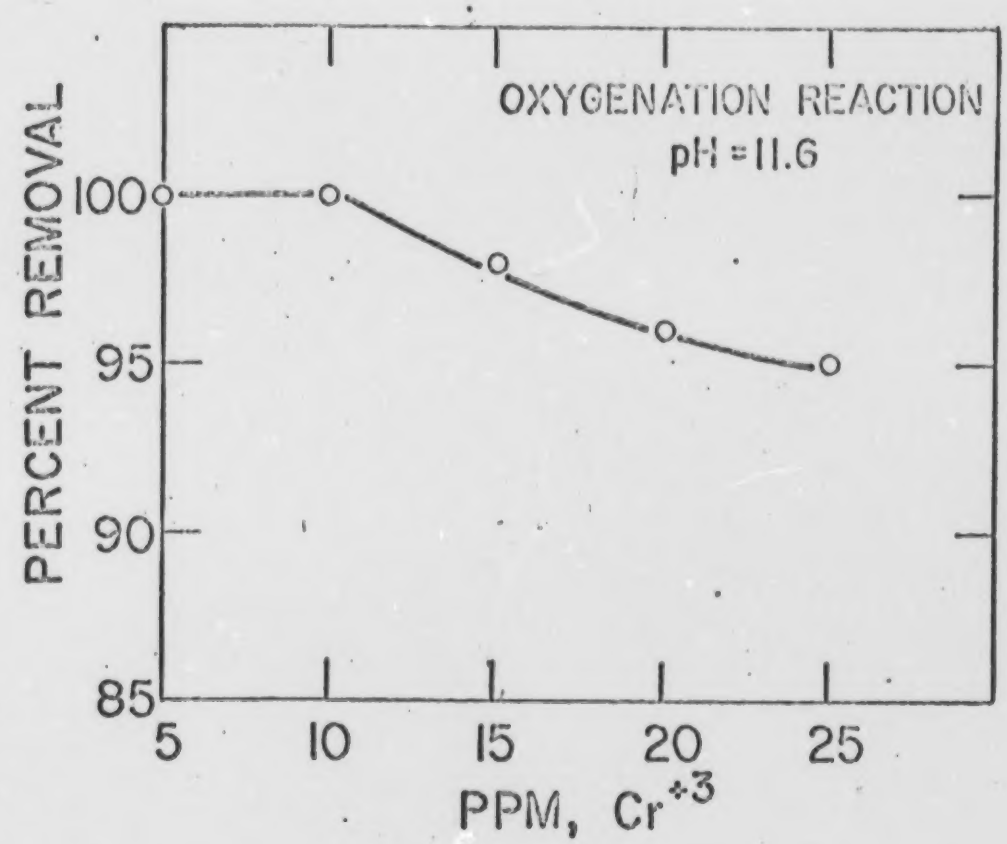
OXYGENATION REACTION
pH = 11.6
PERCENT REMOVAL
100
95
90
85
5
10
15
20
25
PPM, Cr+3

Fig. 27

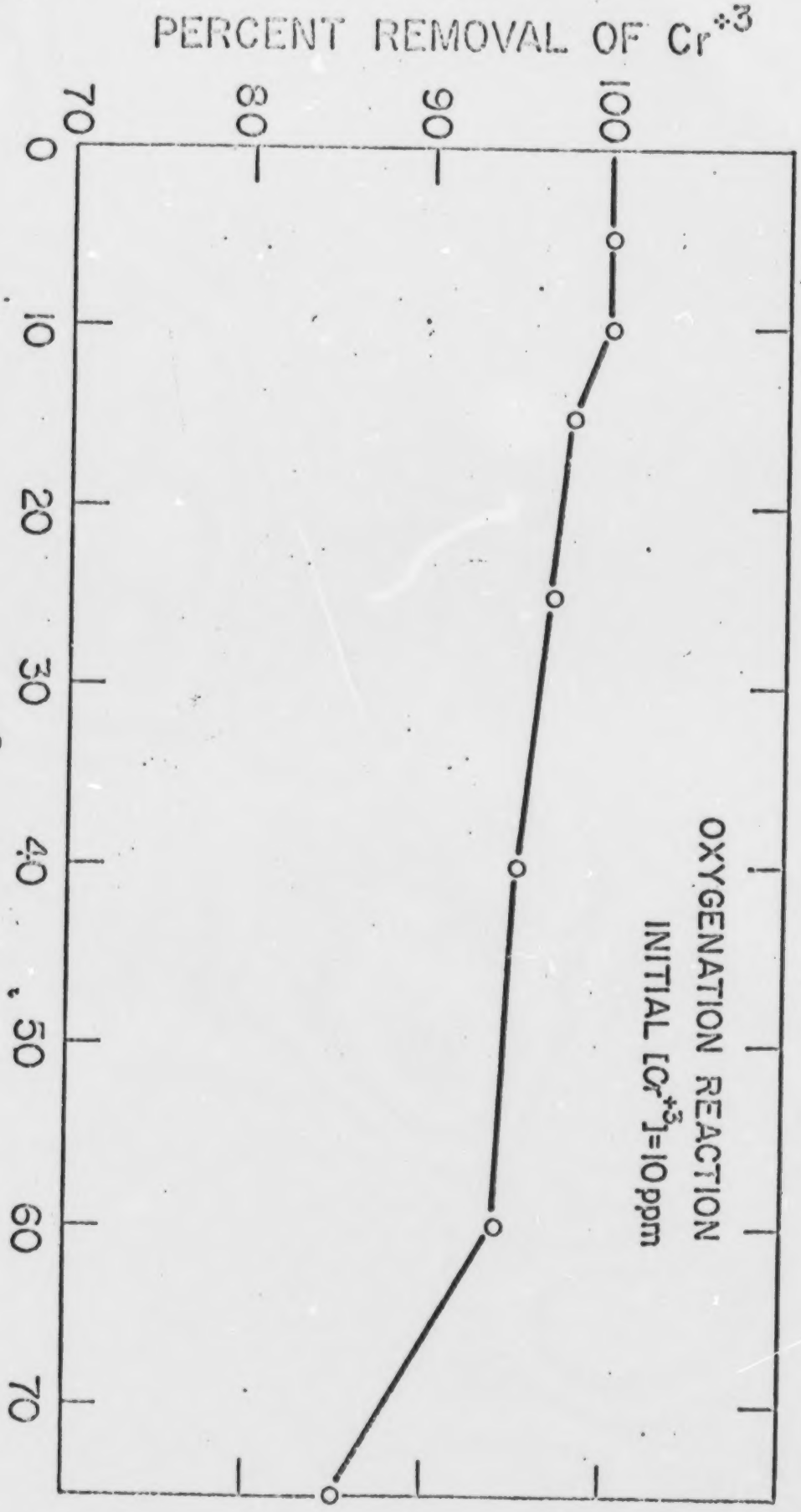
PERCENT REMOVAL OF Cr^{+3}
70
80
90
100
0
10
20
30
40
50
60
70
Ca^{+2}, PPM
OXYGENATION REACTION
INITIAL $[Cr^{+3}]$=10 ppm

Fig. 28

Fig. 27

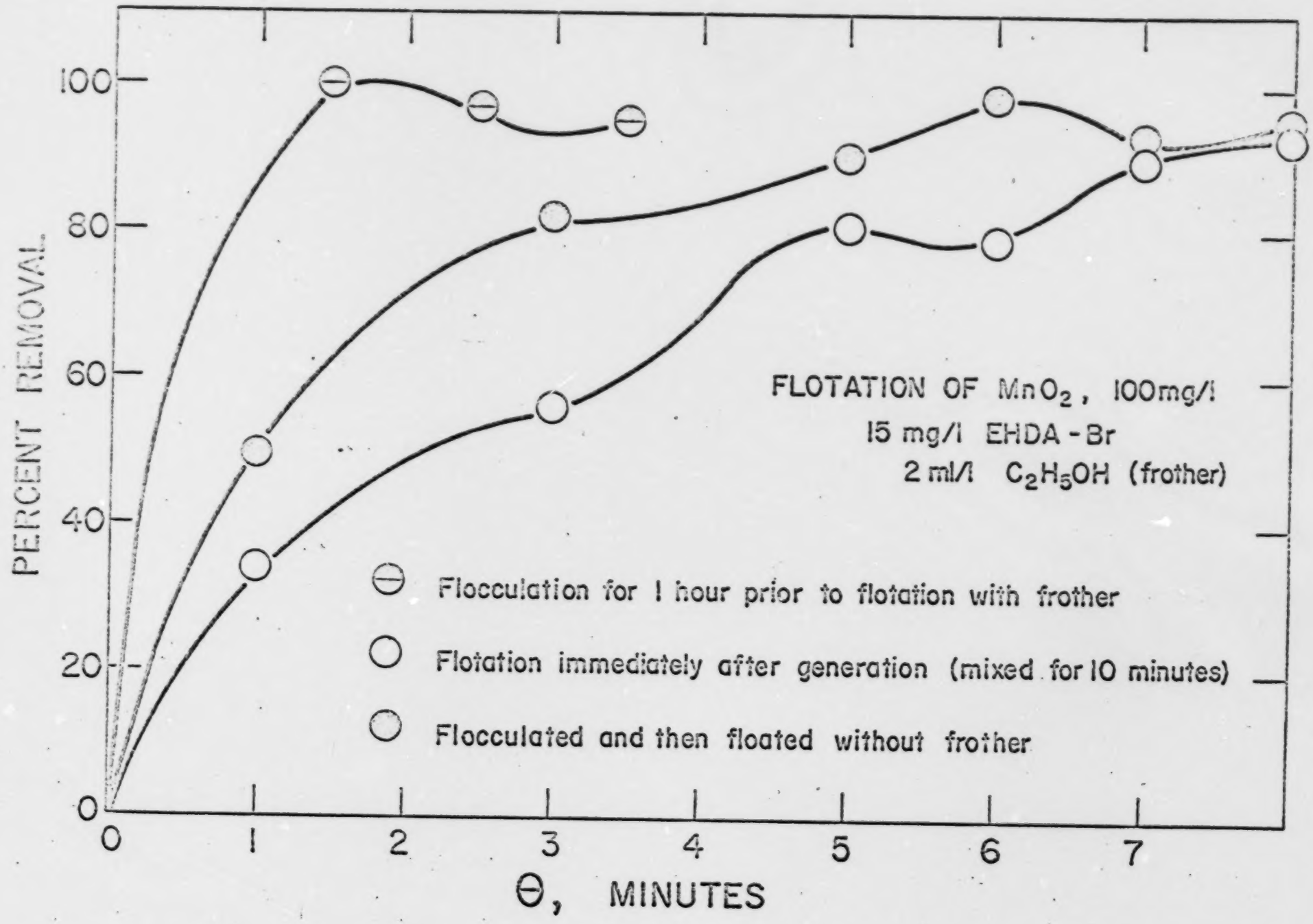
PERCENT REMOVAL
100
80
60
40
20
0
0
1
2
3
4
5
6
7
Θ, MINUTES
FLOTATION OF MnO_2, 100mg/l
15 mg/l EHDA - Br
2 ml/l C_2H_5OH (frother)
Θ Flocculation for 1 hour prior to flotation with frother
Flotation immediately after generation (mixed for 10 minutes)
Flocculated and then floated without frother

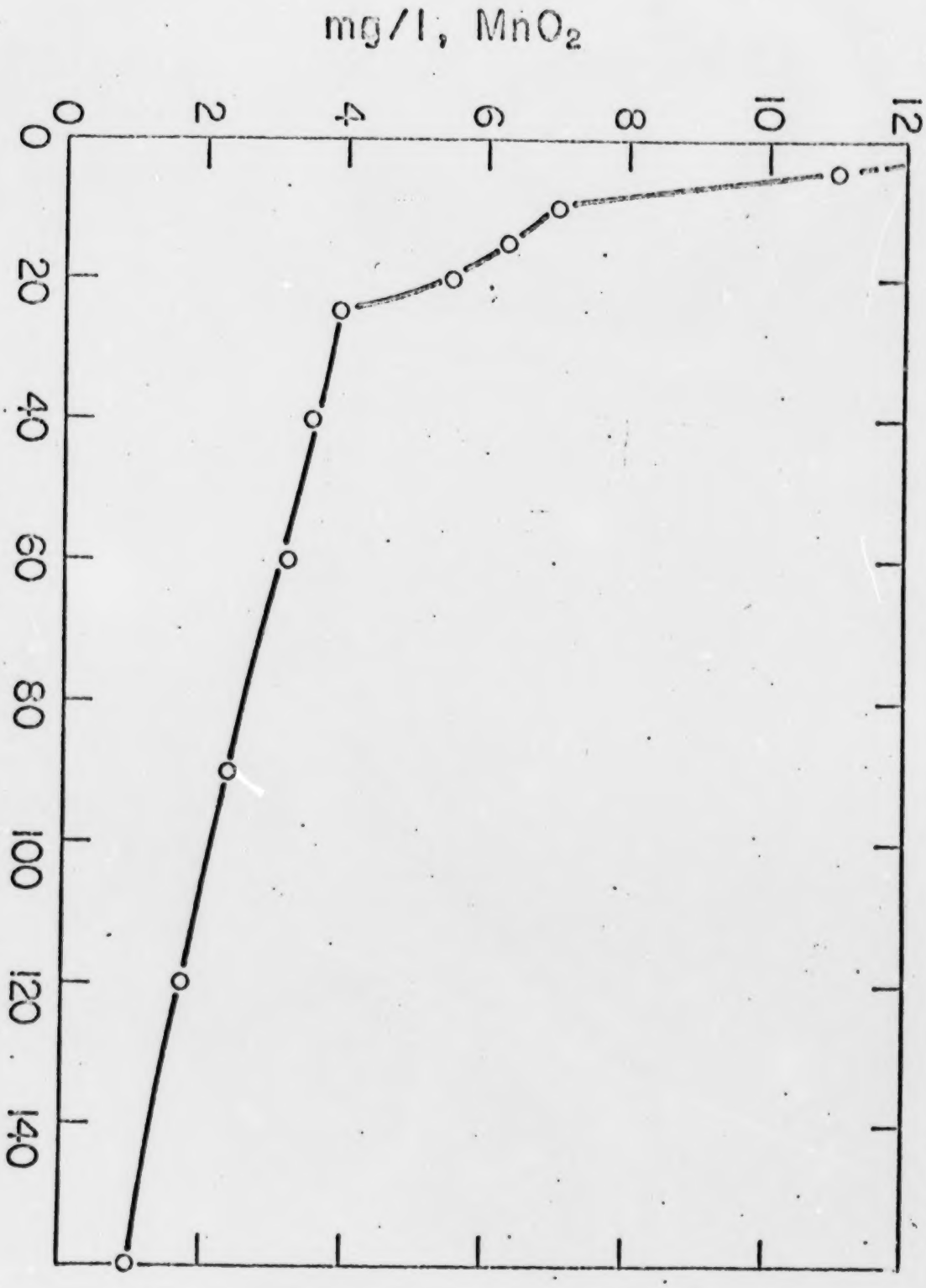
mg/l, MnO_2
0
2
4
6
8
10
12
0
20
40
60
80
100
120
140
STANDING TIME, MINUTES

Fig. 30